



SCHOOL of
GRADUATE STUDIES
EAST TENNESSEE STATE UNIVERSITY

East Tennessee State University
Digital Commons @ East
Tennessee State University

Electronic Theses and Dissertations

Student Works

12-2015

Characterization of SBIP68: A Putative Tobacco Glucosyltransferase Protein and Its Role in Plant Defense Mechanisms

Abdulkareem O. Odesina
East Tennessee State University

Follow this and additional works at: <https://dc.etsu.edu/etd>

 Part of the [Biology Commons](#), [Molecular Biology Commons](#), and the [Plant Biology Commons](#)

Recommended Citation

Odesina, Abdulkareem O., "Characterization of SBIP68: A Putative Tobacco Glucosyltransferase Protein and Its Role in Plant Defense Mechanisms" (2015). *Electronic Theses and Dissertations*. Paper 2598. <https://dc.etsu.edu/etd/2598>

This Thesis - Open Access is brought to you for free and open access by the Student Works at Digital Commons @ East Tennessee State University. It has been accepted for inclusion in Electronic Theses and Dissertations by an authorized administrator of Digital Commons @ East Tennessee State University. For more information, please contact digilib@etsu.edu.

Characterization of SBIP68: A Putative Tobacco Glucosyltransferase Protein and Its
Role in Plant Defense Mechanisms

A thesis

presented to

the faculty of the Department of Biological Sciences

East Tennessee State University

In partial fulfillment

of the requirement for the degree

Master of Science in Biology

by

Abdulkareem Olakunle Odesina

December 2015

Dhirendra Kumar, Chair, PhD

Cecilia A. McIntosh, PhD

Jonathan Peterson, PhD

Keywords: *Nicotiana tabacum*, SA, SABP2, SBIP68, Glucosyltransferase, *Pichia pastoris*, *E. coli*

ABSTRACT

Characterization of SBIP68: A Putative Tobacco Glucosyltransferase Protein and Its Role in Plant Defense Mechanisms

by

Abdulkareem Olakunle Odesina

Plant secondary metabolites are essential for normal growth and development in plants ultimately affecting crop yield. They play roles ranging from appearance of the plants to defending against pathogen attack and herbivory. They have been used by humans for medicinal and recreational purposes amongst others. Glucosyltransferases catalyze the transfer of sugars from donor substrates to acceptors. Glucosyltransferases are a specific type of glycosyltransferases known to transfer glucose molecules from a glucose donor to a glucose acceptor (aglycone) producing the corresponding glucose secondary metabolite or glycone, in this case glucosides. It was hypothesized that SBIP68, a tobacco putative glucosyltransferase-like protein glucosylated salicylic acid. Salicylic acid is an essential plant defense secondary metabolite. SBIP68 was cloned and heterologously expressed in both prokaryotic and eukaryotic systems. Results from activity screening suggest that SBIP68 is a UDP-glucose flavonoid glucosyltransferase with broad substrate specificity. Further studies are required to fully characterize SBIP68.

DEDICATION

To my beloved parents Dr. Idowu Adekunle Odesina and Mrs. Olajumoke Oluwatoyin Odesina who inspire me and have never failed to support me in fulfilling my aspirations, and to my Lord, in whom I place my trust.

ACKNOWLEDGEMENTS

I would like to express my gratitude to members of my committee, Dr. Dhirendra Kumar, Dr. Cecilia McIntosh, and Dr. Jonathan Peterson, for their guidance, support, and constructive criticisms. I would like to specially thank Dr. Dhirendra Kumar for his guidance, and the knowledge and skills I acquired during the course of this research. I would like to thank the staff/ faculty of the Department of Biological Sciences here at ETSU. I would like to acknowledge the support of my colleagues in the lab, both graduates and undergraduates. Special thanks to Dr. Shivakumar Devaiah, Preethi Sathanantham, and Sangam Kandel of Dr. Cecilia McIntosh's laboratory for their help during this research, and the ETSU School of Graduate Studies for the tuition scholarship. This research was supported by a grant from the National Science Foundation (MCB#1022077) to DK and funds from the Department of Biological Sciences, ETSU. Lastly, to my sister, Abisola, my friend and brother, Jubril, and all the members of my family, and my friends, here in the United States and back home, I would like to say thank you for their unrelenting support and encouragement throughout my stay at ETSU.

TABLE OF CONTENTS

	Page
ABSTRACT	2
ACKNOWLEDGEMENTS	4
LIST OF TABLES	9
LIST OF FIGURES.....	10
Chapter	
1. INTRODUCTION	12
Salicylic Acid Binding Protein 2 (SABP2)	24
UGTs, SA, and the Significance of Glucosylation	27
Hypothesis	32
2. MATERIALS AND METHODS	33
Plant Materials	33
Chemicals and Reagents	33
Cells and Vectors	35
Oligonucleotides	35
Apparatus	36
Methods	36
Cloning and Expression of SBIP68 in <i>E. coli</i>	36
Total RNA Extraction	37
cDNA Synthesis.....	39
Polymerase Chain Reaction (PCR)	39
Agarose Gel Electrophoresis	40
Purification of PCR Product	41
Construction of pGEMT-SBIP68 Clone	41
Preparation of Fresh Competent DH5 α Cells	42
Transformation of <i>E. coli</i> DH5 α with pGEMT-SBIP68 Plasmid DNA	43
Verification of pGEMT-SBIP68 Plasmid by Colony PCR.....	43
Plasmid DNA Isolation from pGEMT-SBIP68 Clones	44
Sequencing of pGEMT-SBIP68 Recombinant Plasmid	44
Cloning of SBIP68 into <i>E. coli</i> Expression Plasmid pET-28a.....	45

Transformation of <i>E. coli</i> BL21(DE3) pLysE with pET-28a-SBIP68 Plasmid	46
Test for Recombinant pET-28a-SBIP68 Protein Expression	46
Sodium Dodecyl Sulfate Polyacrylamide Gel Electrophoresis (SDS-PAGE)	47
Western Blot Analysis	47
Recombinant pET-28a-SBIP68 Protein Solubility Test	49
Optimization of Conditions for Protein Solubility	50
Cell Lysis and Purification of Recombinant SBIP68 Protein	51
Analysis of Glucosyltransferase Activity Reaction Products using HPLC	52
Cloning and Expression of SBIP68 in <i>P. pastoris</i>	53
PCR Amplification of <i>SBIP68</i> for Cloning into pPICZA	53
Purification of PCR Product	54
Construction of pGEMT-SBIP68' Clone	55
Recombinant Plasmid pGEMT-SBIP68' Propagation and Isolation	55
Sequencing of pGEMT-SBIP68' Recombinant Plasmid	55
Digestion of pGEMT-SBIP68' Plasmid and pPICZA Vector	55
Ligation of <i>SBIP68'</i> into pPICZA	56
Transformation of <i>E. coli</i> DH5 α with pPICZA-SBIP68' Plasmid DNA	56
Verification of the Presence of pPICZA-SBIP68' Plasmid by Colony PCR	57
Recombinant Plasmid pPICZA-SBIP68' Propagation and Isolation	57
Sequencing of pPICZA-SBIP68' Recombinant Plasmid	58
Preparing pPICZA-SBIP68' DNA for Transformation into <i>Pichia pastoris</i>	58
Preparation of Electrocompetent <i>Pichia pastoris</i> X-33 Mut ⁺ Cells	59
Transformation of <i>P. pastoris</i>	60
Direct PCR Screening of <i>P. pastoris</i> Clones	60
Time Course Expression of Recombinant SBIP68'	61
Preparing Samples for SDS-PAGE and Western Blot Analysis	62
Sodium Dodecyl Sulfate Polyacrylamide Gel Electrophoresis (SDS-PAGE)	63
Western Blot Analysis	63
Large Scale Expression of <i>Pichia</i> -SBIP68'	63
Purification of Recombinant SBIP68' Protein Expressed in <i>Pichia pastoris</i>	64
Purification of Recombinant SBIP68' using Anion Exchange Chromatography ..	65
Analysis of Glucosyltransferase Activity using Radioactive Method	65

Analysis of Glucosyltransferase Activity Reaction Products using HPLC	66
3. RESULTS	68
Cloning and Expression of SBIP68 in <i>E. coli</i>	68
Bioinformatics Analyses of SBIP68	68
Subcellular Localization of SBIP68.....	70
RNA Extraction	71
cDNA Synthesis.....	71
PCR Amplification of <i>SBIP68</i>	72
Purification of PCR Product.....	73
Cloning <i>SBIP68</i> in pGEMT Plasmid	73
Plasmid Isolation and DNA Sequencing of pGEMT-SBIP68	74
PCR Screening of pET-28a-SBIP68 Bacterial Clones.....	83
Test for Recombinant pET-28a-SBIP68 Protein Expression	84
Recombinant pET-28a-SBIP68 Protein Solubility Test	86
Optimization of Conditions for Protein Solubility	87
Affinity Purification of Recombinant SBIP68 Protein.....	90
HPLC Analysis of Glucosyltransferase Activity Assay Products.....	92
Cloning and Expression of SBIP68 in <i>P. pastoris</i>	98
PCR Amplification of <i>SBIP68</i> with Modified Ends for Cloning into pPICZA	98
Sequencing of pGEMT-SBIP68' Recombinant Plasmid	99
PCR Screening of pPICZA-SBIP68' Transformed Bacterial Clones	102
Sequencing of pPICZA-SBIP68' Recombinant Clones	102
Transformation of pPICZA-SBIP68' Plasmid DNA into <i>Pichia pastoris</i>	105
Screening of <i>P. pastoris</i> Clones	106
Expression of Recombinant SBIP68' in <i>Pichia pastoris</i>	107
Large Scale Expression and Purification of Recombinant SBIP68' Protein	110
Purification of recombinant SBIP68' using Anion Exchange Chromatography .	111
Analysis of Glucosyltransferase Activity of SBIP68' using Radioactive Method	114
Analysis of Glucosyltransferase Activity using HPLC	116
4. DISCUSSION.....	120
Future Directions	136
REFERENCES.....	137

APPENDICES	154
Appendix A – Abbreviations	154
Appendix B – Buffers, Reagents, and Media	155
VITA	167

LIST OF TABLES

Table	Page
1. Primers Used in This Study.....	35
2. Activity Screening of SBIP68' using UDP- ¹⁴ C-glucose	115

LIST OF FIGURES

Figures	Page
1. Chemical Structure of Abscisic Acid.....	19
2. Chemical Structure of Ethylene.....	20
3. Chemical Structure of Jasmonic Acid.....	21
4. Chemical Structure of Salicylic Acid.....	22
5. Salicylic Acid Biosynthetic Pathways.....	23
6. Schematic Representation of Systemic Acquired Resistance in Plants.....	24
7. Amino Acid Sequence of NtGT4.....	26
8. Possible Role of SBIP68 in Plants.....	27
9. Map of <i>E. coli</i> Expression Plasmid pET-28a.....	37
10. Map of pGEM-T Easy Vector.....	42
11. Map of pPICZ Vector.....	54
12. Nucleotide and Translated Amino Acid Sequence of SBIP68.....	68
13. Flavonoid Glucosyltransferase (<i>NtGT4</i>) Accession Number BAD93688.1.....	69
14. Subcellular Localization Prediction using MultiLoc2.....	70
15. Subcellular Localization Prediction using Target v1.1.....	70
16. Localization of SBIP68 as Predicted by PSORT.....	70
17. Scan from Nanodrop Spectrophotometer.....	71
18. PCR Amplification of <i>EF1α</i>	72
19. RT-PCR Amplification of <i>SBIP68</i>	72
20. Purified <i>SBIP68</i> PCR Products.....	73
21. Screening of <i>SBIP68</i> Inserts by Colony PCR.....	74
22. Nucleotide Sequence Alignment of <i>NtGT4</i> and pGEMT-SBIP68 Clones.....	79
23. Amino Acid Sequence Alignment of <i>NtGT4</i> and pGEMT-SBIP68 Clones.....	80
24. Full Length <i>SBIP68</i> Sequence Cloned from <i>Nicotiana tabacum</i>	81
25. SBIP68 Protein BLAST Query.....	82
26. Alignment of SBIP68 with Other Similar Glucosyltransferases.....	83
27. Colony PCR Screening of pET28a-SBIP68 Clones.....	84
28. SDS-PAGE of pET-28a-SBIP68 (644 & 645) Expressed in <i>E. coli</i>	85
29. Test for Expression of pET28a-SBIP68 (644) and (645) in <i>E. coli</i>	86
30. Solubility Test of Expressed pET28a-SBIP68 (644) and (645).....	87

31. Optimization of Protein Solubility.....	89
32 A-J. Ni-NTA Purification of SBIP68 Expressed in <i>E. coli</i>	91
33 A-D. GT Assay using <i>E. coli</i> Expressed SBIP68 (645).....	94
34 A-D. GT Assay using <i>E. coli</i> Expressed SBIP68 (644).....	96
35. PCR Amplification of <i>SBIP68</i> for Cloning into pPICZA	98
36. Verification of pGEMT-SBIP68' Clones	99
37. Alignment of Cloned <i>SBIP68'</i> in pGEMT with Reference Gene	101
38. Colony PCR to Verify Presence of <i>SBIP68'</i> in pPICZA Plasmid	102
39. Nucleotide Sequence Alignment of Cloned <i>SBIP68'</i> in pPICZA.....	104
40. Amino Acid Sequence of pPICZA-SBIP68' Clone # C4.....	105
41. Agarose Gel Electrophoresis of pPICZA-SBIP68' Plasmid DNA.....	105
42. Agarose Gel Showing Colony PCR of <i>P. pastoris</i> Clones	106
43. Recombinant SBIP68' Expression in <i>P. pastoris</i>	108
44. Time Course Expression of Recombinant SBIP68'	109
45. Ni-NTA Affinity Chromatography Purification of SBIP68'	111
46. Ni-NTA Affinity Chromatography Purification of SBIP68'	112
47. Chromatogram Showing Purification of SBIP68' on MonoQ Column	113
48. MonoQ Anion Exchange Chromatography Purification of SBIP68'	114
49. Relative Activity of SBIP68' with Different Potential Acceptor Substrates	116
50.A-E: Identification of Reaction Products by HPLC.....	117
51. Model Suggesting SBIP68 Function <i>in planta</i>	134

CHAPTER 1

INTRODUCTION

Plant disease refers to an abnormal condition that causes damages to a plant, leading to a subsequent reduction in its productivity. The disease could be caused by a biotic agent or abiotic factors (McMullen and Lamey, 2001). Given the importance of plants and their products on our daily lives, the study of plant diseases is of utmost importance. Between 1845 and 1852, the great famine in Ireland led to the starvation, death of about one million people and caused one million more to emigrate from Ireland (Ross, 2002). The famine was a result of Potato Blight Disease. In the United States alone, an estimated \$30 billion is lost every year as a result of plant diseases (Pimentel et al., 2000; Pimentel and Burgess, 2014). The ever increasing world population and resulting higher demands for food supplies makes the control of plant diseases even more critical (Emmert and Handelsman, 1999). Various means have been employed to prevent/control herbivory and plant diseases; among them is the use of chemicals called pesticides. Fungicides, herbicides, insecticides and the like, are all pesticides employed in the protection of plants (Rangwala et al., 2013). In the United States alone, more than \$10 billion is spent yearly on the use of pesticides (Pimentel et al., 1994; Pimentel and Burgess, 2014). Pesticides play a major role in maintaining food production globally, as it has been estimated that without the use of pesticides, there would be a 10% increase in losses due to pests. The use of pesticides, however, may not necessarily result in a decrease in crop losses (Pimentel et al., 1992). For instance, in the United States, losses due to pests from 1945 to 1989 nearly doubled from 7% to

13% despite the ten-fold increase in the use of insecticides (Pimentel et al., 1991; Pimentel and Burgess, 2014).

In recent times, there have been concerns over the excessive use of pesticides (Pimentel et al., 1992; Pimentel and Burgess, 2014). Approximately 355,000 people die as a result of unintentional poisonings yearly (WHO, 2003). Pesticides and other toxic chemicals have been strongly associated with two-thirds of these deaths (Goldman and Tran, 2002; FAO/UNEP/WHO, 2004). Dibromo-chloro-propane (DBCP, a banned pesticide) was found to cause testicular dysfunction in animals (Foote et al., 1986) and associated with infertility in humans exposed to it (Potashnik and Yanai-Inbar, 1987). Reports from animal studies have shown that pesticides can cause immune dysfunction (Thomas and House, 1989). Chronic health problems have been linked to organophosphorus pesticides (Ecobichon et al., 1990) resulting in irreversible neurological defects (Lotti, 1984). Neurotoxic effects have been found to persist following poisoning (Ecobichon et al., 1990). Other issues related to the use of pesticides include: poisoning in bees and reduced pollination, destruction of crop and crop products, contamination of surface and ground water and fishery losses among others. Despite their negative effects, pesticides still remain valuable pest control tools (Pimentel et al., 1992; Pimentel and Burgess, 2014).

Cultivated plants such as Chinese cabbage, cowpea, cucumber, melon, potato, strawberry, tobacco, tomato, water melon, are known to be attacked by viral pathogens such as cucumber green mottle mosaic virus (CGMMV), cucumber mosaic virus (CMV), lettuce mosaic virus (LMV), melon necrotic spot virus (MNSV), potato virus X (PVX), and tobacco mosaic virus (TMV), etc. (Shigematsu et al., 1978). These plant viruses are

ubiquitous, occurring in plants, seeds, and soil, and readily infect plants by the suction of plant juices by insects, contact with virus-containing soil during planting, and contact with farm equipment, or humans (Shigematsu et al., 1978). A number of chemicals are known to control these viruses, these include antibiotics and nucleic acid-like compounds, both of which function by suppressing the proliferation of plant viruses (Shigematsu et al., 1978). These substances however, are toxic to humans, plants, and animals, and have not been applied practically except in the case of one chemical that contains sodium alginate as its main component (Shigematsu et al., 1978).

Despite advances in agriculture, certain cultural practices have been known to augment the devastating potential of plant diseases (De Waard et al., 1993). Some of these practices include the growth of plant cultivars that are vulnerable to pathogens, the propagation of genetically similar crop plants in monoculture, and the application of inorganic fertilizers at concentrations that increase disease susceptibility (De Waard et al., 1993). Crop losses due to pathogenic fungi are estimated at approximately 30 % (Schwinn, 1992). The control of plant diseases is heavily dependent on fungicides to attack the plethora of fungal diseases that threaten the productivity of agricultural crops (Schwinn, 1992). For farmers, the obtainability of progressively effective fungicides has varied remarkably in its impact. These benefits include the reduction of yield losses, and the prevention of complete crop losses, e.g. the preservation of potato from *Phytophthora infestans* in Western Europe (Schwinn and Margot, 1991).

Fungicides have been known to improve crop quality, enhancing marketability and food safety (Ragsdale et al., 1991). Improved food safety is associated with the reduction of mycotoxins and phytoalexins (De Waard et al., 1993). Mycotoxins are

capable of being carried over from fungal infections of live plants to stored plant material, and decomposing plant matter (De Waard et al., 1993). They constitute a threat in food technology, greater than the misuse of fungicides (Natl Acad Sci, 1987). Mycotoxins are ubiquitous, they include tenuazonic acid, patulin, fusarium toxins, ergot toxins, and aflatoxins (Ragsdale et al., 1991; Schwinn, 1992). Certain phytoalexins known to occur in potato and leguminous plants are toxic to humans and other higher animals (Ragsdale et al., 1991). Fungicides are capable of preventing and/or diminishing the production of these toxic compounds (De Waard et al., 1993). Without doubt, fungicides play a significant role in the defense against plant pathogens, however, there are emerging concerns on the use of fungicides.

Ethylene-bis-dithiocarbamate (mancozeb) is a widely used fungicide that has been found to induce embryo apoptosis in mice (Paro et al., 2012). Mancozeb was shown to affect oocyte meiotic spindle morphology, and impair the rate at which fertilization occurs, even when used at very low concentrations (Paro et al., 2012). It is a reproductive toxicant that affects the somatic cells of the mammalian ovarian follicles, by inducing a premalignant-like status in both mouse and human granulosa cells (Paro et al., 2012). The fungicide residues benomyl, dichlofluanid, iprodione, procymidone, and vinclozolin found in red and white bottled wines, were shown to have a negative effect on yeast growth, with dichlofluanid and benomyl being the most toxic (Calhelha et al., 2006). In wheat seedlings, carbendazim was found to alter biochemical parameters such as protein content, carbohydrate content, total chlorophyll, chlorophyll a, chlorophyll b, and alkaline protease activity (Rangwala et al., 2013). An increase in concentration of the fungicide brought about a decrease in the concentration of protein,

carbohydrate, total chlorophyll, chlorophyll a, and chlorophyll b, and an increase in alkaline protease activity (Rangwala et al., 2013). A maximum decline in the concentration of protein (– 62.49%), carbohydrate (– 62.5%), total chlorophyll (-57.44%), chlorophyll a (-47.89%) and chlorophyll b (-63.44%), and a maximum elevation in alkaline protease activity (152%) was obtained at a fungicide concentration of 2500 mg/l (Rangwala et al., 2013).

The fungicides azoxystrobin, boscalid, chlorothalonil, fenarimol, fludioxonil, myclobutanil, pyraclostrobin, pyrimethanil, and zoxamide are emerging chemicals of concern due to their increasing rates of use globally, the frequency at which they are detected in surface waters, and their likely persistence in the environment (Elskus, 2014). Significant sublethal effects of fungicides on aquatic invertebrates and ecosystems, fish reproduction and immune function, zooplankton community, metabolic enzymes, and ecosystem processes such as leaf decomposition in streams, have been observed (Elskus, 2014). Some of these effects are known to occur at concentrations well below single-species acute lethality values, killing 50 percent of the organisms within 48 to 96 hours (Elskus, 2014). This is an indication that single-species toxicity values may be a misrepresentation of the toxic effects of certain fungicides (Elskus, 2014). Fungicides are also capable of showing synergistic effects when used in combination with other fungicides and insecticides (Elskus, 2014). The frequency of fungicide use is projected to increase drastically in the next few years (Troy, 2011), making them an emerging concern in freshwater systems in the United States (Elskus, 2014).

More recently, there's been an increase in the use of nonchemical based pest control methods commonly called "biological control" (Emmert and Handelsman, 1999), as most of the synthetic pesticides are likely to lose their usefulness over time, arising from revised safety regulations (Duke et al., 1993; Benbrook et al., 1996; NRC Report, 1996), development of resistance in pathogens (Russell, 1995), and negative effects on non-target organisms (Felton and Dahlman, 1984; Guy et al., 1989; Dernoeden and McIntosh, 1991; Elmholt, 1991). Biological controls, such as microbes, are much more environmental friendly compared to the use of pesticides in controlling plant diseases. Apart from being environment friendly, the rich diversity of microbes makes them a seemingly endless resource and a better alternative to the use of pesticides (Emmert and Handelsman, 1999). Some rhizobacteria that function as effective biocontrol substances by suppressing a number of economically important plant pathogens usually promote plant growth and yield, either when applied to crop seed or into the soil (Burr et al., 1978; Kloepper et al., 1980a, 1980b; Kloepper et al., 1989; Brown and Surgeoner, 1991; Turner and Backman, 1991; Bashan, 1998). These bacterial strains promote plant growth even in the absence of pathogens (Harris et al., 1994). They are referred to as plant growth promoting rhizobacteria, PGPR (Kloepper et al., 1989).

In-depth analysis into various plant defense mechanisms and the biocontrol of plant diseases is essential to the development of better and safer disease control methods. The innate immune system otherwise referred to as the "non-specific immune system" (Grasso, 2002) is the first line of defense against invading pathogens. Unlike the adaptive immune system found in vertebrates, the innate immune system does not keep memory of antigens / pathogens and therefore does not provide an organism with

long-lasting immunity (Alberts et al., 2003). Because plants possess neither mobile defender cells nor the adaptive immune system characteristic of mammals, they defend themselves against pathogens using the innate immunity of individual cells and systemic signals produced by infected cells (Dangl and Jones, 2001; Ausubel, 2005; Chisholm et al., 2006; Bent and Mackey, 2007).

Plants respond to a number of chemical stimuli produced by the soil and plant-associated microbes (Pal and Gardener, 2006). These stimuli are capable of inducing plant host defenses via biochemical changes that boost resistance against subsequent infections by different pathogens (Pal and Gardener, 2006). Depending on the type, source, and amount of stimuli, the induction of the host defense mechanisms could be local and/or systemic (Pal and Gardener, 2006). Attempts are being made by plant pathologists to fully characterize the components of pathways involved in induced resistance triggered by biological control agents and other non-pathogenic microorganisms. Upon pathogen infection, large amounts of salicylic acid is produced, leading to the expression of pathogenesis-related (PR) proteins (Yalpani et al., 1991). PR proteins consist of a variety of enzymes with different modes of action (Yalpani et al., 1991). Some PR proteins lyse invading cells, others reinforce the host cell wall, and some trigger localized cell death (Pal and Gardener, 2006).

In hypersensitive response (HR; a form of innate immunity), pathogen attack triggers rapid cell death at the site of infection and immediate surrounding cells (Agrios, 1988; Goodman and Novacky, 1994). HR can be triggered by an array of pathogens and it occurs within a few hours upon pathogen contact (Morel and Dangl, 1997). In addition to HR, plants have a form of secondary resistance referred to as systemic

acquired resistance (SAR) (Morel and Dangl, 1997). SAR is an inducible defense mechanism that is activated in the distal uninfected parts of plants in response to a local infection by pathogens (reviewed in Shah et al., 2014). It confers non-specific and prolonged levels of resistance in uninfected parts of a plant to secondary infections by a wide range of pathogens (Ryals et al., 1996). SAR is triggered by pathogens that cause cell death due to HR (Morel and Dangl, 1997). However, HR is not required to generate the SAR signal (Mishina and Zeier, 2007). Plants defend themselves against pathogens through an interconnection of signaling pathways involving three signal molecules: ethylene, jasmonic acid and salicylic acid (Kunkel and Brooks, 2002).

Absciscic acid (ABA; Fig. 1), is a phytohormone that also plays an important part in plant responses to environmental stress and in defense against plant pathogens

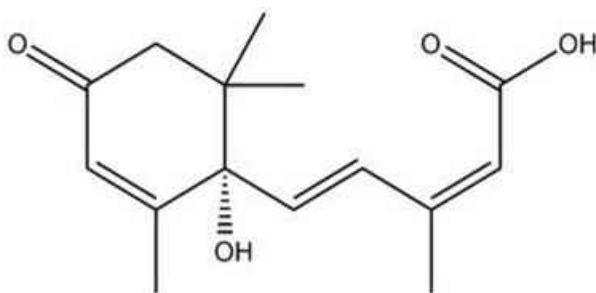


Figure 1: Chemical Structure of Absciscic Acid

(Swamy and Smith, 1999; Chinnusamy et al., 2004). ABA is known to play an essential role in various coordinating cellular processes including seed germination, seed development, dormancy, and growth with responses to environmental changes. These involve complex regulatory mechanisms that regulate its biosynthesis, catabolism, perception, and transduction (Xiong and Zhu, 2003). It is produced in response to different forms of stress which include but are not limited to cold, salinity and drought

(Wu et al., 1997). It reduces water loss due to transpiration by triggering the closing of stomata (Schroeder et al., 2001). ABA's glucose ester is gradually dispersed from leaves recovering from water stress thereby maintaining abscisic acid levels for a period of time after the leaves have regained turgor (Hiron and Wright, 1973). Apart from its role in environmental stress, ABA-mediated signaling is also important in plant – pathogen interactions (Seo and Koshiba, 2002). It is involved in increasing resistance to pathogens by plants through its positive effect on callose deposition (Mauch-Mani and Mauch, 2005). Wounding induces an increase in the synthesis of ABA.

Ethylene (Fig. 2), is a gaseous phytohormone with roles in various processes in plants such as growth and development (Yang and Hoffman, 1984). It is also a regulator

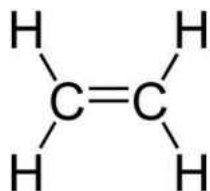


Figure 2: Chemical Structure of Ethylene

of fruit ripening (Van Loon et al., 2006). Its biosynthesis in plants has been found to increase rapidly following exposure to pathogens (Ecker and Davis, 1987). The increase in ethylene biosynthesis in infected plants brings about a subsequent increase in chitinase activity in these plants (Roby et al., 1986) and the deposition of hydroxyproline in the cell walls of the infected tissues (Roby et al., 1985). Hydroxyproline rich glycoproteins are the major structural proteins present in plant cell walls. Chitinases are enzymes that are responsible for the breakdown of glycosidic bonds in chitin (Jollès and

Muzzarelli, 1999) which is an important component of fungal cell-walls and the exoskeleton of arthropods, thereby conferring protection against fungal attack and attack from arthropods on plant cells. Ethylene effects the accumulation of mRNAs of genes responsible for plant defense (Ecker and Davis, 1987). Ethylene has been found to contribute to disease resistance in some interactions (Thomma et al., 1999; Norman-Setterblad et al., 2000), while it is known to promote disease in other interactions (Bent et al., 1992; Lund et al., 1998; Hoffman et al., 1999).

Jasmonic acid (JA; Fig. 3), is a phytohormone with a number of physiological roles including regulation of growth and development and response to biotic and abiotic

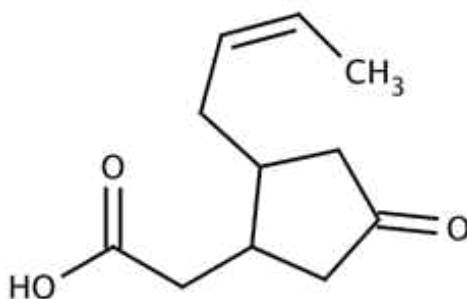


Figure 3: Chemical Structure of Jasmonic Acid

stress factors (Creelman and Mullet, 1995). JA, derived from lipids (Schaller and Stintzi, 2009) is biosynthesized from linolenic acid (Creeman and Mullet, 1995). JA also controls pollen maturation and wound responses (Turner et al., 2002). JA and its ester methyl jasmonate (MeJA) promote senescence (cell death), acting as growth regulators as mentioned earlier (Creelman and Mullet, 1997). Inhibiting the biosynthesis of JA in *Arabidopsis thaliana* greatly increases plant susceptibility to a wide array of pathogens (Staswick et al., 1998; Thomma et al., 1998; Vijayan et al., 1998; Norman-Setterblad et al., 2000).

Salicylic acid (SA; Fig. 4), is a phenolic phytohormone that is widely distributed in

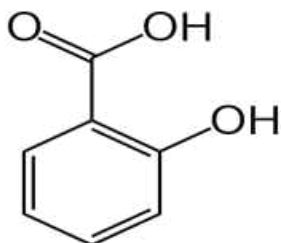


Figure 4: Chemical Structure of Salicylic Acid

plants, with its basal levels differing by as much as 100-fold between different plant species (Raskin et al., 1990). It has various roles in plants ranging from growth and development, ion transport, photosynthesis, response to abiotic stresses including drought (Munne´-Bosch and Penuelas, 2003; Chini et al., 2004), heat (Larkindale and Knight, 2002; Larkindale et al., 2005), osmotic stress (Borsani et al., 2001) and heavy metal tolerance (Metwally et al., 2003; Yang et al., 2003; Freeman et al., 2005). It is well studied for its involvement in plant defense signaling against pathogen infections (Hayat and Ahmad, 2007; Kumar, 2014) in which case it induces the production of PR proteins (Hooft van Huijsdijnen et al., 1986). SA induces resistance in uninfected parts of plants through SAR (Fig. 6). SAR induces resistance against pathogens in other nearby plants too by gaseous diffusion of methyl salicylate (MeSA), a salicylic acid ester (Shulaev et al., 1997). MeSA is likely converted into SA to induce resistance (Shulaev et al., 1997). SA biosynthesis occurs through two differentiated pathways (Fig. 5), that make use of different precursors: the phenylpropanoid (phenylalanine dependent) and the isochorismate (non-phenylalanine dependent) pathways in the cytoplasm and chloroplast, respectively (Rivas-San Vicente and Plasencia, 2011; Kumar 2014). The

isochorismate pathway involves isochorismate synthase and isochorismate pyruvate lyase, and is responsible for synthesizing most of the pathogen-induced salicylic acid in *Arabidopsis* (Wildermuth et al., 2001), *Nicotiana benthamiana* (Catinot et al., 2008), and tomato (Uppalapati et al., 2007). Upon infection, SA concentration increases at the pathogen infection sites, leading to the formation of necrotic lesions from hypersensitive response. This activates the SAR pathway (Ryals et al., 1996) and activation of SAR produces a broad-spectrum systemic resistance (Hunt and Ryals, 1996; Neuenschwander et al., 1996).

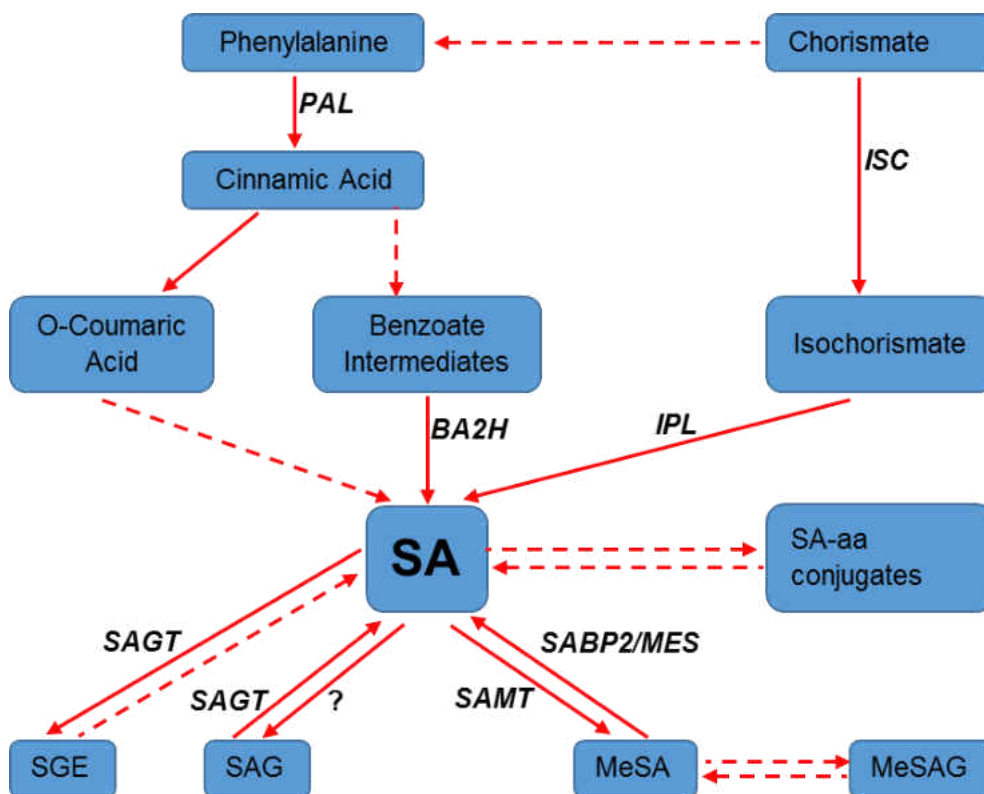


Figure 5: Salicylic Acid Biosynthetic Pathways. Enzymes are shown in italics. PAL, Phenylalanina Ammonia Lyase; ISC, Isochorismate Synthase; BA2H, Benzoic Acid 2-Hydroxylase; IPL, Isochorismate Pyruvate Lyase; SAGT, Salicylic Acid Glucosyltransferase; SAMT, Salicylic Acid Methyltransferase; SABP2, Salicylic Acid Binding Protein 2; MES, Methyl Esterase; SGE, Salicyoyl Glucose Ester; SAG, Salicylic Acid O-β-Glucoside; MeSA, Methyl Salicylate (Figure adapted from Vlot et al. 2009).

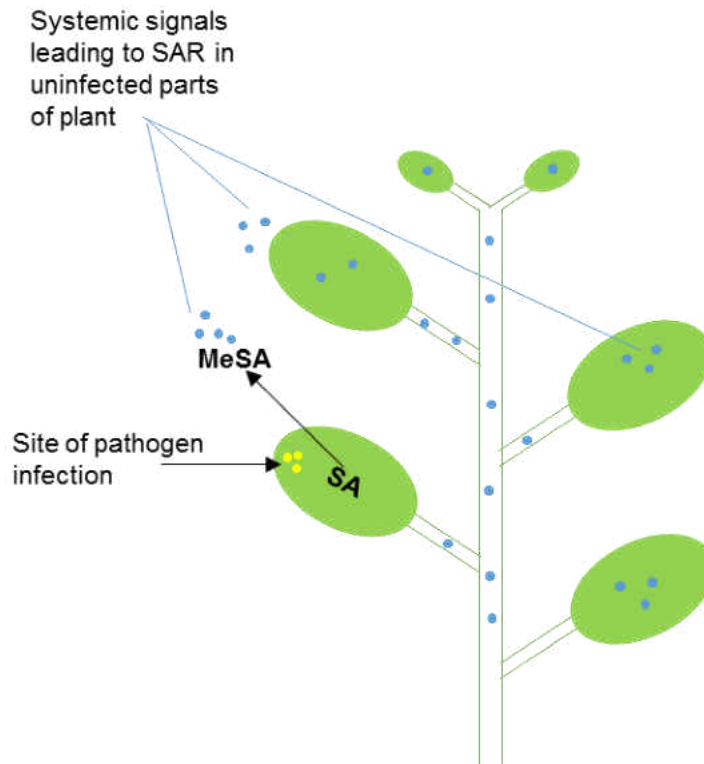


Figure 6: Schematic Representation of Systemic Acquired Resistance (SAR) in Plants. Volatile MeSA diffuses to uninfected parts and neighboring plants to induce pathogen resistance.

Salicylic Acid Binding Protein 2 (SABP2)

There are four proteins that currently are known to bind SA in tobacco and these are collectively referred to as salicylic acid binding proteins (SABP) (Vlot et al., 2009), although recent studies suggest the presence of additional new SABPs in Arabidopsis (Kumar, 2014; Manohar et al., 2014). One of the SABP, salicylic acid binding proteins 2 (SABP2) has the highest affinity for salicylic acid (Du and Klessig, 1997). It is a 29 kDa protein required for both local resistance and SAR after infection by tobacco mosaic virus (TMV) (Kumar and Klessig, 2003). It catalyzes the synthesis of methyl salicylic acid (MeSA) into SA to induce SAR (Forouhar et al., 2005). Exogenous application of

SA or its analog acibenzolar-S-methyl (ASM) also induces SAR as SABP2 catalyzes the conversion of ASM into acibenzolar which induces SAR (Tripathi et al., 2010). SABP2-silenced tobacco plants neither express PR-1 proteins nor induce SAR expression to a significant level when treated with ASM (Tripathi et al., 2010). Conversely, treatment of the same type of plants with acibenzolar induces full SAR indicating that SABP2 is required for induction of resistance (Kumar and Klessig, 2003; Tripathi et al., 2010). SABP2 is feedback inhibited by reverse binding of the product of the reaction it catalyzes, SA. This inhibition promotes the accumulation of the more volatile MeSA to be translocated through the phloem to uninfected parts of the plant (Forouhar et al., 2005; Park et al., 2007).

To better understand the role of SABP2 in inducing SAR, an attempt was made to identify its interacting proteins. One of the best ways to identify interacting proteins is to use a yeast two-hybrid screen (Y2H). Y2H is a technique used in the discovery of protein–protein interactions (Young, 1998) and also protein–DNA interactions (Joung et al., 2000; Hurt et al., 2003) by testing for physical interactions between two proteins or a protein and a DNA molecule. Typically one of the proteins, the known one, is termed the ‘bait’ and the unknown one(s) the ‘prey’. Interaction between the proteins causes activation of a reporter gene which could be detected by change of color, antibiotic resistance growth on depleted minimal media. With the aid of Y2H using full length SABP2 as a bait, a number of interacting tobacco proteins were discovered. These interacting proteins have been collectively referred to as ‘SABP2 interacting proteins’ (SBIPs). SBIP68, the focus of this research, is one of the interacting proteins. Bioinformatics analyses revealed that the partial amino acid sequence of SBIP68 is

100% identical to an annotated putative UDP-glucose: flavonoid glucosyltransferase from *Nicotiana tabacum* (Fig. 7), with NCBI accession number BAD93688.1. It is a B

```
1  MATQVHKLHF  ILFPLMAPGH  MIPMIDIAKL  LANRGVITTI  ITTPVNANRF  SSTITRAIKS
61  GLRIQILTLK  FPSVEVGLPE  GCENIDMLPS  LDLASKFFAA  ISMLKQQVEN  LLEGINSPSP
121 CVISDMGFPW  TTQIAQNFNI  PRIVFHGTCC  FSL LCSYKIL  SSNILENITS  DSEYFVVPDL
181 PDRVELTKAQ  VSGSTKNNTS  VSSSVLKEVT  EQIRLAEESS  YGVIVNSFEE  LEQVYEKEYR
241 KARGKKVWCV  GPVSLCNKEI  EDLVTRGNKT  AIDNQDCLKW  LDNFETESVV  YASLGSL SRL
301 TLLQMVELGL  GLEESNRPFV  WVLGGGDKLN  DLEKWILENG  FEQRIKERV  LIRGWAPQVL
361 ILSHPAIGGV LTHCGWNSTL EGISAGLPMV TWPLFAEQFC NEKLVVQVLK  IGVSLGVKVP
421 VKWGDEENVG  VLVKKDDVKK  ALDKLMDEGE  EGQVRRTKAK  ELGELAKKAF  GEGGSSYVNL
481 TSLIEDIEEQ  QNHKEK
```

Figure 7: Amino Acid Sequence of NtGT4. The PSPG Motif is shown in bold, amino acid residues numbers 355–398.

type (fold) glycosyltransferase with 496 amino acid residues in its primary chain (NCBI). It is encoded by the *NtGT4* gene with a protein coding region that is 1491 base pairs long (NCBI).

SBIP68 has the 44 amino acid C-terminal signature motif characteristic of family 1 of plant GT's (UGT's), the plant secondary product glycosyltransferase (PSPG) box (Fig. 7; amino acid residues numbers 355 - 398), which is thought to be responsible for binding the glucose donor substrate, UDP-glucose (Hughes and Hughes 1994). Results from the Y2H screening showing that SBIP68 interacts with SABP2, which has high affinity for SA (Kumar and Klessig, 2003), and bioinformatics analyses predicting SBIP68 to be a UGT, both indicate that SBIP68 might be involved in the glucosylation of SA during stress responses in plants (Fig. 8).

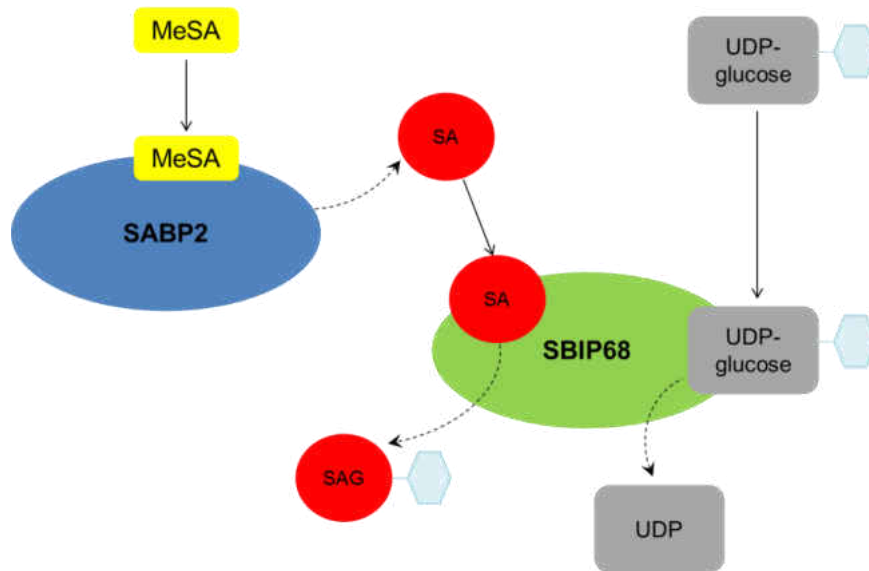


Figure 8: Possible Role of SBIP68 in Plants. SBIP68 might be involved in the glucosylation of SA during stress responses.

UGTs, SA, and the Significance of Glucosylation

Based on bioinformatics analyses, SBIP68 shows similarity (24% - 52% identity) with many UDP-glycosyltransferases in Arabidopsis. UGT group D family includes 13 members in Arabidopsis and it also contains genes identified in other plant species, including tobacco, to be involved in plant stress responses (Langlois-Meurinne et al., 2005). However, different patterns of expression in response to pathogens and defense signal molecules such as SA, MeJA and H₂O₂ have been observed (Langlois-Meurinne et al., 2005). None of them are induced by MeJA even though *UGT73B* genes (B1-B5) expression are induced upon wounding (Langlois-Meurinne et al., 2005). Only three of them, *UGT73B3*, *UGT73B5*, and *UGT73C1* have been found to respond to H₂O₂ (Langlois-Meurinne et al., 2005). Most of them respond to SA treatment (Langlois-Meurinne et al., 2005). *UGT73C6*, a UDP-glucose: flavonol glucosyltransferase

belonging to the Arabidopsis UGT group D, has been found to glucosylate the 7-OH position of kaempferol-3-O-rhamnoside and quercetin-3-O-rhamnoside, respectively (Jones et al., 2003). Presently, it is the only Arabidopsis UGT group D enzyme for which the endogenous substrates are known (Langlois-Meurinne et al., 2005).

Salicylic acid has been found to be glycosylated at both the hydroxyl and the carboxyl groups (Song, 2006). In TMV or *Pseudomonas syringae* pv. *phaseolicola* - inoculated tobacco (*Nicotiana tabacum* cv. Xanthi-nc NN genotype) leaves, newly synthesized SA is converted primarily to SA 2-O- β -D-glucoside (SAG) by glucosylation at the hydroxyl group, and to glucosyl salicylate (GS), a relatively minor metabolite, by glucosylating the carboxyl group, implying this to be a general process in tobacco plants (Lee and Raskin, 1998). GS is rapidly produced while levels of SAG increases gradually over a longer period of time making it a more stable metabolite of SA (Lee and Raskin, 1998). Biosynthesis of GS and SAG are catalyzed by UDPG/SA carboxyl glucosyltransferase (SACGT) and UDPG/SA 2-O-glucosyltransferase (SAGT), respectively (Lee and Raskin, 1998).

Unlike methyl salicylate, the glucosylated conjugates of SA accumulate only in and around inoculated (or infected) parts of the plants where hypersensitive necrotic lesions are formed, as there are no detectable levels of glucosylated SA in phloem sap or uninoculated areas of TMV-inoculated plants (Enyedi et al., 1992 ; Malamy et al., 1992). This suggests that glucosylation is not necessary for long distance signaling during systemic acquired resistance (SAR) (Lee and Raskin, 1998). Just as inoculation of tobacco leaves with TMV causes the activity of β -GTase to increase significantly as a result of increased SA biosynthesis, exogenous application of SA produces similar

results, showing that tobacco does not differentiate between endogenously produced SA and exogenously supplied SA with regards to compartmentalization and biological activity (Enyedi and Raskin, 1993).

Like most other enzymes, glucosyltransferases show substrate specificity. Most plant glucosyltransferases are specific for UDP-glucose and a given phenolic compound (Bechthold et al., 1991; Sun and Hrazdina, 1991; Fukuchi-Mizutani et al., 2003). An exception to this is UDP-glucose:cinnamic acid glucosyltransferase present in sweet potato that is involved in the conjugation of a range of phenolic compounds (Shimizu and Kojima, 1984). Tobacco UDP-glucose: salicylic acid 3-O-glucosyltransferase (β -GTase) has been found to be specific for the UDP-glucose as sugar donor and SA as glucose acceptor (Enyedi and Raskin, 1993).

Because tobacco leaves rapidly metabolize SA to β -O-D-glucosylsalicylic acid (GSA), most of the SA in TMV-inoculated leaves of tobacco is present in the form of GSA (Enyedi et al., 1992; Malamy et al., 1992). Induction of β -GTase activity by SA has been found to be inhibited by RNA synthesis inhibitors applied to cell-suspension cultures of *M. japonicus* (Tanaka et al., 1990) and roots of oat plants (Yalpani et al., 1992) indicating that SA triggers the *de novo* synthesis of β -GTase (Enyedi and Raskin, 1993). However, high concentrations of SA may inhibit plant growth (Pareek and Gaur, 1973; Chou and Patrick, 1976) by SA-induced disruption of membrane and inhibition of ion absorption (Glass, 1973; Harper and Balke, 1981; Macri et al., 1986). Conversion of SA to GSA may be required for sequestering excessive SA in the vacuole (Ben-Tal and Cleland, 1982), hence protecting plant tissues from excessive damage by SA. This makes sense as SA is required in a certain amount for increased activity of β -GTase

and a subsequent increase in GSA. GSA may also serve to store metabolized SA during plant defense (Enyedi and Raskin, 1993).

In strawberry plants, the expression of FaGT6 and FaGT7 glucosyltransferases were found to be induced by certain plant defense signals suggesting their involvement in stress responses (Griesser et al., 2008). Both glucosyltransferases were found to glucosylate a number of exogenous substrates which do not occur in strawberry fruits *in vitro*, suggesting they may have a role in detoxification (Griesser et al., 2008).

In *Picrorhiza*, MeJA treatment resulted in the upregulated expression of UGTs UGT86C4 and UGT94F2. UGT86C4 expression was observed to increase 8-fold 12 hours post-application of MeJA and the expression of UGT94F2 increased 15-fold 24 hours post MeJA application (Bhat et al., 2013). Upon application of SA, UGT94F2 displayed maximum increase by 10-fold, 12 hours after induction while a 16-fold increase in expression levels occurred with UGT86C4, 6 hours after induction (Bhat et al., 2013). The rapid increase in the transcript levels of these UGT genes post application of MeJA or SA is indicative of a possible role for these UGTs in plant defense responses (Bhat et al., 2013).

Glycosylation is just one of the many mechanisms involved in the maintenance of cellular homeostasis in plants. Glycosides are known to perform a number of functions in plants including but not limited to serving as high-energy donors and signaling molecules. They are involved in the biosynthesis of plant cell walls (Ostrowski and Jakubowska, 2014). UGT's catalyze the conjugation of plant hormones, a regulatory mechanism that may serve to check the concentration of physiologically active plant hormones during growth and development (Ostrowski and Jakubowska,

2014). Mutations leading to loss of function in UGT genes are known to have adverse effects on the phenotype of the plants involved (Ostrowski and Jakubowska, 2014).

The significant role of SA in plants responding to stress suggests that it makes use of an important signaling molecule whose concentration must be strictly controlled (Ostrowski and Jakubowska, 2014). Even though the biological importance of SA conjugates is still not fully understood, it is assumed that some of them serve to increase the polarity of SA, thereby enabling its accumulation in plant vacuoles and protection from degradation (Ostrowski and Jakubowska, 2014). Based on these, SA glucosides may serve to transport and store SA (Ostrowski and Jakubowska 2014). Further studies on the role of UGT's in plants will enable us to come up with ways to better control plant diseases and improve crop yield, by enhancing the resistance of plants to pathogens and diseased conditions and consequently improve the life of animals and humans alike.

This research aims at cloning the full length SBIP68, expression and purification using a heterologous system (*E. coli* and/or yeast) and functionally characterizing by testing a number of potential substrates (including but not limited to salicylic acid) with the recombinant purified protein *in vitro*. Attempts will be made to understand the effect of interaction of SBIP68 with SABP2, effect of SA on SBIP68, and its possible role (if any) in the plants defense signaling mechanism.

Hypothesis

Hypothesis: SBIP68 is a UDP-glucosyltransferase which glucosylates salicylic acid.

Yeast two hybrid screening revealed that SBIP68 interacts with SABP2 which has high affinity for SA (Kumar and Klessig, 2003), and bioinformatics analyses predicted SBIP68 to be a UGT. Based on these, it was hypothesized that SBIP68 is a UDP-glucosyltransferase which glucosylates salicylic acid. It is also possible that SBIP68 does not glucosylate SA, instead it glucosylates other molecules with important roles in SA-mediated defense signaling in tobacco plants and its interaction with SABP2 modulates its activity or vice-versa.

CHAPTER 2

MATERIALS AND METHODS

Plant Materials

Nicotiana tabacum cv. Xanthi-nc NN (XNN) plants were utilized for the purpose of this experiment. Soil containing peat moss (Fafard Canadian growing mix F-15, Agawam, MA) was used to cultivate the plants. The soil was autoclaved for 20 minutes and allowed to cool to room temperature, after which an average of 20 seeds were sown in a 4 x 4 inch plastic container. The container with the seeds was placed in a controlled environment, a growth chamber (PGW 36, Conviron, Canada) set at 16-h day cycle and 22 °C, the plants would be maintained under these conditions through the course of the experiment. After 14 days, seedlings were transferred to 4 x 4 inch pots (2 per pot), and maintained in these for 3 weeks. Young plants were then transferred one per 8" pot. Fertilizer (nitrogen, phosphorus, and potassium; 21:5:20) was diluted and applied to the plants 3 days after transferring to 8" pots. The plants were grown until they were 6 to 8 weeks old before using them for the experiments.

Chemicals and Reagents

Agar (Acros organics), agarose (SeaKem), ammonium persulfate (APS), ammonium sulfate ($(\text{NH}_4)_2\text{SO}_4$), benzamidine-HCl, β -mercaptoethanol (β -ME), bovine serum albumin (BSA), chloroform, coomassie brilliant blue G-250, coomassie brilliant blue R-250, ethylenediaminetetraacetic acid (EDTA), glycerol, glycine, imidazole, isopropanol, magnesium chloride (MgCl_2), methanol, phenylmethanesulfonyl fluoride (PMSF), ponceau-S, sodium chloride (NaCl), potassium phosphate dibasic (K_2HPO_4), potassium phosphate monobasic (KH_2PO_4), sodium dodecyl sulfate (SDS),

tetramethylethylenediamine (TEMED), TRIS base, tween-20, ethidium bromide, phenol, isoamyl alcohol, 100% ethanol, glacial acetic acid, yeast extract, yeast nitrogen base powder, and all other standard chemicals were purchased from Fisher Scientific (Pittsburgh, PA). Liquid nitrogen (Airgas, TN), proteose peptone 3 (Becton and Dickenson), dithiothreitol (DTT), diethylpyrocarbonate (DEPC), TRI reagent, mouse monoclonal anti poly-histidine antibody, HRP conjugated goat anti-mouse IgG, mouse anti c-myc monoclonal antibody, lyticase enzyme from *Arthobacter luteus*, and acid washed glass beads (0.5mm), were purchased from Sigma-Aldrich. Acrylamide solution (30%), pre-stained low molecular weight marker, SDS sample buffer, and Gene Pulser cuvettes (0.2 cm) were purchased from Bio-Rad, Hercules, CA. Pierce ECL Western blotting substrate was purchased from Thermo Scientific, Rockford, IL. WesternSure PREMIUM Chemiluminescent Substrate was purchased from LI-COR, Lincoln, NE. Polyvinylidene fluoride (PVDF) membranes were purchased from Millipore, Billerica, MA. Oligo dT-20, and Taq DNA polymerase were purchased from Invitrogen, CA. RNase free DNase, recombinant RNAsin, and MMLV reverse transcriptase were purchased from Promega. dNTP, 100 bp and 1 kb DNA ladders, and restriction enzymes (New England Biolabs), and gel loading dye (Bio-Rad). Zeocin™ was purchased from Research Products International Corps (Illinois). QIAprep Spin Miniprep Kit, QIAGEN Plasmid Midi Kit, and QIAquick Gel Extraction Kit were purchased from Qiagen (Valencia, CA). Advantage HF 2 PCR Kit was purchased from Clontech.

Cells and Vectors

pGEM®-T easy vector was purchased Promega, pET-28a vector from Novagen, and pPICZA vector from Invitrogen (Carlsbad, CA). X-33 strain of *Pichia pastoris* was a gift from Dr. Cecilia McIntosh, East Tennessee State University (Johnson City, TN).

Oligonucleotides

All the primers used in this study were custom synthesized by Eurofins MWG Operon (Huntsville, AL). The lyophilized oligonucleotides were re-suspended in nuclease-free water and diluted to give a final concentration of 10 µM. Table 1 lists all the primers and their respective uses.

Table 1: Primers Used in This Study

Primers	Sequence (5' – 3')	T _m	Purpose
DK639 forward	GCCTCGAGGTCATGGCAACTCAAGTGAC AACTTCATTTTCATACTATTC	72.9	Cloning in <i>P. pastoris</i>
DK640 reverse	GAGGGCCCTTTTTCCTTGTGATTTTGTTC TCAATGATGTCTTCAATCAG	72.1	Cloning in <i>P. pastoris</i>
DK641 forward	GACTGGTTCCAATTGACAAGC	60.6	Sequencing in <i>P. pastoris</i>
DK642 reverse	GCAAATGGCATTCTGACATCC	60.6	Sequencing in <i>P. pastoris</i>
DK643 forward	GGATCCATGGCAACTCAAGTGACAAACT TCATTTTCATACTATTC	70.2	Cloning in <i>E. coli</i>
DK644 reverse	CTCGAGCTATTTTTCCTTGTGATTTTGTTC CTCAATGATGTCTTC	69.3	Cloning in <i>E. coli</i>
DK645 reverse	CTCGAGTTTTTTCCTTGTGATTTTGTTC CTCAATGATGTCTTCAAT	68.4	Cloning in <i>E. coli</i>
DK551 forward	GTAAAACGACGGCCAG	56.7	Sequencing
DK552 reverse	CAGGAAACAGCTATGAC	54.8	Sequencing

Apparatus

Mastercycler (Eppendorf, NY), ND-1000 nanodrop spectrophotometer (Thermo scientific), agarose gel electrophoresis apparatus (Fisher Biotech) and SDS-PAGE apparatus (BIO-RAD), Gene Pulser (BIO-RAD), Western blot apparatus (BIO-RAD), gel doc (UVP) system, pH meter (Beckman), high speed centrifuge (Sorvall RT6000 refrigerated centrifuge, DuPont, Waltham, MA), UV transilluminator (UVP Bioimaging Systems), LI-COR C-DIGIT Western blot imager (LI-COR). Spectrophotometer, French press (Thermo Scientific), centrifuge (Beckman, model J2-21 or Sorvall RC5B), sonicator, AKTA purifier 10 (GE) system, Beckman LS 6500 scintillation counter (McIntosh lab, ETSU), Waters Breeze HPLC system (McIntosh lab, ETSU).

Methods

Cloning and Expression of SBIP68 in *E. coli*

To clone and express SBIP68 in *E. coli*, gene specific primers (DK 643, DK644 and DK645) were synthesized and used. All primers were designed with a restriction enzyme site to enable cloning into an *E. coli* expression plasmid. The forward primer DK643, had a BamHI restriction endonuclease site. Both the reverse primers, DK644 and DK645 had Xho I restriction endonuclease sites. The plasmid pET-28a (Figure 9) used for cloning and expression of SBIP68 in *E. coli* has both an N- and C- terminal 6x polyhistidine tag coding sequence to help ease purification of recombinant proteins. The reverse primer DK644 was designed to have the original stop codon present in the SBIP68 gene, in which case the expressed protein was expected to be fused to the N-terminal 6x polyhistidine tag of the pET-28a vector. Reverse primer DK645 on the other

hand did not have the stop codon of the SBIP68 gene in it, the expressed protein in this case was to be fused to either the C-terminal 6x polyhistidine tag or both the N and C - terminal 6x polyhistidine tags of the pET-28a vector.

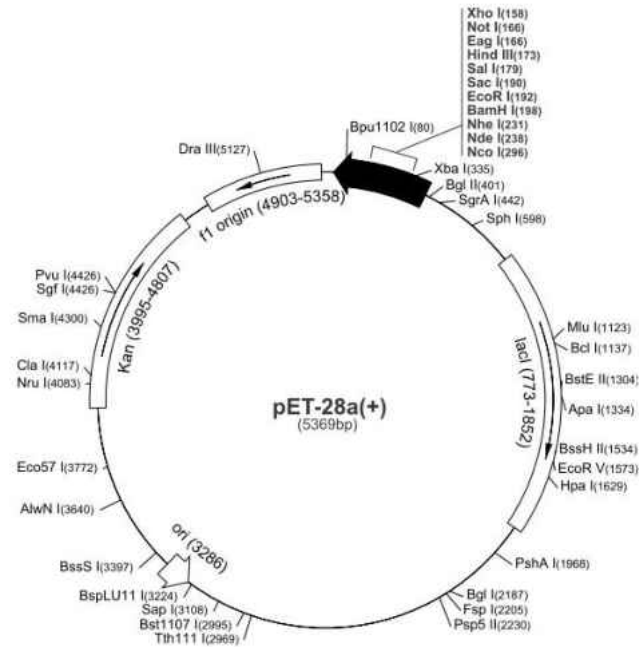


Figure 9: Map of *E. coli* Expression Plasmid pET-28a (Novagen). Bam HI and Xho I restriction sites of the multiple cloning area were used to clone SBIP68 in *E. coli*.

Total RNA Extraction

To minimize degradation during total RNA isolation, all material used were either disposable or sterilized by autoclaving. Fresh DEPC treated water (Appendix B) was autoclaved and was used. Leaf discs were obtained from wild type tobacco XNN plants with the aid of a cork borer. The discs were transferred into eppendorf tubes, and snap frozen by dropping into liquid nitrogen. The frozen tissues were homogenized to fine

powder using a mechanical grinder and liquid nitrogen. To the finely ground leaf powder (~50-100 mg), 1 ml TRI reagent was added and vortexed. The sample mixture was incubated for 5 mins at room temperature. Two hundred microliters of chloroform was added to the sample mixture, mixed gently by inverting the tubes several times, and incubated at room temperature for 3 minutes. Following incubation, the sample was centrifuged at 12,000 x g for 10 minutes at 4 °C. The supernatant resulting from the centrifugation step was transferred to a fresh eppendorf tube. To the supernatant, 500 µl isopropanol was added, mixed and followed by a 10 minute incubation period at 28 °C. The sample was centrifuged at 12,000 x g for 10 minutes at 4 °C and the supernatant was discarded, while making sure the pellets remained in the tube. The pellet was resuspended in 1 ml of 75 % cold ethanol (prepared with DEPC treated water) and centrifuged at 7500 x g for 5 minutes at 4 °C. The supernatant was discarded and the pellet was air dried for 5-10 minutes. The pellet was resuspended in 43 µl DEPC-treated (ribonuclease free) water and incubated at 37 °C for 5 minutes. Five microliters DNase buffer and 2 µl DNase (RNase free) were added to the sample, mixed, and incubated at 37 °C for 20 minutes. To the sample, 0.5 ml of TRI reagent was added and vortexed, followed by a 5 minute incubation at room temperature. One hundred microliters of chloroform was added to the sample, mixed very gently and incubated at room temperature for 3 minutes. The sample was centrifuged at 12,000 x g for 10 minutes at 4 °C and the resulting supernatant was transferred to a fresh tube. To this, 250 µl isopropanol was added followed by a 10 minute incubation period at 28 °C. The sample was centrifuged at 12,000 x g for 10 minutes at 4 °C. The supernatant was carefully decanted. To the pellet, 0.5 ml of 75 % cold ethanol was added. The sample

was centrifuged at 7500 x g for 5 minutes at 4 °C. The supernatant was discarded, the pellet air dried for 10 minutes and resuspended in 20 µl DEPC-treated water. The sample was incubated at 55 °C for 10 minutes after which RNA concentration was determined using a nanodrop spectrophotometer at 260 nm. The purity of the sample was also determined from the value of OD₂₆₀:OD₂₈₀ (>1.8 shows low protein contamination).

cDNA Synthesis

In synthesizing first strand cDNA, 1 µl (0.5 µg/µl) of oligo-dT was added to 9 µl (1 µg) of total RNA. The sample was mixed and incubated at 75 °C for 10 minutes in a thermocycler and then cooled to 4 °C for annealing to occur. In a separate tube, 10 µl of RT (reverse transcriptase) reaction mix was made. The RT reaction mix constituted 3 µl of DEPC-treated water, 4 µl of 5 x RT buffer, 1 µl of 10 mM dNTP, 1 µl RNasin (RNase inhibitor), and 1 µl MMLV reverse transcriptase (RT) enzyme. Ten microliters of the RT mix was added to 10 µl of the RNA/oligo-dT mix. This new 20 µl sample was briefly vortexed and incubated in a thermocycler at 42 °C for 60 minutes and at 70 °C for 10 minutes for reverse transcription and inactivation of the RT enzyme to occur, respectively. One microliter of the newly synthesized cDNA was used to carry out a polymerase chain reaction (PCR) of the tobacco housekeeping gene *EF1α* to check the integrity of cDNA. The 10 µl PCR reaction mix composed of 1 µl cDNA, 1 µl of 10 x *Taq* polymerase buffer, 1 µl of 10 x dNTP mix, 0.2 µl of 10 µM forward primer, 0.2 µl of 10 µM reverse primer, 0.2 µl of *Taq* DNA polymerase, 6.4 µl of H₂O. The PCR conditions were as follows: hot start and initial denaturation at 94 °C for 2 minutes, 30 cycles of denaturation, annealing, and elongation at 94 °C, 55 °C, and 72 °C, for 30 seconds, 30

seconds, and 45 seconds respectively, and a final extension step at 72 °C for 5 minutes. The rest of the cDNA was preserved at - 20 °C for future use.

Polymerase Chain Reaction (PCR)

The *SBIP68* gene was PCR amplified using cDNA prepared from tobacco leaves and Advantage HF 2 PCR Kit (Clontech) following manufacturer's instructions.

Advantage HF 2 polymerase contains a mixture of *Taq* DNA polymerase and a proofreading enzyme. Each PCR reaction mix composed 3 µl cDNA, 5 µl of 10 x HF2 PCR Buffer, 1 µl of 50 x HF dNTP mix, 1 µl of 10 µM forward primer, 1 µl of 10 µM reverse primer, 1 µl of 50 x Advantage HF polymerase mix, 40 µl of H₂O. The PCR conditions were as follows: hot start and initial denaturation at 94 °C for 4 minutes, 30 cycles of denaturation, annealing, and elongation at 94 °C, 55 °C, and 72 °C, for 30 seconds, 30 seconds, and 90 seconds respectively, and a final extension step at 72 °C for 10 minutes. DK643 forward primer, and DK644 reverse primer (with the *SBIP68* stop codon) were used to facilitate cloning into *E.coli* with a 6xHis fusion tag at the 5' end of the gene. DK643 forward primer, and DK645 reverse primer (without the *SBIP68* stop codon) were used to facilitate cloning into *E.coli* with a 6xHis tag codon at both the 5' and 3' ends of the gene.

Agarose Gel Electrophoresis

Agarose gel electrophoresis was used to separate nucleic acids based on size differences. The PCR products were analyzed by gel electrophoresis using 1.2 % agarose gel containing ethidium bromide. Ten microliters of 6 x DNA loading dye was mixed with 50 µl of PCR product. Eight microliters (25 ng/µl) of a 1 kb DNA ladder was

loaded into the first well, and the samples were loaded into the other wells. The gel was run at 80 volts for ~ 90 minutes and visualized on a UV transilluminator.

Purification of PCR Product

SBIP68 DNA bands were cut out and purified using Qiagen Gel Extraction kit following the manufacturer's instructions. The purified DNA was quantified using a Nanodrop spectrophotometer at 260 nm and subsequently analyzed on a 1.2 % agarose gel as previously described.

Construction of pGEMT-SBIP68 Clone

Taq DNA polymerase adds a single deoxyadenosine nucleotide base to the 3'-ends of PCR amplified fragments, in a template-independent fashion (Zhou and Gomez-Sanchez, 2000). Cloning into pGEMT easy vector (Promega) is made possible due to these deoxyadenosine bases added to the PCR amplicons. The vector, pGEMT, is provided as a linear plasmid with single terminal thymidine bases added to both 3' ends (Fig. 10). The single 3'-T overhangs present at the insertion site of the vector greatly improve the efficiency of ligation of PCR amplicons having 3'-deoxyadenosine bases into the plasmids by preventing recircularization of the vector and providing a compatible overhang for these PCR products (Zhou and Gomez-Sanchez, 2000; Promega). The plasmid, pGEMT allows for blue/white screening on indicator plates and carries an ampicillin resistant gene (Promega).

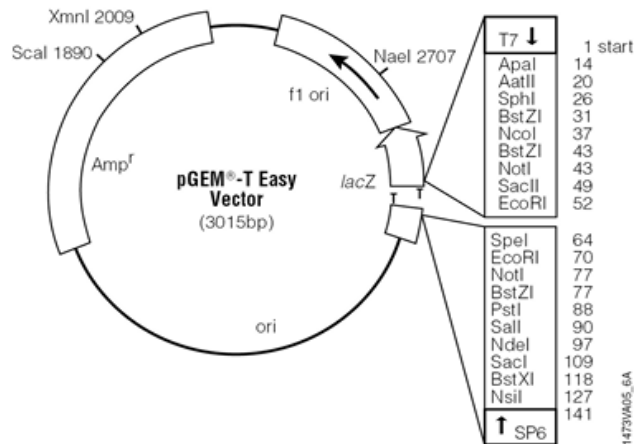


Figure 10: Map of pGEM-T Easy Vector (Promega)

A 10 μ l ligation reaction was set up as follows: 5 μ l 2 x rapid ligation buffer, 1 μ l pGEMT easy vector, 2 μ l purified PCR product, 1 μ l T4 DNA ligase, and 1 μ l H₂O. The 2 x rapid ligation buffer was vortexed vigorously before use. A control reaction which had all the constituents of the standard reaction without the PCR products was also set up. Ligation reactions were incubated overnight at 4 °C for maximum number of transformants.

Preparation of Fresh Competent DH5 α Cells

E. coli DH5 α cells from a glycerol stock stored at -80 °C freezer were streaked on an LB plate and incubated overnight at 37 °C. The following day, single isolated colonies from the plate were used to inoculate 3 ml of LB-broth and grown at 37 °C and 250 rpm until the cultures had an OD₆₀₀ of ~ 0.45. The cultures were transferred to pre-chilled tubes (on ice) for 15 minutes. They were then centrifuged at 3000 x g for 10 minutes at 4 °C. The pellet was gently resuspended in 0.6 ml of ice cold sterile 0.1 M

CaCl₂ and incubated on ice for 30 minutes. The bacterial suspensions were centrifuged at 3000 x g for 10 minutes at 4 °C, the supernatants were discarded, and the pellet resuspended in 120 µl of ice cold 0.1 M CaCl₂. The resuspended cells (50 µl) were used for transformation.

Transformation of *E. coli* DH5α with pGEMT-SBIP68 Plasmid DNA

The ligation reactions were vortexed briefly and 2 µl of each ligation reaction was added to 50 µl of freshly prepared competent cells in a 1.5 ml tube. The tubes were gently flicked and incubated on ice for 20 minutes. After 20 minutes, the cells were heat-shocked for 50 seconds in a water bath at 42 °C and immediately returned to ice for 2 minutes. Following incubation, 950 µl LB medium was added to each tube containing transformation mix. The samples were incubated for 90 minutes at 37 °C with shaking at 150 rpm. The transformation mix was centrifuged at 5,000 x g for 1 min and pellet was resuspended in 200 µl LB medium (Appendix B). The resuspended transformation mix was spread on LB/ampicillin/IPTG/X-Gal plates (Appendix B) using sterile glass beads and incubated overnight at 37 °C. The following morning, white colonies were selected for further analysis for the presence of insert using colony PCR.

Verification of pGEMT-SBIP68 Plasmid by Colony PCR

A colony PCR was performed to screen for positive clones containing SBIP68. Single isolated white bacterial colonies were picked using sterile tips from the plates and streaked on a fresh LB/ampicillin plate. Each colony was assigned a number for future reference. Following streaking, each tip was put in a 0.2 ml PCR tube containing 40 µl of sterile water and pipetted up and down a few times to suspend the remaining

bacteria. Ten microliters bacterial suspension from each colony was used as template in the PCR reaction. Each PCR reaction mix was composed of 10 µl bacterial suspension, 2 µl of 10 x PCR Buffer, 2 µl of 0.1 M dNTP mix, 0.8 µl of M13 forward primer, 0.8 µl of M13 reverse primer, 0.5 µl *Taq* DNA polymerase, and 3.9 µl sterile H₂O. The PCR conditions were as follows: 94 °C for 4 minutes, 30 cycles of denaturation, annealing, and elongation at 94 °C, 55 °C, and 72 °C, for 30 seconds, 30 seconds, and 90 seconds respectively. The PCR products were analyzed by agarose gel electrophoresis as described earlier.

Plasmid DNA Isolation from pGEMT-SBIP68 Clones

Positive clones following confirmation by colony PCR, were selected for plasmid purification. Corresponding colonies from master plate were used to inoculate 3 ml LB broth containing ampicillin (100 µg/ml). The bacterial cultures were grown at 37 °C and 250 rpm overnight. Plasmid DNA's were isolated from the overnight cultures using the QIAprep Spin Miniprep kit according to the manufacturer's instructions. The concentration and purity of the isolated plasmids were determined using a nanodrop spectrophotometer at 260 nm. The quality of the plasmid DNA was also checked using a 0.8 % agarose gel as described earlier.

Sequencing of pGEMT-SBIP68 Recombinant Plasmid

The purified plasmid DNA (0.5 – 1.0 µg each), were sent to the DNA Analysis Facility at Yale University to be sequenced. The Sanger DNA Sequencing method was employed in sequencing the pGEMT-SBIP68 constructs. The plasmids were sequenced using M13 forward and M13 reverse primers. Analysis of the sequencing results helped

in identifying clones with the highest similarities to the database gene sequence (*NtGT4*). Of the 1,488 nucleotides in the protein coding sequence, there was only one nucleotide difference, at position 552. This was a pyrimidine to pyrimidine (T to C) base change and upon translation did not result in an amino acid change in the primary sequence of the protein.

Cloning of SBIP68 into *E. coli* Expression Plasmid pET-28a

The positive pGEMT-SBIP68 clone following DNA sequence analysis was selected for further cloning into pET-28a. To excise out SBIP68 from pGEMT, the pGEMT+SBIP68 plasmid was restriction digested with BamHI and Xho I restriction enzymes. Similarly, the destination plasmid pET-28a was also restriction digested with BamHI and Xho I. The reaction mixture for the pGEMT-SBIP68 plasmids included: 10 µl pGEMT-SBIP68 plasmid-DNA, 2 µl NEB buffer #3, 2 µl BSA (10mg/ml), 4 µl sterile H₂O, 1 µl BamHI, and 1 µl Xho I. The digestion reaction for the pET-28a vector included: 5 µl pET-28a vector, 2 µl NEB buffer 3, 2 µl BSA (10mg/ml), 9 µl sterile H₂O, 1 µl BamHI, and 1 µl Xho I. The reactions were incubated at 37 °C for 3 hours. The restriction digested plasmid DNA were separated by running on a 0.8 % agarose gel. The DNA band corresponding to SBIP68 was excised out and purified using QIAquick Gel Extraction Kit according to the manufacturer's instructions. Similarly the BamHI and Xho I restriction digested pET-28a was also gel purified. Concentration and purity for SBIP68 and pET-28a were determined using a nanodrop spectrophotometer at 280 nm.

After gel purification, SBIP68 was ligated into pET-28a using T4 DNA ligase following manufacturer's instructions. Each reaction mixture consisted of 3 µl SBIP68-

644 (24.1 ng μ l⁻¹) or SBIP68-645 (28.6 ng μ l⁻¹) DNA, 2 μ l pET-28a vector (14.5 ng μ l⁻¹), 1 μ l 10 x ligase buffer, 1 μ l T4 DNA ligase, and 3 μ l H₂O. The reaction mixtures were incubated at 16 °C overnight for ligation.

Transformation of *E. coli* BL21(DE3) pLysE with pET-28a-SBIP68 Plasmid

The ligated products from pET-28a-SBIP68 were used to transform *E. coli* BL21 (DE3) pLysE competent bacterial cells. The competent cells were prepared (as described earlier) and stored at – 80 °C. Frozen competent cells were thawed by placing them on ice for ~ 5 minutes. Two microliters of ligation products were added to 1.5 ml eppendorf tubes containing 50 μ l competent cells. The contents of the tubes were mixed gently and incubated on ice for 20 minutes. Cells were heat-shocked for 45 seconds using a water bath at 42 °C and the tubes were immediately returned to ice for 2 minutes. To the transformation mixture, 950 μ l of LB broth was added and incubated at 37 °C for 1 hour at ~ 150 rpm. Transformed bacterial cells were plated on LB/Kanamycin (50 μ g/ml) plates using sterilized glass beads as described earlier. Plates were incubated at 37 °C overnight.

Test for Recombinant pET-28a-SBIP68 Protein Expression

Colony PCR using pET-28a specific primers was performed as described earlier to test for clones containing the plasmid of interest. Positive clones were used to inoculate 3 ml LB broth containing kanamycin (50 μ g/ml). Cell cultures were incubated at 37 °C with shaking at 250 rpm for 2 hours. One milliliter of each culture was transferred into a 1.5 ml microcentrifuge tube and centrifuged at maximum speed for 3 minutes. The supernatants were discarded and the pellets (uninduced controls) stored

at - 20 °C. To the remaining 2 ml cultures, 4 µl of 0.5 M isopropyl-beta-D-thiogalactopyranoside (IPTG) was added to a final concentration of 1mM for the induction of recombinant protein expression. Induction was carried out at 37 °C and 250 rpm for 3 hours. After 3 hours, the bacterial cultures were centrifuged at 5000 x g for 3 minutes, the supernatants were discarded and the pellets stored at – 20 °C. The pellets from both induced and uninduced samples were heated. They were analyzed by SDS-polyacrylamide gel electrophoresis.

Sodium Dodecyl Sulfate Polyacrylamide Gel Electrophoresis (SDS-PAGE)

SDS-PAGE was performed by mixing each protein sample with an equivalent amount of 2 x SDS sample buffer containing 5 % βME added just before use. The mixtures were placed in a boiling water bath for 5 minutes and centrifuged at 16,200 x g for 10 minutes at room temperature. The samples were loaded on an SDS gel and run using electrophoresis at 200 volts until the dye reached the bottom of the gel ~ 50 minutes. The gel was stained using coomassie blue stain for 20 minutes and subsequently destained with a destaining solution (Appendix B) to remove the background dye as much as possible to make separated proteins visible.

Western Blot Analysis

Upon the separation of protein samples using SDS-PAGE, the proteins were transferred from the gel to a membrane by electroblotting. The membrane used throughout this study was PVDF (polyvinylidene difluoride) membrane. Prior to electroblotting, the PVDF membrane was incubated in 100% methanol for 15 seconds after which it was rinsed with water for 2 minutes. The membrane was placed in 1x

Western blot transfer buffer (Appendix B) and allowed to shake gently on a platform shaker for 10 minutes. The foam pads and 3 mm Whatman papers were presoaked in the 1x Western blot transfer buffer to be used for electroblotting. The gel and PVDF membrane were sandwiched in between the Whatman papers which were sandwiched between the foam pads. A roller was used to remove any air bubbles trapped in the sandwich. The sandwich was placed in the gel cassette holder such that the gel was on the black colored (negative) side of the gel cassette holder and the membrane was on the clear side (positive) of the gel cassette holder. A small magnetic stir bar was placed in the electrophoresis tank which was to be placed on a magnetic stirrer. A cold ice pack was also placed in the electrophoresis tank. The cassette holding the gel and membrane was placed in the electrophoresis tank such that the black colored side of the cassette and the electrophoresis unit were in contact and the clear side of the cassette was towards the red side of the electrophoresis unit.

Electroblotting was carried out at ~ 96 volts for 1 hour at 4 °C. After 1 hour, the PVDF was taken out of the cassette, rinsed with methanol for 15 seconds, and allowed to air dry for about 1 minute. The membrane was again rinsed with 100% methanol for 15 seconds and then placed in ponceau S stain (Appendix B) for 2 minutes to verify protein transfer. The membrane was rinsed with deionized water and visualized for protein transfer. Ponceau S stain was washed off with 1x PBS (phosphate buffered saline, Appendix B). Once the membrane was clear of the ponceau S stain, the PBS was discarded and blocking buffer (1 % non-fat dry milk, 3 % BSA in 1 x PBS, Appendix B) containing mouse monoclonal anti-polyhistidine primary antibody (1:2,500) was added to the membrane. The membrane with primary antibody was incubated on a

rocking platform overnight at 4 °C. The next morning, the membrane was sequentially washed twice with 1 x PBS, twice with 1 x PBS containing 3 % tween 20, and twice with 1 x PBS for a duration of 5 minutes per wash step. The membrane was then incubated with anti-mouse IgG conjugated with horseradish peroxidase in blocking buffer (1:5,000) at room temperature for 2 hours on a rocking platform. The membrane was washed as described above. After washing, the membrane was incubated in 2 ml of WesternSure PREMIUM Chemiluminescent Substrate for 5 minutes at room temperature making sure the entire surface area of the membrane was covered by the substrate. The membrane was removed from the substrate and the excess substrate left on the membrane was allowed to drip off. The membrane was placed protein side down in a C-Digit Blot Scanner and a plastic wrap was placed on top of the membrane. The blot was scanned for 12 minutes for maximum sensitivity and several pictures were captured. Following scanning, the blot was stained with coomassie blue.

Recombinant pET-28a-SBIP68 Protein Solubility Test

To check if recombinant pET-28a-SBIP68 protein was present in soluble or insoluble form, a solubility test was carried out. Positive bacterial colonies were used to inoculate 3 ml of LB with kanamycin (50µg/ml). Cell cultures were incubated at 37 °C with shaking at ~ 250 rpm for 2 hours. After 2 hours, 1 ml of each culture was centrifuged and the pellets preserved at –20 °C to serve as uninduced controls. To the remaining 2 ml cultures, 4 µl of 0.5 M isopropyl-beta-D-thiogalactopyranoside (IPTG) was added to give a final concentration of 1 mM for the induction of protein expression. Induction was carried out at 37 °C and 250 rpm for 3 hours. After 3 hours, the bacterial cultures were centrifuged at maximum speed (18,800 x g) for 3 minutes, the

supernatants were discarded and the pellets preserved at – 20 °C. The following day, pellets from both induced and uninduced 1 ml samples were resuspended in 100 µl of Ni-NTA binding buffer each. The samples were sonicated while placed on ice at an amplitude of 10 % for 5 seconds and a 15 second interval for 3 times. The samples were centrifuged at 16,200 x g for 5 minutes at 4 °C. Supernatants were transferred into fresh microcentrifuge tubes and mixed with 2 x SDS sample buffer ratio 1:1. These were placed in a boiling water bath for 5 minutes. The samples were centrifuged at 16,200 x g for 2 minutes and analyzed using SDS-PAGE and Western blot. To the pellets derived just before placing the supernatants in the water bath above, 200 µl of SDS sample buffer was added to each. These were placed in a boiling water bath for 5 minutes after which they were analyzed using SDS-PAGE and Western blot as described earlier.

Optimization of Conditions for Protein Solubility

Protein expression at 37 °C and 1mM IPTG concentration resulted in mostly insoluble recombinant SBIP68 and a small amount of soluble protein. To increase the solubility of recombinant SBIP68, the expression conditions were fine-tuned by lowering the incubation temperature for expression to 17 °C and lowering the concentration of IPTG (0.1 mM, and 0.01 mM). Induction at 37 °C and 1 mM IPTG concentration was also performed simultaneously to serve as a control. Single colonies from the plates were used to inoculate 3 ml LB/kan media which were incubated at 37 °C and 250 rpm overnight. The following morning, 1 ml of each culture was used to inoculate 100 ml of LB/kan medium each. One hundred milliliter cultures were grown at 37 °C and 250 rpm until the OD600 was within 0.6 – 0.7. One milliliter samples were taken from each culture to serve as uninduced controls. To the remaining 99 ml cultures, 198 µl, 19.8 µl,

and 1.98 μ l of 0.5 M IPTG were added to a final IPTG concentration of 1 mM, 0.1 mM, and 0.01 mM, respectively, to induce SBIP68 expression. The 37 °C cultures were incubated for 3 hours at 250 rpm, while the 17 °C cultures were incubated overnight at 250 rpm. Upon the completion of incubation, 1 ml of each culture was put in separate 1.5 ml tubes to be processed by Western blot analysis of SBIP68 solubility as previously described. The remaining 99 ml cultures were transferred to separate tubes and centrifuged at 21,000 x g for 10 minutes at 4 °C. The supernatants were discarded and the cell pellets saved at - 20 °C until they were purified for recombinant SBIP68 protein.

Cell Lysis and Purification of Recombinant SBIP68 Protein

Each pellet from 100 ml culture was resuspended in 3 ml of 1 x Ni-NTA binding buffer containing 30 μ l PMSF (phenylmethylsulfonyl flouride – a protease inhibitor, Appendix B), and 15 mM imidazole. Bacterial cells were lysed 3 times using a French press mini cell (stored at 4 °C prior to use) at 20,000 psi and the lysed samples were collected on ice. Samples were centrifuged at 21,000 x g for 15 minutes at 4 °C. The soluble fractions (supernatants) were collected in fresh tubes and the pellets were stored at - 20°C. Twenty-five milliliters of 1 x Ni-NTA binding buffer was used to equilibrate 2 ml of Ni-NTA resin. Each soluble fraction was gently transferred to the respective Ni-NTA column with the aid of a pipette and allowed to settle. The stop valve was opened to collect flow-through and the column was washed with at least 15 ml of 1 x Ni-NTA wash / binding buffer (containing 15 mM imidazole). The bound 6xHis-tag SBIP68 protein was eluted with 1 x Ni-NTA elution buffer (pH 8.0) containing 250 mM imidazole at room temperature. The eluted proteins were collected in 0.5 ml fractions which were stored at 4 °C. SDS-PAGE and Western blot analysis were performed to

verify the presence of the protein of interest in the purified samples. Fractions with highest recombinant SBIP68 were pooled, concentrated, and used for GT activity.

Analysis of Glucosyltransferase Activity Reaction Products using HPLC

GT activity assays were carried out using purified recombinant SBIP68 and HPLC was performed to identify the products of the glucosyltransferase reactions (Owens and McIntosh, 2009). Each 150 μ l reaction mix consisted of 10 μ l acceptor substrate (100 nmol aglycone in ethylene glycol monomethyl ether), 100 μ l assay buffer (50 mM sodium phosphate buffer pH 7.5, 14 mM β ME), 20 μ l donor substrate (200 nmol UDP-glucose), and 20 μ l (34 μ g, of which SBIP68 was about a tenth or less of this) partially purified SBIP68 recombinant enzyme. The acceptor substrates used were kaempferol, quercetin, naringenin, or hesperetin. The reaction mix was incubated with gentle shaking at 37 °C for 120 minutes. After 120 minutes, 30 μ l 6 M HCl was added to the sample tube and mixed by vortexing briefly. Five hundred microliters of ethyl acetate was added to the sample to separate the formed glucosides from unincorporated UDP-glucose, the reaction tube was vortexed and centrifuged very briefly. Three hundred microliters from the upper organic phase of the sample (containing the reaction products) was transferred to a fresh tube. The reaction products were dried using nitrogen gas. The dried components were redissolved in 60 μ l of HPLC grade methanol and 10 μ l of this was run on a Waters Breeze HPLC system that consists of an in-line degasser AF, a binary HPLC pump 1525 and a dual wavelength absorbance detector 2487 operated by Breeze software version 3.30 (Waters, Milford, MA). The mobile phase was acetic acid:water (15:85) and a gradient of 95:5 acetonitrile:water was the organic phase over a period of 28 minutes. Sample fractionation was performed at room

temperature using a Nova-Pak® C18 (3.9 x 150 mm) column at a flow rate of 1.0 ml/min. The wavelengths used for detection were 290 and 365 nm. Kaempferol, kaempferol 3-*O*-glucoside, quercetin, quercetin 3-*O*-glucoside, naringenin, naringenin 7-*O*-glucoside, and hesperetin were used as standards in the identification of the reaction products.

Cloning and Expression of SBIP68 in *P. pastoris*

Two gene specific primers, a forward primer DK639 and a reverse primer DK640 were utilized in the cloning of SBIP68 in *P. pastoris*. Both primers were designed to carry a restriction enzyme site to enable cloning into an expression system. The forward primer DK639, had an Xho I restriction endonuclease site, while the reverse primer DK640 had an Apa I restriction endonuclease site. The vector pPICZA (Fig. 11), containing a c-myc epitope tag coding sequence and a C-terminal 6x polyhistidine tag coding sequence to facilitate the detection and purification of recombinant proteins respectively (Invitrogen) was used for cloning and expression of recombinant SBIP68. The reverse primer DK640 was designed without the stop codon present in the SBIP68 gene thereby making use of the stop codon just after the C-terminal 6x polyhistidine tag in the vector.

PCR Amplification of *SBIP68* for Cloning into pPICZA

SBIP68 was PCR amplified using a verified pGEMT-SBIP68 clone as a template. The PCR reaction mix composed of 3µl pGEMT-SBIP68_plasmid DNA, 5 µl of 10 x HF2 PCR Buffer, 1 µl of 50 x HF dNTP mix, 1 µl of 10 µM forward primer, 1 µl of 10 µM reverse primer, 1 µl of 50 x Advantage HF polymerase mix, 40 µl of H₂O. The PCR

conditions were as follows: hot start and initial denaturation at 94 °C for 4 minutes, 30 cycles of denaturation, annealing, and elongation at 94 °C, 55 °C, and 72 °C, for 30 seconds, 30 seconds, and 90 seconds respectively, and a final extension step at 72 °C for 10 minutes.

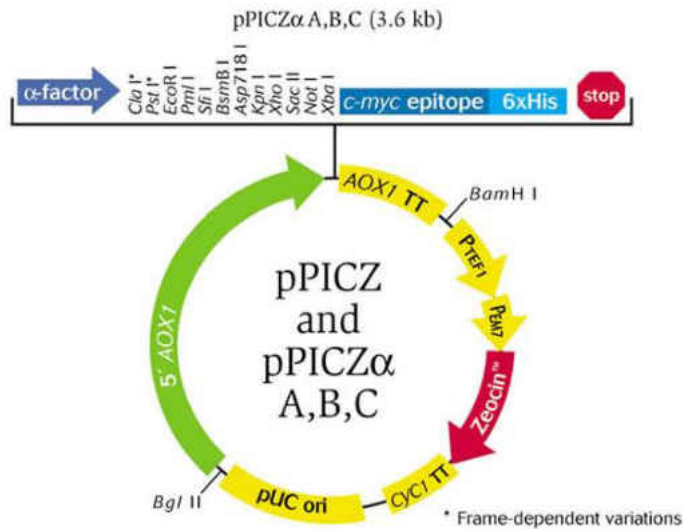


Figure 11: Map of pPICZ Vector (Invitrogen). The restriction sites Xho I and Apa I were used in cloning SBIP68 in *P. pastoris*

Purification of PCR Product

The products of the PCR reaction (*SBIP68'*) were analyzed using agarose gel electrophoresis as described earlier. *SBIP68'* DNA bands were cut out for purification following gel electrophoresis. The bands were purified using Qiagen Gel Extraction kit following the manufacturer's instructions. The purified products were quantified using a nanodrop spectrophotometer and subsequently analyzed on 0.8 % agarose gel.

Construction of pGEMT-SBIP68' Clone

Gel purified *SBIP68'* was ligated into pGEMT easy vector and transformed into competent DH5 α cells as described earlier. The cells were plated on LB/ampicillin containing IPTG/X-Gal and incubated overnight at 37 °C. The following morning, white colonies were selected and streaked on fresh LB/ampicillin plates. The colonies were also tested for presence of *SBIP68'* using colony PCR as described earlier.

Recombinant Plasmid pGEMT-SBIP68' Propagation and Isolation

Positive clones were propagated and used for plasmid purification using the QIAprep Spin Miniprep kit. The concentration and purity of the isolated plasmids were determined as previously described.

Sequencing of pGEMT-SBIP68' Recombinant Plasmid

Each of the purified plasmids (0.5 – 1.0 μ g) was sent to the DNA Analysis Facility at Yale University to be sequenced. The plasmids were sequenced using M13 forward (DK551) and M13 reverse primers (DK552). Analysis of the sequencing results helped in identifying clones whose protein coding sequence were 100 % identical to pGEMT-SBIP68 used for PCR amplification.

Digestion of pGEMT-SBIP68' Plasmid and pPICZA Vector

pGEMT-SBIP68' plasmid and pPICZA plasmid were both digested with Xho I and Apa I. The digestion reaction for the pGEMT-SBIP68' plasmids included in each tube: 10 μ l pGEMT-SBIP68' plasmid-DNA, 2 μ l CutSmart buffer, 6 μ l sterile H₂O, 1 μ l Xho I, and 1 μ l Apa I. The digestion reaction for the pPICZA vector included: 5 μ l pPICZA

vector, 2 μ l CutSmart buffer, 11 μ l sterile H₂O, 1 μ l Xho I, and 1 μ l Apa I. All the constituents of each of the reactions were added at the initial stage with the exclusion of the Xho I enzyme. The samples were incubated at 25 °C (optimum temperature for Apa I) for ~ 2 hours. After about 2 hours, Xho I was added to each sample and the samples were incubated at 37 °C for 3 hours. Both enzymes were heat inactivated at 65 °C for ~ 20 minutes. The digested samples were gel purified as described earlier. The concentration and purity of digested DNA and vector was determined using a nanodrop spectrophotometer as previously described.

Ligation of *SBIP68'* into pPICZA

After purification, the products of the digestion reactions were ligated to create pPICZA-SBIP68' constructs. Each reaction contained a mixture of 10 μ l SBIP68' DNA, 1.3 μ l pPICZA vector, 2 μ l 10 x ligase buffer, 1 μ l T4 DNA ligase, and 5.7 μ l H₂O. A control reaction was also set up that had 1.3 μ l pPICZA vector, 2 μ l 10 x ligase buffer, 1 μ l T4 DNA ligase, and 15.7 μ l H₂O. The reactions were incubated at 16 °C overnight.

Transformation of *E. coli* DH5 α with pPICZA-SBIP68' Plasmid DNA

The ligation reaction mix was centrifuged briefly and 2 μ l was added to a sterile 1.5 ml tube on ice containing 50 μ l of freshly prepared DH5 α competent cells. All steps were followed as described earlier. The cells were plated on low salt LB plates (Appendix B) with 25 μ g/ml zeocin and incubated overnight at 37 °C. The following morning, colonies were streaked on fresh low salt LB/zeocin plates. The colonies were tested for incorporation of the SBIP68' plasmid using colony PCR.

Verification of the Presence of pPICZA-SBIP68' Plasmid by Colony PCR

A colony PCR was performed to screen for positive clones containing the pPICZA-SBIP68' target plasmid. Two hundred microliter PCR tubes containing 40 µl of water each were numbered serially. Single isolated white positive colonies were picked from the low salt LB/zeocin plate and streaked on fresh low salt LB/zeocin plates divided into numbered sections, these were to be the master plates. It is important that low salt LB media be used for efficient selection as zeocin is only active under conditions of low salt concentration and a pH of 7.5 (Invitrogen). The colonies were streaked using sterile micropipette tips. Each of the tips was put in a PCR tube containing 40 µl of sterile water and pipetted up and down a few times to suspend the bacteria. Ten microliters each of the bacterial suspensions would serve as cDNA templates in the PCR amplification of pPICZA-SBIP68' target plasmids. Each PCR reaction mix was composed of 10 µl bacterial suspension, 2 µl 10x PCR Buffer, 2 µl 0.1M dNTP mix, 0.8 µl 5' AOX1 (DK 641) forward primer, 0.8 µl 3' AOX1 (DK 642) reverse primer, 0.5 µl *Taq* polymerase, and 3.9 µl sterile H₂O. The PCR conditions were as follows: 94 °C for 4 minutes, 30 cycles of denaturation, annealing, and elongation at 94 °C, 55 °C, and 72 °C, for 30 seconds, 30 seconds, and 120 seconds respectively, and a final extension step at 72 °C for 10 minutes. The PCR products were analyzed by agarose gel electrophoresis using 0.8 % agarose gels as previously described.

Recombinant Plasmid pPICZA-SBIP68' Propagation and Isolation

Positive clones from the master plate as confirmed by colony PCR were selected for plasmid propagation and purification using the QIAGEN CompactPrep Plasmid Midi

Kit according to the manufacturer's instructions. The concentration and purity of the isolated plasmids were determined as previously described.

Sequencing of pPICZA-SBIP68' Recombinant Plasmid

The plasmids were sequenced using 5' AOX1 forward and 3' AOX1 reverse primers. One hundred percent positive plasmids were used to transform *P. pastoris*.

Preparing pPICZA-SBIP68' DNA for Transformation into *Pichia pastoris*

To transform *P. pastoris*, ~ 10 µg of pPICZA-SBIP68' plasmid DNA was linearized by digesting with the restriction enzyme Pme I. Linearization of plasmid DNA prior to transformation is not obligatory but is strongly recommended as linear DNA is capable of generating extremely stable transformants of *Pichia pastoris* via homologous recombination between the transforming DNA and regions of homology present within the *P. pastoris* genome (Cregg et al. 1985; Cregg et al. 1989). The digestion reaction mix contained: 6 µl plasmid DNA, 1 µl 10 x CutSmart buffer, 1 µl Pme I restriction enzyme, 2 µl autoclaved milliQ water. The reactions were incubated at 37 °C for 4 hours. After 4 hours, 1 µl of Pme I was added to each reaction and incubated at 37 °C overnight. The following morning the enzyme was heat inactivated by incubating the reactions at 65 °C for 20 minutes. To ensure complete linearization, the digested DNA mixture were analyzed by running 2 µl of each on a 0.8 % agarose gel. Following verification, the total volume of linearized DNA was adjusted to 300 µl using sterile water. Three hundred microliters phenol:chloroform:isoamyl alcohol (25:24:1) was added to each 300 µl of linearized DNA. This mixture was vortexed for 20 seconds, and centrifuged at 16,000 x g for 5 minutes. The upper aqueous phase of each mixture was

carefully transferred to a fresh tube making sure none of the middle layer (phenol) was transferred with it. Ethanol precipitation was performed by adding 0.1 volume of 3 M sodium acetate (Appendix B) and then adding 2.5 volumes of 100 % ethanol. Samples were mixed and incubated at - 80 °C for 1 hour and centrifuged at 16,000 x g for 30 minutes at 4° C. The supernatants were carefully decanted without disturbing the DNA pellets. To each pellet, 500 µl of ice cold 80 % ethanol was added, and they were centrifuged at 16,000 x g for 15 minutes at 4 °C. The ethanol was discarded, and the pellets were air dried and then re-suspended in 10 µl each of sterile deionized water. DNA concentration and purity were determined using a nanodrop spectrophotometer. DNA was used to transform *P. pastoris*.

Preparation of Electrocompetent *Pichia pastoris* X-33 Mut⁺ Cells

Pichia pastoris strain X-33 Mut⁺ glycerol stock was used to inoculate 5 ml of YPD (Appendix B) which was grown at 30 °C and 250 rpm overnight in a 50 ml flask. The following day, 0.2 ml of the overnight culture was used to inoculate 200 ml of fresh YPD medium. The culture was again grown overnight at 30 °C and 250 rpm overnight in a 1 L flask until its OD₆₀₀ was within 1.3 – 1.5. The cells were centrifuged at 1500 x g for 5 minutes at 4 °C. Cells were resuspended with 200 ml of ice cold sterile water and centrifuged at 1500 x g for 5 minutes at 4 °C. Cells were resuspended with 100 ml of ice cold sterile water and centrifuged at 1500 x g for 5 minutes at 4 °C. Cells were resuspended in 8 ml of ice cold sterile 1 M sorbitol and centrifuged at 1500 x g for 5 minutes at 4 °C. Finally the cells were resuspended in 0.4 ml of ice cold sterile 1 M sorbitol (Appendix B). The cells were kept on ice and used the same day.

Transformation of *P. pastoris*

To transform *P. pastoris* with pPICZA-SBIP68', both linearized and circular DNAs were used in two separate transformation reactions. Transformation was achieved by electroporation of freshly prepared electrocompetent *P. pastoris*. In one tube, 80 μ l of the cells was mixed with \sim 10 μ g of linearized pPICZA-SBIP68' DNA, while in the other tube 80 μ l of cells was mixed with \sim 40 μ g of circular pPICZA-SBIP68' DNA. These were transferred to pre-chilled 0.2 cm electroporation cuvettes. The cuvettes with the cells were incubated on ice for 5 minutes, after which they were each pulsed once at 1.5 volts using BIORAD Gene Pulser. Immediately after pulsing, 1 ml of ice cold 1 M sorbitol was added to each cuvette. The contents of the cuvettes were each transferred to separate sterile 15 ml tubes and were incubated at 28 °C for \sim 2 hours without shaking. Transformed cells (10 μ l, 25 μ l, 50 μ l, 100 μ l, and 200 μ l) were spread using glass beads on YPDS/zeocin (100 μ g/ml) plates (Appendix B). The plates were incubated at 28 °C until colonies formed, at approximately 2.5 days.

Direct PCR Screening of *P. pastoris* Clones

Colony PCR was performed to screen for positive *Pichia* clones containing the pPICZA-SBIP68' target DNA. PCR tubes (0.2 ml), each containing 15 μ l of sterile water were numbered serially. Single isolated *Pichia* colonies were picked (and numbered for identification purposes) from the YPDS/zeocin plates with the aid of sterile micropipette tips. Each tip was dipped in each PCR tube containing 15 μ l of sterile water and pipetted up and down a few times to suspend the cells. Ten microliters of each cell suspension was mixed with 5 μ l of a 5 U/ μ l solution of the enzyme lyticase in TE buffer.

These were incubated at 37 °C, - 80 °C, and 95 °C, for 30 minutes, 10 minutes, and 10 minutes respectively. The addition of lyticase to the cells and their subsequent freezing and heating treatment are necessary to lyse the cells as yeast cells are known to have tough chitinous cell walls. The 5 µl of each cell lysate (cell suspension with lyticase, after cold and heat treatment) would serve as the DNA template to be amplified during the PCR. Each PCR mix was composed of 5 µl cell lysate, 1 µl 10 x PCR Buffer, 1 µl 0.1 M dNTP mix, 0.5 µl 5' *AOX1* forward primer, 0.5 µl 3' *AOX1* reverse primer, 0.5 µl *Taq* polymerase, and 1.5 µl sterile H₂O. The PCR conditions were as follows: 95 °C for 5 minutes, 30 cycles of denaturation, annealing, and elongation at 95 °C, 50 °C, and 72 °C, for 30 seconds, 30 seconds, and 90 seconds respectively. A 0.8 % agarose gel was used to analyze the PCR products using agarose gel electrophoresis. Clones that tested positive were used to inoculate YPD/zeocin media and grown overnight at 30 °C with shaking at 250 rpm. These overnight cultures were used in the preparation of *Pichia*-SBIP68' glycerol stocks.

Time Course Expression of Recombinant SBIP68'

Pichia pastoris containing SBIP68' from glycerol stocks were streaked on YPD/zeocin plates and incubated at 28 °C until colonies formed (~ 2.5 days). A few single isolated colonies were each used to inoculate 3 ml of YPD/zeocin media and grown at 30 °C in a shaker at 250 rpm overnight. To start a large scale liquid culture, 100-125 µl of the overnight grown cultures were used to inoculate 25 ml of BMGY medium (Appendix B) each in a 250 ml baffled conical flask. BMGY cultures were grown at 29 °C and 250 rpm until their OD₆₀₀ = 2-6 (log-phase growth) approximately 15-18 hours. The cells were harvested by centrifuging at 2,500 x g for 5 minutes at room

temperature. The supernatants were discarded and the pellets were washed to remove all traces of glycerol from the BMGY medium. Cells were washed by resuspending each cell pellet in 30 ml BMMY (Appendix B) media and centrifuging at 2,500 x g for 5 minutes at room temperature. The washing step was repeated once. Cell pellets were resuspended in BMMY media to an OD₆₀₀ of 1.0 (typical resuspension volumes were between 75 - 250 ml) in 1 L autoclaved baffled flasks. One milliliter samples were taken from the cultures to serve as 0 hour post-induction time points. The flasks were covered with 2 - 4 layers of sterile cheesecloth and incubated at 29 °C and 250 rpm. Every 24 hours, 100 % methanol was added to each culture to give a final methanol concentration of 0.5 %. One milliliter samples were taken from the cultures at different times post-induction to determine the optimal post-induction time to harvest. Time point samples were centrifuged at 16,200 x g for 3 minutes at room temperature, supernatants were discarded, and pellets were frozen in liquid nitrogen and stored at – 80 °C until ready to assay. Pellets were later analyzed for protein expression using SDS-PAGE and Western blot.

Preparing Samples for SDS-PAGE and Western Blot Analysis

Pichia- SBIP68' cell pellets were removed from the – 80 °C freezer and placed on ice briefly to thaw. Each 1 ml sample pellet was re-suspended in 100 µl of breaking buffer (Appendix B). An equal volume of 0.5 mm acid-washed glass beads was added to each sample. The samples were alternately vortexed for 30 seconds and rested on ice for 30 seconds, this was repeated for a total of 8 times. The cell lysates together with the pellets (total cell protein) were analyzed by Western blot.

Sodium Dodecyl Sulfate Polyacrylamide Gel Electrophoresis (SDS-PAGE)

SDS-PAGE was performed by adding 200 µl of 2 x SDS sample buffer (containing 5 % βME added just before use) to each sample. The samples were placed in a boiling water bath for 10 minutes and 10 µl of each sample was loaded on an SDS gel and run by electrophoresis at 200 volts.

Western Blot Analysis

Upon the separation of protein samples using SDS-PAGE, the proteins were transferred from the gels to PVDF (polyvinylidene difluoride) membranes as described earlier. After electroblotting, the PVDF membranes were taken out of the cassettes and processed for Western blot analysis using anti-polyhistidine primary antibody as described earlier.

Large Scale Expression of *Pichia*-SBIP68'

Pichia-SBIP68' cells from glycerol stocks were streaked on an YPD/zeocin plates and incubated at 28 °C until colonies formed, ~ 2.5 days. A few single isolated colonies were each used to inoculate 3 ml of YPD/zeocin media and grown at 30 °C and 250 rpm overnight. To inoculate 25 ml of BMGY medium each in a 250 ml baffled conical flask, 100-125 µl of overnight culture was used. BMGY cultures were grown at 29 °C and 250 rpm until their OD₆₀₀ was within 2 – 6 (log-phase growth) approximately 15 – 18 hours. The cells were harvested by centrifuging at 2,500 x g for 5 minutes at room temperature. The supernatants were discarded and the pellets were washed to remove all traces of glycerol from the BMGY medium. Cells were washed by resuspending each cell pellet in 30 ml BMMY media (Appendix B) and centrifuging at 2,500 x g for 5

minutes at room temperature. The washing step was repeated once. Cell pellets were resuspended in BMMY media to an OD₆₀₀ of 1.0 (typical resuspension volumes were between 75 – 250 ml) in 1 liter sterile baffled flasks. One milliliter samples were taken from the cultures to serve as 0 hour control. The flasks were covered with 2 - 4 layers of sterile cheesecloth and incubated at 29 °C and 260 rpm. Every 24 hours, 100 % methanol was added to each culture to give a final methanol concentration of 0.5 %. Cells were grown for a total of 96 hours and harvested by centrifuging at 2,500 x g for 5 minutes at room temperature. Pellets were saved at – 80 °C until they were processed for purification of target protein.

Purification of Recombinant SBIP68' Protein Expressed in *Pichia pastoris*

Each pellet derived from the 530 ml culture was resuspended in 40 ml of 1 x Ni-NTA binding buffer containing PMSF. Cells were lysed using a French press 40K cell at 20,000 psi at least 5 times, and lysate was collected on ice. Sample was centrifuged at 20,000 x g for 15 minutes at 4 °C. The soluble fraction (supernatant) was collected in a fresh tube and the pellet stored at – 80 °C. Soluble SBIP68' was purified on Ni-NTA column as previously described. After purification, the fractions with the highest concentration of proteins were pooled and concentrated using a centrifugal filter unit (Amicon Centricon Centrifugal Filter, 30 kDa cut off) at 4,700 x g and 4 °C until the sample volume was reduced to 500 µl. Two milliliters of enzyme assay buffer was added to the sample and centrifuged again until the volume was 500 µl. Western blot analysis was performed to verify the presence of SBIP68' in the eluted purified fractions and in the concentrated sample. The concentrated Ni-NTA purified SBIP68' was used for glucosyltransferase activity assay.

Purification of Recombinant SBIP68' using Anion Exchange Chromatography

Fractions 7 - 13 containing SBIP68' (as confirmed by Western blot analysis) from the Ni-NTA affinity chromatography were pooled and desalted on a Hi-Trap Desalting Column (2x5 ml) (GE Healthcare). The desalted sample (9 ml) was further purified using a Mono-Q anion exchange column (Mono-Q 5/50 GL, GE Healthcare) on AKTA purifier 10. The bound proteins were eluted with a linear gradient of 0-500 mM sodium chloride in potassium phosphate buffer pH 7.5 (Appendix B) and collected as 1 ml fractions. Western blot was performed to determine which fractions contained SBIP68'.

Analysis of Glucosyltransferase Activity using Radioactive Method

Recombinant purified SBIP68 was screened for glucosyltransferase activity following a method developed by McIntosh et al. (1990). Briefly, radioactive (^{14}C) UDP-glucose was used as the sugar donor substrate and the amount of radioactive ^{14}C -glucose incorporated into the reaction product was measured. Each 75 μl reaction mix composed of 5 μl acceptor substrate (50 nmol aglycone in ethylene glycol monomethyl ether), 50 μl assay buffer (50 mM sodium phosphate buffer pH 7.5, 14 mM βME), 10 μl donor substrate (UDP-[U- ^{14}C] glucose, 0.025 μCi , 19,670 cpm), 10 μl (34 μg , of which SBIP68 was about a tenth or less of this) semi-purified and concentrated recombinant SBIP68 enzyme. A control reaction with 60 μl assay buffer and no enzyme and kaempferol was used as the acceptor substrate. Each reaction mix was incubated with gentle shaking at 37 $^{\circ}\text{C}$ for 10 minutes. A total of 14 potential acceptor substrates were tested, these are: salicylic acid, methyl salicylate, benzoic acid, azelaic acid, *p*-hydroxybenzoic acid, kaempferol, quercetin, hesperetin, naringenin, gossypetin, 4'-

acetoxy-7-hydroxy-6-methoxyisoflavone, apigenin, luteolin, and fisetin. The reactions were terminated by the addition of 15 μ l 6 M HCl and mixed by vortexing briefly. Two hundred and fifty microliters of ethyl acetate was added to each tube to separate the formed glucosides from unincorporated UDP-[U- 14 C] glucose, the reaction tubes were vortexed and centrifuged briefly. A hundred and fifty microliters of the upper organic phase of each sample was transferred to separate 7 ml scintillation vials containing 2 ml of scintillation fluid each. The radioactive count for each reaction product was determined using a scintillation counter (Beckman LS 6500).

Analysis of Glucosyltransferase Activity Reaction Products using HPLC

HPLC was performed to identify the products formed from separate glucosyltransferase reactions involving kaempferol, quercetin, naringenin, hesperetin, and salicylic acid as acceptor substrates (Owens and McIntosh, 2009). Each 150 μ l reaction mix composed of 10 μ l acceptor substrate (100 nmol aglycone in ethylene glycol monomethyl ether for flavonoid substrates, 100 nmol aglycone in water (pH 7) for salicylic acid), 100 μ l assay buffer (50 mM sodium phosphate buffer pH 7.5, 14 mM β ME), 20 μ l donor substrate (200 nmol UDP-glucose), and 20 μ l (68 μ g, of which SBIP68 was about a tenth or less of this) partially purified SBIP68 recombinant enzyme. The reaction mix was incubated with gentle shaking at 37 $^{\circ}$ C for 120 minutes. For reactions involving flavonoid substrates, after 120 minutes, 30 μ l 6 M HCl was added to the sample tube and mixed by vortexing briefly. Five hundred microliters of ethyl acetate was added to the sample to separate the formed glucosides from unincorporated UDP-glucose, the reaction tube was vortexed and centrifuged very briefly. Three hundred microliters from the upper organic phase of the sample (containing the reaction

products) was transferred to a fresh tube. The reaction products were dried using nitrogen gas. The dried components were redissolved in 60 μ l of HPLC grade methanol and 10 μ l of this was run on a Waters HPLC system that consists of an in-line degasser AF, a binary HPLC pump 1525 and a dual wavelength absorbance detector 2487 operated by Breeze software version 3.30 (Waters, Milford, MA). The mobile phase was acetic acid:water (15:85) and a gradient of 95:5 acetonitrile:water was the organic phase over a period of 28 minutes. Sample fractionation was performed at room temperature using a Nova-Pak[®] C18 (3.9 x 150 mm) column at a flow rate of 1.0 ml/min. The wavelength used for detection was 365 nm. Kaempferol, kaempferol 3-O-glucoside, quercetin, quercetin 3-O-glucoside, naringenin, naringenin 7-O-glucoside, and hesperetin were used as standards in the identification of the reaction products. For the reaction involving salicylic acid as substrate, after 120 minutes, 300 μ l of ethanol was added to the sample tube and mixed by vortexing briefly. The sample was cooled to – 80 °C for 120 minutes, and centrifuged for 30 minutes at 21,000 x g and 4 °C. The supernatant was transferred to a fresh tube and the volume was reduced to 60 μ l using a concentrator (Thermo Electron Corporation Savant ISS110 SpeedVac Concentrator) with the drying rate set to low, and 10 μ l of this was run on the Waters HPLC system as described for the other reactions. Detection of reaction products was at 296 nm. Salicylic acid was used as a standard in the identification of the reaction products.

CHAPTER 3

RESULTS

Cloning and Expression of SBIP68 in *E. coli*

Bioinformatics Analyses of SBIP68

Previous work involving a yeast two-hybrid screening using SABP2 as a bait and tobacco leaf proteins as prey led to the identification of several putative SABP2 interacting proteins. The nucleotide sequence (Fig. 12A) of one of the SABP2 interacting proteins, SBIP68, was translated to protein (Fig. 12B) and used to perform a BLAST analysis using the NCBI database.

A.

```
AGGGGTAATAAACTGCAATTGATAATCAAGATTGCTTGAAATGGTTAGATAAATTTGAAAC
AGAATCCGTGGTTTATGCAAGTCTTGGAAAGTTTATCTCGTTTGACATTATTGCAAATGGTGG
AACTTGGTCTTGGTTTAGAAGAGTCAAATAGGCCTTTTGTATGGGTATTAGGAGGAGGTGAT
AAATTAATGATTTAGAGAAATGGATTCTTGAGAATGGATTTGAGCAAAGAATTAAGAAAG
AGGAGTTTTGATTAGAGGATGGGCTCCTCAAGTGCTTATACTTTCACACCCTGCAATTGGTG
GAGTATTGACTCATTGCGGATGGAATTCTACATTGGAAGGTATTTTCAGCAGGATTACCAATG
GTAACATGGCCACTATTTGCTGAGCAATTTTGAATGAGAAGTTAGTAGTCCAAGTGCTAAA
AATTGGAGTGAGCCTAGGTGTGAAGGTGCCTGTCAAATGGGGAGATGAGGAAAATGTTGGAG
TTTTGGTAAAAAAGGATGATGTTAAGAAAGCATTAGACAAACTAATGGATGAAGGAGAAGAA
GGACAAGTAAGAAGAACAAAAGCAAAAGAGTTAGGAGAATTGGCTAAAAAGGCATTTGGAGA
AGGTGGTTCTTCTTATGTTAACTTAACATCTCTGATTGAAGACATCATTGAGCAACAAAATC
ACAAGGAAAAATAGTATATTATGATTATTTTTTTTTTCTAATAAAAAAAAAAAAAAAAAAAAA
AAAACAC
```

B.

```
RGNKTAIDNQDCLKWLDNFETESVYASLGSLSRLLQLQMVLEGLGLEESNRPFVWVLGGGD
KLNDLEKWILENGFEQRIKERGVLRGWAPQVLILSHPAIGGVLTGCGWNSTLEGISAGLPM
VTWPLFAEQFCNEKLVVQVLKIGVSLGVKVPVKWGDEENVGLVKKDDVKKALDKLMDEGEE
GQVRRTKAKELGELAKKAFGEGGSSYVNLTSIEDIIEQQNHKEK
```

Figure 12: Nucleotide and Translated Amino Acid Sequence of SBIP68 Obtained from Yeast Two-Hybrid Screening. A. Nucleotide sequence. B. Translated amino acid sequence of SBIP68.

The bioinformatics revealed that SBIP68 showed 100% identity to the C-terminal of a putative UDP-glucose: flavonoid glucosyltransferase with NCBI accession number BAD93688.1, that has 496 amino acids (Fig. 13A) and is encoded by the tobacco *NtGT4* gene with an open reading frame that is 1,488 bp long (Fig. 13B). The

A.

MATQVHKLHFILFPLMAPGHMIPMIDIAKLLANRGVITTTIITTPVNNANRFSSTITRAIKSGLRIQIL
 TLKFPSVEVGLPEGCENIDMLPSLDLASKFFAAISMLKQQVENLLEGINPSPSCVISDMGFPWTTQI
 AQNFNIPRIVFHGTCCFSLLCYKILSSNILENITSDSEYFVVPDLPDRVELTKAQVSGSTKNNTSV
 SSSVLKEVTEQIRLAEESSYGVIVNSFEELEQVYEKEYRKARGKKVWCVPVSLCNKEIEDLVTRGN
KTAINQDCLKWLDNFETESVYASLGSLSRLTLLQMVLEGLGLEESNRPFVWVLGGGDKLNDLEKW
I LENGFEQRIKERGV LIRGWAPQV LILSHPAIGGVLTHCGWNSTLEGI SAGLPMVTWPLFAEQFCNE
KLVVQVLKIGVSLGVKVPVKWGD EENVGVLVKDDVKKALDKLMDEGEEGQVRRTKAKELGELAKKA
FGEGSSSYVNLTS LI EDI IEQQNHKEK

B.

ATGGCAACTCAAGTGCACAACTTCATTTCATACTATTCCCTTTAATGGCTCCAGGCCACATGATTC
 CTATGATAGACATAGCTAAACTTCTAGCAAATCGCGGTGTCATTACCACTATCATCACCCTCCAGT
 AAACGCCAATCGTTTCAGTTCAACAATTACTCGTGCCATAAAAATCCGGTCTAAGAATCCAAATCTT
 ACACTCAAATTTCCAAGTGTAGAAGTAGGATTACCAGAAGGTTGCGAAAATATTGACATGCTTCCTT
 CTCTTGACTTGGCTTCAAAGTTTTTTTGCTGCAATTAGTATGCTGAAACAACAAGTTGAAAATCTCTT
 AGAAGGAATAAAATCCAAGTCCAAGTTGTGTTATTTTCAGATATGGGATTTCCCTTGGACTACTCAAAT
 GCACAAAATTTTAAATATCCCAAGAATTGTTTTTCATGGTACTTGTGTTTTCTCACTTTTATGTTCCCT
 ATAAAATACTTTCCCTCCAACATTCTTGA AAAATATAACCTCAGATTCAGAGTATTTTGTGTTCCCTGA
 TTTACCCGATAGAGTTGAACTAACGAAAGCTCAGGTTTCAGGATCGACGAAAAATACTACTTCTGTT
 AGTTCCTTCTGTATTGAAAGAAGTTACTGAGCAAATCAGATTAGCCGAGGAATCATCATATGGTGTA
 TTGTTAATAGTTTTGAGGAGTTGGAGCAAGTGTATGAGAAAGAATATAGGAAAGCTAGAGGGAAAAA
 AGTTTGGTGTGTTGGTCCCTGTTTCTTTGTGTAATAAGGAAATGAAGATTTGGTTACAAGGGGTAAT
 AAACTGCAATTGATAATCAAGATTGCTTGA AATGGTTAGATAATTTTGAACAGAATCTGTGGTTT
 ATGCAAGTCTTGAAGTTTATCTCGTTTGACATTATTGCAAATGGTGAACCTGGTCTTGGTTTGA
 AGAGTCAAATAGGCCTTTTGTATGGGTATTAGGAGGAGGTGATAAATTAATGATTTAGAGAAATGG
 ATTCTTGAGAATGGATTTGAGCAAAGAATTAAGAAAGAGGAGTTTTGATTAGAGGATGGGCTCCTC
 AAGTGCTTATACTTTACACCCCTGCAATTGGTGGAGTATTGACTCATTGCGGATGGAATTCTACATT
 GGAAGGTATTTGAGCAGGATTACCAATGGTAACATGGCCACTATTTGCTGAGCAATTTTGAATGAG
 AAGTTAGTAGTCCAAGTGCTAAAAATGGAGTGAGCCTAGGTGTGAAGGTGCCTGTCAAATGGGGAG
 ATGAGGAAAAATGTTGGAGTTTTGGTAAAAAAGGATGATGTTAAGAAAGCATTAGACAAACTAATGGA
 TGAAGGAGAAGAAGGACAAGTAAGAAGAACAAAAGCAAAGAGTTAGGAGAATGGCTAAAAAGGCA
 TTTGGAGAAGGTGGTTCTTCTTATGTTAACTTAACATCTCTGATTGAAGACATCATTGAGCAACAAA
 ATCACAAGGAAAAATAG

Figure 13: Flavonoid Glucosyltransferase (*NtGT4*) Accession Number BAD93688.1. A. Amino acid sequence, the underlined sequence shows 100% identity to the SBIP68 sequence in figure 13B. B. Open reading frame of *NtGT4* gene.

smaller size and exact match of the SBIP68 to the C-terminus of NTGT4 indicated that it is a partial sequence and lacks N-terminus.

Subcellular Localization of SBIP68

Various subcellular localization prediction software was used to predict the subcellular localization of SBIP68 (Figs. 14-16). Most analyses predicted SBIP68 to be

Protein: SBIP68
 Predicted Location: **cytoplasmic**: 0.5 **extracellular**: 0.12 **peroxisomal**: 0.11 **Golgi apparatus**: 0.07 **plasma membrane**: 0.06 **mitochondrial**: 0.05 **vacuolar**: 0.04 **ER**: 0.03
 nuclear: 0.01 chloroplast: 0.01

Figure 14: Subcellular Localization Prediction using MultiLoc2. This predicts that the protein is most probably a cytoplasmic protein with the highest score of 0.5.

Name	Len	cTP	mTP	SP	other	Loc	RC
SBIP68	496	0.018	0.046	0.469	0.118	S	4
cutoff		0.000	0.000	0.000	0.000		

Figure 15: Subcellular Localization Prediction using Target v1.1. This indicates that SBIP68 is most probably a secretory protein (SP) and neither a mitochondrial transfer protein (mTP) nor a chloroplast transfer protein (cTP).

```

endoplasmic reticulum (membrane) --- Certainty= 0.550(Affirmative) < succ>
  endoplasmic reticulum (lumen) --- Certainty= 0.100(Affirmative) < succ>
    outside --- Certainty= 0.100(Affirmative) < succ>
  microbody (peroxisome) --- Certainty= 0.100(Affirmative) < succ>
  
```

Figure 16: Localization of SBIP68 as Predicted by PSORT.

neither a mitochondrial nor a chloroplast localized protein. MultiLoc 2 predicted it to be a cytoplasmic protein (Fig. 14), while Target v1.1 predicted it to be a secretory protein

(Fig. 15) and PSORT predicted to be endoplasmic reticulum membrane localized protein (Fig. 16).

RNA Extraction

Total RNA from young tobacco leaves was purified and quantitated using a nanodrop spectrophotometer. The result is as shown in Fig. 17. The concentration of the purified total RNA was 637.2 ng/ μ l and the A260/280 ratio was 2.01 which showed high purity level.

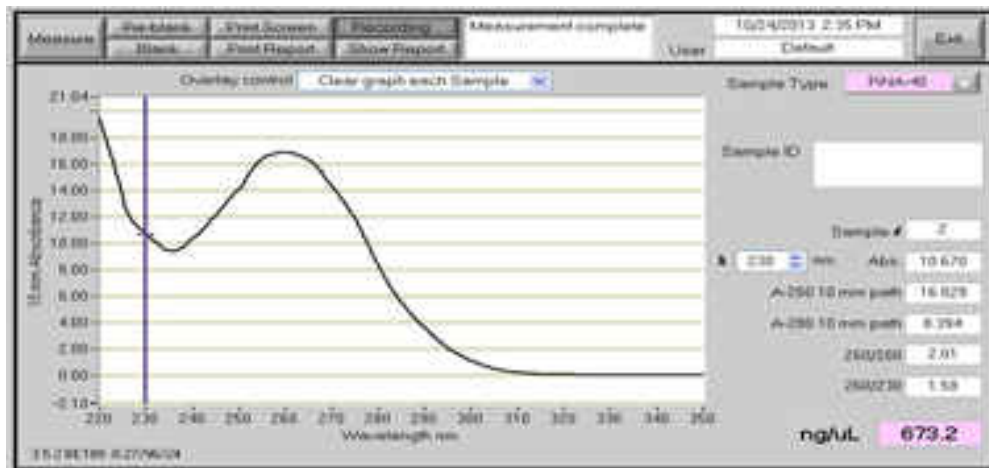


Figure 17: Scan from Nanodrop Spectrophotometer.

cDNA Synthesis

The endogenous tobacco *EF1 α* was amplified via PCR to check the quality of the newly synthesized cDNA. Figure 18 shows agarose gel picture of the PCR amplified *EF1 α* with expected size of 550 bp. The other thick diffused bands at the bottom are likely from primer dimers. Lane numbers 2 and 3 are duplicate samples of the same cDNA preparation.

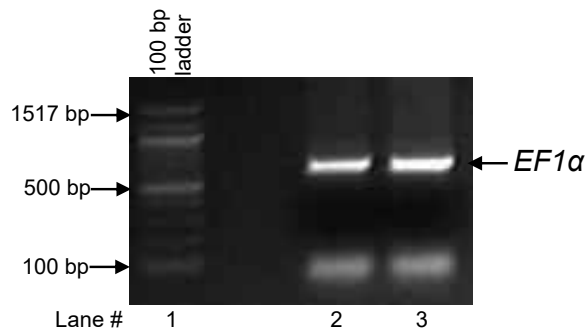


Figure 18: PCR Amplification of *EF1α*. DNA ladder (100 bp) was used to compare size of purified products.

PCR Amplification of *SBIP68*

To amplify full length *SBIP68*, PCR amplification was performed using primers specific for *SBIP68*. Three separate cDNA preparations (lane #2, 3, & 4) were used (Fig. 19). Full length *SBIP68* (~1491 bp) was amplified but some unexpected products were also amplified (lane #2) as shown in Figure 18. This was probably due to non-specific binding of the primers used for PCR, to templates other than *SBIP68* cDNA.

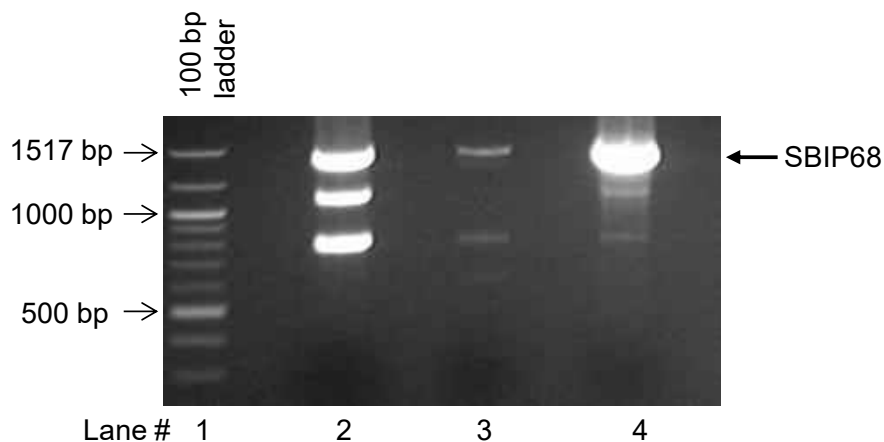


Figure 19: RT-PCR Amplification of *SBIP68*. Ethidium bromide stained 1.2 % agarose gel showing amplification of *SBIP68* (~1491bp).

Purification of PCR Product

The RT-PCR amplified *SBIP68* was gel purified as described in material and methods before using them for other downstream applications. Figure 20 shows aliquots of the gel purified PCR products.

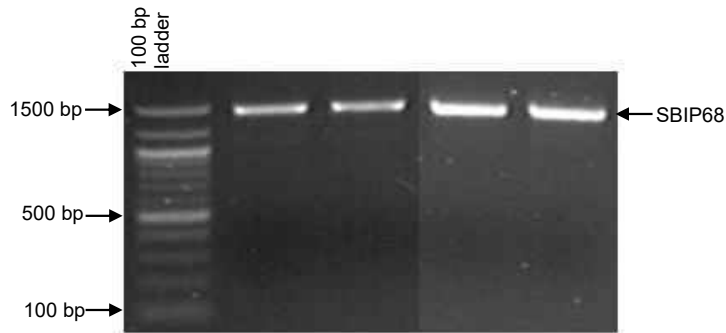


Figure 20: Purified *SBIP68* PCR Products. Ethidium bromide stained 1.2 % agarose gel showing *SBIP68* purified PCR products. DNA ladder (100 bp) was used to compare size of purified products.

Cloning *SBIP68* in pGEMT Plasmid

The purified *SBIP68* PCR amplified products were ligated into pGEMT plasmids via TA cloning. Ligated products were transformed into freshly prepared competent cells. Transformed cells were plated on selective media (LB/ampicillin), and incubated at 37 °C overnight. Isolated colonies were tested for the presence of pGEMT-*SBIP68* using colony PCR, and the PCR amplified products were analyzed by electrophoresis on a 0.8 % agarose gel (Fig. 21). Several clones containing the expected size bands (#2, 3, 4 and #6 -10 for DK644) (#3 - 6 and 8 -10 for DK645) were selected for plasmid DNA isolation followed by DNA sequencing. Clones in lane #5 (Fig. 21A), and lane #2 and 7 (Fig. 21B) showed faint and smaller sized bands. The fact that these clones grew

as white colonies on selective media meant two things: they were transformed by the vector which conferred resistance to ampicillin, and they were not transformed by empty vectors otherwise they would have shown up as blue colonies due to α -complementation and the presence of X-Gal.

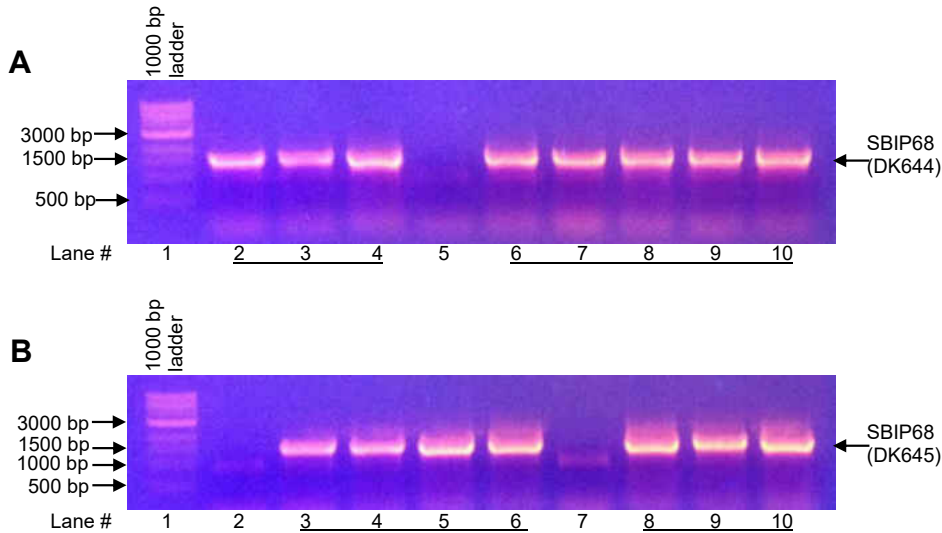


Figure 21: Screening of *SBIP68* Inserts by Colony PCR. Agarose gel (0.8%) showing PCR amplified *SBIP68*. Lane numbers 2 through 10 are individual clones. Clones that tested positive for the inserts of interest have been underlined. **A.** Shows colony PCR of 644. **B.** Shows colony PCR of 645 in pGEMT. Plasmid specific M13 forward primer, and gene specific DK644 and DK645 reverse primers were used for PCR amplifications.

Plasmid Isolation and DNA Sequencing of pGEMT-SBIP68

Ten clones (five each of pGEMT-SBIP68 (644) and pGEMT-SBIP68 (645)) were selected for plasmid DNA isolation. Plasmid DNA was isolated and sequenced. Of the ten clones, seven of them had good quality readable sequences. These were compared to the *NtGT4* sequence from the NCBI database. All clones showed over 90% identity to the reference sequence (*NtGT4*). Four of these clones, C2, C15, C18, and C20, showed

99% identity to *NtGT4*. These four clones differed from the reference sequence (*NtGT4*) by one nucleotide change at base number 552 (Fig. 22). This single nucleotide difference was a pyrimidine (T) to pyrimidine (C) change. Upon translation this resulted in no change in amino acid (Fig. 23). C2 is pGEMT-SBIP68 (644) with the stop codon as present in *NtGT4*, while C15, C18, and C20, are pGEMT-SBIP68 (645) without the stop codon. Full length *SBIP68* nucleotide sequence and translated amino acid sequence are shown in Figure 24A and Figure 24B respectively. Figure 25 shows the result of a protein blast performed on NCBI with full length SBIP68 protein, showing SBIP68 to belong to the glycosyltransferase_GTB_type superfamily. It has a putative GT1_Gtf_like conserved protein domain (276 - 464) and a putative UDP-glucuronosyl and UDP-glycosyltransferase (UDPGT, 287 - 408) conserved domain. Full length SBIP68 showed homology to enzymes of glycosyltransferase family 1 (Fig. 26). It showed 100 % similarity to a predicted: UDP-glycosyltransferase from *Nicotiana tomentosiformis* (NCBI reference sequence: XP_009623864.1), which also has 496 amino acids and is yet to be characterized. This 100 % similarity did not come as a surprise as *N. tabacum* (a tetraploid) from which SBIP68 was derived is supposedly a hybrid of *N. tomentosiformis* and *N. sylvestris* (Ren and Timko, 2001; Siervo et al., 2014). SBIP68 also showed 88 % similarity to a putative glycosyltransferase UGT73E5 from *Lycium barbarum* (GenBank: BAG80535.1) with 503 amino acids (Noguchi et al., 2008). UGT73E5 was cloned alongside other LbGT's including UGT73A10 (49 % similarity to SBIP68). UGT73E5 and UGT73A10 belong to the same phylogenetic cluster and UGT73A10 has been shown to be a flavonoid: UDP-glycosyltransferase with regio-specific activity towards flavan-3-ols (Noguchi et al., 2008). UGT73A10 is highly

specific for the donor substrate UDP-glucose has broad acceptor substrate specificity with the highest preference for naringenin (Noguchi et al., 2008).

SBIP68 also showed 58 % similarity to a putative flavonoid UDP-glucosyltransferase 2 from *Citrus paradisi* (GenBank: AIS39471.1) with 491 amino acids (Devaiah et al., in review). A previously characterized salicylic acid glucosyltransferase, UDP-glucose: salicylic acid glucosyltransferase (SA GTase) from *Nicotiana tabacum* (GenBank: AAF61647.1) with 459 amino acids showed only 29 % similarity to SBIP68 (Lee and Raskin, 1999). SA GTase uses UDP-glucose as the sole sugar donor to glucosylate SA forming SA 2-O-beta-D-glucoside (SAG) and glucosyl salicylate (GS) and has broad acceptor substrate specificity to simple phenolics. SA GTase mRNA is also induced by SA and incompatible pathogens. “Currently, PSPG function and specificity cannot be fully predicted based on sequence information alone” (Noguchi et al., 2008).

```

C15      GGATCCATGGCAACTCAAGTGCACAAACTTCATTTTCATACTATTCCCTTTAATGGCTCCA
C18      GGATCCATGGCAACTCAAGTGCACAAACTTCATTTTCATACTATTCCCTTTAATGGCTCCA
C20      GGATCCATGGCAACTCAAGTGCACAAACTTCATTTTCATACTATTCCCTTTAATGGCTCCA
NtGT4    -----ATGGCAACTCAAGTGCACAAACTTCATTTTCATACTATTCCCTTTAATGGCTCCA
C2       GGATCCATGGCAACTCAAGTGCACAAACTTCATTTTCATACTATTCCCTTTAATGGCTCCA
          *****

C15      GGCCACATGATTCCCTATGATAGACATAGCTAAACTTCTAGCAAATCGCGGTGTCATTACC
C18      GGCCACATGATTCCCTATGATAGACATAGCTAAACTTCTAGCAAATCGCGGTGTCATTACC
C20      GGCCACATGATTCCCTATGATAGACATAGCTAAACTTCTAGCAAATCGCGGTGTCATTACC
NtGT4    GGCCACATGATTCCCTATGATAGACATAGCTAAACTTCTAGCAAATCGCGGTGTCATTACC
C2       GGCCACATGATTCCCTATGATAGACATAGCTAAACTTCTAGCAAATCGCGGTGTCATTACC
          *****

C15      ACTATCATCACCCTCCAGTAAACGCCAATCGTTTCAGTTCAACAATTACTCGTGCCATA
C18      ACTATCATCACCCTCCAGTAAACGCCAATCGTTTCAGTTCAACAATTACTCGTGCCATA
C20      ACTATCATCACCCTCCAGTAAACGCCAATCGTTTCAGTTCAACAATTACTCGTGCCATA
NtGT4    ACTATCATCACCCTCCAGTAAACGCCAATCGTTTCAGTTCAACAATTACTCGTGCCATA
C2       ACTATCATCACCCTCCAGTAAACGCCAATCGTTTCAGTTCAACAATTACTCGTGCCATA
          *****

```

Figure 22 (continued on next page)

```

C15      AAATCCGGTCTAAGAATCCAAATTCTTACACTCAAATTTCCAAGTGTAGAAGTAGGATTA
C18      AAATCCGGTCTAAGAATCCAAATTCTTACACTCAAATTTCCAAGTGTAGAAGTAGGATTA
C20      AAATCCGGTCTAAGAATCCAAATTCTTACACTCAAATTTCCAAGTGTAGAAGTAGGATTA
NtGT4    AAATCCGGTCTAAGAATCCAAATTCTTACACTCAAATTTCCAAGTGTAGAAGTAGGATTA
C2       AAATCCGGTCTAAGAATCCAAATTCTTACACTCAAATTTCCAAGTGTAGAAGTAGGATTA
          *****
C15      CCAGAAGGTTGCGAAAAATATTGACATGCTTCCTTCTCTTGACTTGGCTTCAAAGTTTTTTT
C18      CCAGAAGGTTGCGAAAAATATTGACATGCTTCCTTCTCTTGACTTGGCTTCAAAGTTTTTTT
C20      CCAGAAGGTTGCGAAAAATATTGACATGCTTCCTTCTCTTGACTTGGCTTCAAAGTTTTTTT
NtGT4    CCAGAAGGTTGCGAAAAATATTGACATGCTTCCTTCTCTTGACTTGGCTTCAAAGTTTTTTT
C2       CCAGAAGGTTGCGAAAAATATTGACATGCTTCCTTCTCTTGACTTGGCTTCAAAGTTTTTTT
          *****
C15      GCTGCAATTAGTATGCTGAAACAACAAGTTGAAAATCTCTTAGAAGGAATAAATCCAAGT
C18      GCTGCAATTAGTATGCTGAAACAACAAGTTGAAAATCTCTTAGAAGGAATAAATCCAAGT
C20      GCTGCAATTAGTATGCTGAAACAACAAGTTGAAAATCTCTTAGAAGGAATAAATCCAAGT
NtGT4    GCTGCAATTAGTATGCTGAAACAACAAGTTGAAAATCTCTTAGAAGGAATAAATCCAAGT
C2       GCTGCAATTAGTATGCTGAAACAACAAGTTGAAAATCTCTTAGAAGGAATAAATCCAAGT
          *****
C15      CCAAGTTGTGTTATTTTCAGATATGGGATTTCCCTGGACTACTCAAATGCACAAAATTTT
C18      CCAAGTTGTGTTATTTTCAGATATGGGATTTCCCTGGACTACTCAAATGCACAAAATTTT
C20      CCAAGTTGTGTTATTTTCAGATATGGGATTTCCCTGGACTACTCAAATGCACAAAATTTT
NtGT4    CCAAGTTGTGTTATTTTCAGATATGGGATTTCCCTGGACTACTCAAATGCACAAAATTTT
C2       CCAAGTTGTGTTATTTTCAGATATGGGATTTCCCTGGACTACTCAAATGCACAAAATTTT
          *****
C15      AATATCCCAAGAATTGTTTTTCATGGTACTTGTTGTTTCTCACTTTTATGTTCTTATAAAA
C18      AATATCCCAAGAATTGTTTTTCATGGTACTTGTTGTTTCTCACTTTTATGTTCTTATAAAA
C20      AATATCCCAAGAATTGTTTTTCATGGTACTTGTTGTTTCTCACTTTTATGTTCTTATAAAA
NtGT4    AATATCCCAAGAATTGTTTTTCATGGTACTTGTTGTTTCTCACTTTTATGTTCTTATAAAA
C2       AATATCCCAAGAATTGTTTTTCATGGTACTTGTTGTTTCTCACTTTTATGTTCTTATAAAA
          *****
C15      ATACTTTCCTCCAACATTCCTGAAAATATAACCTCAGATTCAGAGTATTTGTTGTTCCCT
C18      ATACTTTCCTCCAACATTCCTGAAAATATAACCTCAGATTCAGAGTATTTGTTGTTCCCT
C20      ATACTTTCCTCCAACATTCCTGAAAATATAACCTCAGATTCAGAGTATTTGTTGTTCCCT
NtGT4    ATACTTTCCTCCAACATTCCTGAAAATATAACCTCAGATTCAGAGTATTTGTTGTTCCCT
C2       ATACTTTCCTCCAACATTCCTGAAAATATAACCTCAGATTCAGAGTATTTGTTGTTCCCT
          *****
C15      GATTTACCCGATAGAGTCGAACTAACGAAAGCTCAGGTTTCAGGATCGACGAAAAATACT
C18      GATTTACCCGATAGAGTCGAACTAACGAAAGCTCAGGTTTCAGGATCGACGAAAAATACT
C20      GATTTACCCGATAGAGTCGAACTAACGAAAGCTCAGGTTTCAGGATCGACGAAAAATACT
NtGT4    GATTTACCCGATAGAGTCGAACTAACGAAAGCTCAGGTTTCAGGATCGACGAAAAATACT
C2       GATTTACCCGATAGAGTCGAACTAACGAAAGCTCAGGTTTCAGGATCGACGAAAAATACT
          *****
C15      ACTTCTGTTAGTTCTTCTGTATTGAAAGAAGTTACTGAGCAAATCAGATTAGCCGAGGAA
C18      ACTTCTGTTAGTTCTTCTGTATTGAAAGAAGTTACTGAGCAAATCAGATTAGCCGAGGAA
C20      ACTTCTGTTAGTTCTTCTGTATTGAAAGAAGTTACTGAGCAAATCAGATTAGCCGAGGAA
NtGT4    ACTTCTGTTAGTTCTTCTGTATTGAAAGAAGTTACTGAGCAAATCAGATTAGCCGAGGAA
C2       ACTTCTGTTAGTTCTTCTGTATTGAAAGAAGTTACTGAGCAAATCAGATTAGCCGAGGAA
          *****
C15      TCATCATATGGTGAATTGTTAATAGTTTTGAGGAGTTGGAGCAAGTGTATGAGAAAGAA
C18      TCATCATATGGTGAATTGTTAATAGTTTTGAGGAGTTGGAGCAAGTGTATGAGAAAGAA
C20      TCATCATATGGTGAATTGTTAATAGTTTTGAGGAGTTGGAGCAAGTGTATGAGAAAGAA
NtGT4    TCATCATATGGTGAATTGTTAATAGTTTTGAGGAGTTGGAGCAAGTGTATGAGAAAGAA
C2       TCATCATATGGTGAATTGTTAATAGTTTTGAGGAGTTGGAGCAAGTGTATGAGAAAGAA
          *****

```

Figure 22 (continued on next page)

```

C15      TATAGGAAAGCTAGAGGGAAAAAAGTTTGGTGTGTTGGTCCTGTTTCTTTGTGTAATAAG
C18      TATAGGAAAGCTAGAGGGAAAAAAGTTTGGTGTGTTGGTCCTGTTTCTTTGTGTAATAAG
C20      TATAGGAAAGCTAGAGGGAAAAAAGTTTGGTGTGTTGGTCCTGTTTCTTTGTGTAATAAG
NtGT4    TATAGGAAAGCTAGAGGGAAAAAAGTTTGGTGTGTTGGTCCTGTTTCTTTGTGTAATAAG
C2       TATAGGAAAGCTAGAGGGAAAAAAGTTTGGTGTGTTGGTCCTGTTTCTTTGTGTAATAAG
*****

C15      GAAATTGAAGATTTGGTTACAAGGGGTAATAAAACTGCAATTGATAATCAAGATTGCTTG
C18      GAAATTGAAGATTTGGTTACAAGGGGTAATAAAACTGCAATTGATAATCAAGATTGCTTG
C20      GAAATTGAAGATTTGGTTACAAGGGGTAATAAAACTGCAATTGATAATCAAGATTGCTTG
NtGT4    GAAATTGAAGATTTGGTTACAAGGGGTAATAAAACTGCAATTGATAATCAAGATTGCTTG
C2       GAAATTGAAGATTTGGTTACAAGGGGTAATAAAACTGCAATTGATAATCAAGATTGCTTG
*****

C15      AAATGGTTAGATAATTTGAAACAGAATCTGTGGTTTATGCAAGTCTTGGAAGTTTATCT
C18      AAATGGTTAGATAATTTGAAACAGAATCTGTGGTTTATGCAAGTCTTGGAAGTTTATCT
C20      AAATGGTTAGATAATTTGAAACAGAATCTGTGGTTTATGCAAGTCTTGGAAGTTTATCT
NtGT4    AAATGGTTAGATAATTTGAAACAGAATCTGTGGTTTATGCAAGTCTTGGAAGTTTATCT
C2       AAATGGTTAGATAATTTGAAACAGAATCTGTGGTTTATGCAAGTCTTGGAAGTTTATCT
*****

C15      CGTTTGACATTATTGCAAATGGTGGAACTTGGTCTTGGTTTAGAAGAGTCAAATAGGCCT
C18      CGTTTGACATTATTGCAAATGGTGGAACTTGGTCTTGGTTTAGAAGAGTCAAATAGGCCT
C20      CGTTTGACATTATTGCAAATGGTGGAACTTGGTCTTGGTTTAGAAGAGTCAAATAGGCCT
NtGT4    CGTTTGACATTATTGCAAATGGTGGAACTTGGTCTTGGTTTAGAAGAGTCAAATAGGCCT
C2       CGTTTGACATTATTGCAAATGGTGGAACTTGGTCTTGGTTTAGAAGAGTCAAATAGGCCT
*****

C15      TTTGTATGGGTATTAGGAGGAGGTGATAAATTAATGATTTAGAGAAATGGATTCTTGAG
C18      TTTGTATGGGTATTAGGAGGAGGTGATAAATTAATGATTTAGAGAAATGGATTCTTGAG
C20      TTTGTATGGGTATTAGGAGGAGGTGATAAATTAATGATTTAGAGAAATGGATTCTTGAG
NtGT4    TTTGTATGGGTATTAGGAGGAGGTGATAAATTAATGATTTAGAGAAATGGATTCTTGAG
C2       TTTGTATGGGTATTAGGAGGAGGTGATAAATTAATGATTTAGAGAAATGGATTCTTGAG
*****

C15      AATGGATTTGAGCAAAGAATTAAGAAAGAGGAGTTTGGATTAGAGGATGGGCTCCTCAA
C18      AATGGATTTGAGCAAAGAATTAAGAAAGAGGAGTTTGGATTAGAGGATGGGCTCCTCAA
C20      AATGGATTTGAGCAAAGAATTAAGAAAGAGGAGTTTGGATTAGAGGATGGGCTCCTCAA
NtGT4    AATGGATTTGAGCAAAGAATTAAGAAAGAGGAGTTTGGATTAGAGGATGGGCTCCTCAA
C2       AATGGATTTGAGCAAAGAATTAAGAAAGAGGAGTTTGGATTAGAGGATGGGCTCCTCAA
*****

C15      GTGCTTATACTTTCACACCCTGCAATTGGTGGAGTATTGACTCATTGCGGATGGAATTCT
C18      GTGCTTATACTTTCACACCCTGCAATTGGTGGAGTATTGACTCATTGCGGATGGAATTCT
C20      GTGCTTATACTTTCACACCCTGCAATTGGTGGAGTATTGACTCATTGCGGATGGAATTCT
NtGT4    GTGCTTATACTTTCACACCCTGCAATTGGTGGAGTATTGACTCATTGCGGATGGAATTCT
C2       GTGCTTATACTTTCACACCCTGCAATTGGTGGAGTATTGACTCATTGCGGATGGAATTCT
*****

C15      ACATTGGAAGGTATTTGAGCAGGATTACCAATGGTAACATGGCCACTATTTGCTGAGCAA
C18      ACATTGGAAGGTATTTGAGCAGGATTACCAATGGTAACATGGCCACTATTTGCTGAGCAA
C20      ACATTGGAAGGTATTTGAGCAGGATTACCAATGGTAACATGGCCACTATTTGCTGAGCAA
NtGT4    ACATTGGAAGGTATTTGAGCAGGATTACCAATGGTAACATGGCCACTATTTGCTGAGCAA
C2       ACATTGGAAGGTATTTGAGCAGGATTACCAATGGTAACATGGCCACTATTTGCTGAGCAA
*****

C15      TTTTGCAATGAGAAGTTAGTAGTCCAAGTGCTAAAAATTGGAGTGAGCCTAGGTGTGAAG
C18      TTTTGCAATGAGAAGTTAGTAGTCCAAGTGCTAAAAATTGGAGTGAGCCTAGGTGTGAAG
C20      TTTTGCAATGAGAAGTTAGTAGTCCAAGTGCTAAAAATTGGAGTGAGCCTAGGTGTGAAG
NtGT4    TTTTGCAATGAGAAGTTAGTAGTCCAAGTGCTAAAAATTGGAGTGAGCCTAGGTGTGAAG
C2       TTTTGCAATGAGAAGTTAGTAGTCCAAGTGCTAAAAATTGGAGTGAGCCTAGGTGTGAAG
*****

C15      GTGCCGTGCAAAATGGGGAGATGAGGAAAATGTTGGAGTTTGGTAAAAAAGGATGATGTT
C18      GTGCCGTGCAAAATGGGGAGATGAGGAAAATGTTGGAGTTTGGTAAAAAAGGATGATGTT
C20      GTGCCGTGCAAAATGGGGAGATGAGGAAAATGTTGGAGTTTGGTAAAAAAGGATGATGTT
NtGT4    GTGCCGTGCAAAATGGGGAGATGAGGAAAATGTTGGAGTTTGGTAAAAAAGGATGATGTT
C2       GTGCCGTGCAAAATGGGGAGATGAGGAAAATGTTGGAGTTTGGTAAAAAAGGATGATGTT
*****

```

Figure 22 (continued on next page)

```

C15      AAGAAAGCATTAGACAAACTAATGGATGAAGGAGAAGAAGGACAAGTAAGAAGAACAAA
C18      AAGAAAGCATTAGACAAACTAATGGATGAAGGAGAAGAAGGACAAGTAAGAAGAACAAA
C20      AAGAAAGCATTAGACAAACTAATGGATGAAGGAGAAGAAGGACAAGTAAGAAGAACAAA
NtGT4    AAGAAAGCATTAGACAAACTAATGGATGAAGGAGAAGAAGGACAAGTAAGAAGAACAAA
C2       AAGAAAGCATTAGACAAACTAATGGATGAAGGAGAAGAAGGACAAGTAAGAAGAACAAA
          *****
C15      GCAAAGAGTTAGGAGAATTGGCTAAAAAGGCATTTGGAGAAGGTGGTTCTTCTTATGTT
C18      GCAAAGAGTTAGGAGAATTGGCTAAAAAGGCATTTGGAGAAGGTGGTTCTTCTTATGTT
C20      GCAAAGAGTTAGGAGAATTGGCTAAAAAGGCATTTGGAGAAGGTGGTTCTTCTTATGTT
NtGT4    GCAAAGAGTTAGGAGAATTGGCTAAAAAGGCATTTGGAGAAGGTGGTTCTTCTTATGTT
C2       GCAAAGAGTTAGGAGAATTGGCTAAAAAGGCATTTGGAGAAGGTGGTTCTTCTTATGTT
          *****
C15      AACTTAACATCTCTGATTGAAGACATCATTGAGCAACAAAATCACAAGGAAAAACTCGAG
C18      AACTTAACATCTCTGATTGAAGACATCATTGAGCAACAAAATCACAAGGAAAAACTCGAG
C20      AACTTAACATCTCTGATTGAAGACATCATTGAGCAACAAAATCACAAGGAAAAACTCGAG
NtGT4    AACTTAACATCTCTGATTGAAGACATCATTGAGCAACAAAATCACAAGGAAAAATAG---
C2       AACTTAACATCTCTGATTGAAGACATCATTGAGCAACAAAATCACAAGGAAAAATAGCTC
          *****

C15      AATCACTAGT---
C18      AATCACTAGT---
C20      AATCACTAGT---
NtGT4    -----
C2       GAGAATCACTAGT

```

Figure 22: Nucleotide Sequence Alignment of *NtGT4* and pGEMT-SBIP68 Clones. Clones C2, C15, C18, and C20. The arrow indicates the single nucleotide difference between *NtGT4* and pGEMT-SBIP68 clones.

```

NtGT4    MATQVHKLHFILFPLMAPGHMIPMIDIAKLLANRGVITTIITT PVNANRFSSTITRAIKS
C2       MATQVHKLHFILFPLMAPGHMIPMIDIAKLLANRGVITTIITT PVNANRFSSTITRAIKS
C15     MATQVHKLHFILFPLMAPGHMIPMIDIAKLLANRGVITTIITT PVNANRFSSTITRAIKS
*****

NtGT4    GLRIQILTLKFPSVEVGLPEGCENIDMLPSLDLASKFFAAISMLKQQVENLLEGINPSPS
C2       GLRIQILTLKFPSVEVGLPEGCENIDMLPSLDLASKFFAAISMLKQQVENLLEGINPSPS
C15     GLRIQILTLKFPSVEVGLPEGCENIDMLPSLDLASKFFAAISMLKQQVENLLEGINPSPS
*****

NtGT4    CVISDMGFPWITQIAQNFNIPRIVFHGTCCFSL LCSYKILSSNILENITSDSEYFVVPDL
C2       CVISDMGFPWITQIAQNFNIPRIVFHGTCCFSL LCSYKILSSNILENITSDSEYFVVPDL
C15     CVISDMGFPWITQIAQNFNIPRIVFHGTCCFSL LCSYKILSSNILENITSDSEYFVVPDL
*****

NtGT4    PDRV ELTKAQVSGSTKNTTSVSSSVLKEVTEQIRLAEESYGVIVNSFEELEQVYEKEYR
C2       PDRV ELTKAQVSGSTKNTTSVSSSVLKEVTEQIRLAEESYGVIVNSFEELEQVYEKEYR
C15     PDRV ELTKAQVSGSTKNTTSVSSSVLKEVTEQIRLAEESYGVIVNSFEELEQVYEKEYR
*****

NtGT4    KARGKVVWCVGPVSLCNKEIEDLVTRGNHTAIDNQDCLKWLDNFETESVVYASLGSL SRL
C2       KARGKVVWCVGPVSLCNKEIEDLVTRGNHTAIDNQDCLKWLDNFETESVVYASLGSL SRL
C15     KARGKVVWCVGPVSLCNKEIEDLVTRGNHTAIDNQDCLKWLDNFETESVVYASLGSL SRL
*****

NtGT4    TLLQMVELGLGLEESNRPFVWVLGGDKLNDLEKWI LENGFEQRIKERGV LIRGWAPQVL
C2       TLLQMVELGLGLEESNRPFVWVLGGDKLNDLEKWI LENGFEQRIKERGV LIRGWAPQVL
C15     TLLQMVELGLGLEESNRPFVWVLGGDKLNDLEKWI LENGFEQRIKERGV LIRGWAPQVL
*****

NtGT4    ILSHPAIGGVLTHCGWNSTLEGISAGLPMVTWPLFAEQFCNEKLVVQVLKIGVSLGVKVP
C2       ILSHPAIGGVLTHCGWNSTLEGISAGLPMVTWPLFAEQFCNEKLVVQVLKIGVSLGVKVP
C15     ILSHPAIGGVLTHCGWNSTLEGISAGLPMVTWPLFAEQFCNEKLVVQVLKIGVSLGVKVP
*****

NtGT4    VKWGDEENVGVLVKDDVKKALDKLMDEGEEGQVRRTKAKELGELAKKAFEGGSSYVNL
C2       VKWGDEENVGVLVKDDVKKALDKLMDEGEEGQVRRTKAKELGELAKKAFEGGSSYVNL
C15     VKWGDEENVGVLVKDDVKKALDKLMDEGEEGQVRRTKAKELGELAKKAFEGGSSYVNL
*****

NtGT4    TSLIEDIIEQQNHKEK
C2       TSLIEDIIEQQNHKEK
C15     TSLIEDIIEQQNHKEK
*****

```

Figure 23: Amino Acid Sequence Alignment of *NtGT4* and pGEMT-SBIP68 Clones, C2 and C15. All sequences are identical.

A**>SBIP68_Nucleotide**

ATGGCAACTCAAGTGCACAAACTTCATTTTCATACTATTCCCTTTAATGGCTCCAGGCCACATGATTCCCTATGAT
AGACATAGCTAAACTTCTAGCAAATCGCGGTGTCATTACCACTATCATCACCCTCCAGTAAACGCCAATCGTT
TCAGTTCAACAATTACTCGTGCCATAAAAATCCGGTCTAAGAATCCAAATTCCTTACACTCAAATTTCCAAGTGTA
GAAGTAGGATTACCAGAAGGTTGCGAAAATATTGACATGCTTCCTTCTCTTGACTTGGCTTCAAAGTTTTTTGC
TGCAATTAGTATGCTGAAACAACAAGTTGAAAATCTCTTAGAAGGAATAAATCCAAGTCCAAGTTGTGTTATTT
CAGATATGGGATTTCCCTGGACTACTCAAATTGCACAAAATTTTAATATCCCAAGAATTGTTTTTTCATGGTACT
TGTTGTTTTCTCACTTTTATGTTCCCTATAAAAATACTTTCTCCAACATTCTTGAAAATATAACCTCAGATTGAGA
GTATTTTGTGTTCCCTGATTTACCCGATAGAGTCGAACTAACGAAAGCTCAGGTTTCAGGATCGACGAAAAATA
CTACTTCTGTTAGTTCCTCTGTATTGAAAGAAGTTACTGAGCAAATCAGATTAGCCGAGGAATCATCATATGGT
GTAATTGTTAATAGTTTTGAGGAGTTGGAGCAAGTGTATGAGAAAGAATATAGGAAAGCTAGAGGGAAAAAAGT
TTGGTGTGTTGGTCCCTGTTTCTTTGTGTAATAAGGAAATTGAAGATTTGGTTACAAGGGGTAATAAAACTGCAA
TTGATAATCAAGATTGCTTGAAATGGTTAGATAATTTTGAAACAGAATCTGTGGTTTATGCAAGTCTTGGAAGT
TTATCTCGTTTTGACATTATTGCAAATGGTGGAACTTGGTCTTGGTTTTAGAAGAGTCAAATAGGCCCTTTTGTATG
GGTATTAGGAGGAGGTGATAAATTAATGATTTAGAGAAATGGATTCTTGAGAATGGATTTGAGCAAAGAATTA
AAGAAAGAGGAGTTTTGATTAGAGGATGGGCTCCTCAAGTGCTTATACTTTACACCCTGCAATTTGGTGGAGTA
TTGACTCATTGCGGATGGAATTCTACATTGGAAGGTATTTGAGCAGGATTACCAATGGTAACATGGCCACTATT
TGCTGAGCAATTTGCAATGAGAAGTTAGTAGTCCAAGTGCTAAAAATTGGAGTGAGCCTAGGTGTGAAGGTGC
CTGTCAAATGGGGAGATGAGGAAAATGTTGGAGTTTTGGTAAAAAAGGATGATGTTAAGAAAGCATTAGACAAA
CTAATGGATGAAGGAGAAGAAGGACAAGTAAGAAGAACAAGCAAAAGAGTTAGGAGAATTGGCTAAAAAGGC
ATTTGGAGAAGGTGGTTCCTTCTTATGTTAACTTAACATCTCTGATTGAAGACATCATTGAGCAACAAAATCACA
AGGAAAAATAG

B**>SBIP68_Protein**

MATQVHKLHFI L FPLMAPGHMIPMIDI AKLLANRGVITTTITTPV N ANRFSSTITRAIKSGLRIQILTLKFPSV
EVGLPEGCENIDMLPSLDLASKFFFAAISMLKQQVENLLEGINPSPSCVISDMGF PWTQIAQNFNIPRIVFHGT
CCFSL L CSYKILSSNILENITSDSEYFVVPDL PDRVELTKAQVSGSTKN TTSVSSSVLKEVTEQIRLAEESSYG
VIVNSFE ELEQVYEKEYRKARGKKVWCVGPVSLCNKEIEDLVTRGNKTAIDNQDCLKWLDNFETESV VYASLGS
LSRLTLLQMVELGLGLEESNRPFVWVLGGDKLNDLEKWILENGFEQRIKERGVLRG **WAPQVLILSHPAIGGV**
LTHCGWNSTLEGISAGLPMVTWPLFAEQFCNEKLVVQVLKIGVSLGVKVPVKWGDEENVGVLVKKDDVKKALDK
LMDEGEEGQVRRTKAKELGELAKKAFGEGGSSYVNLTS LIEDIIEQQNHKEK

Figure 24: Full Length SBIP68 Sequence Cloned from *Nicotiana tabacum*. **A.** Nucleotide sequence. **B.** Translated amino acid sequence, a putative PSPG Box (355-398) is highlighted.

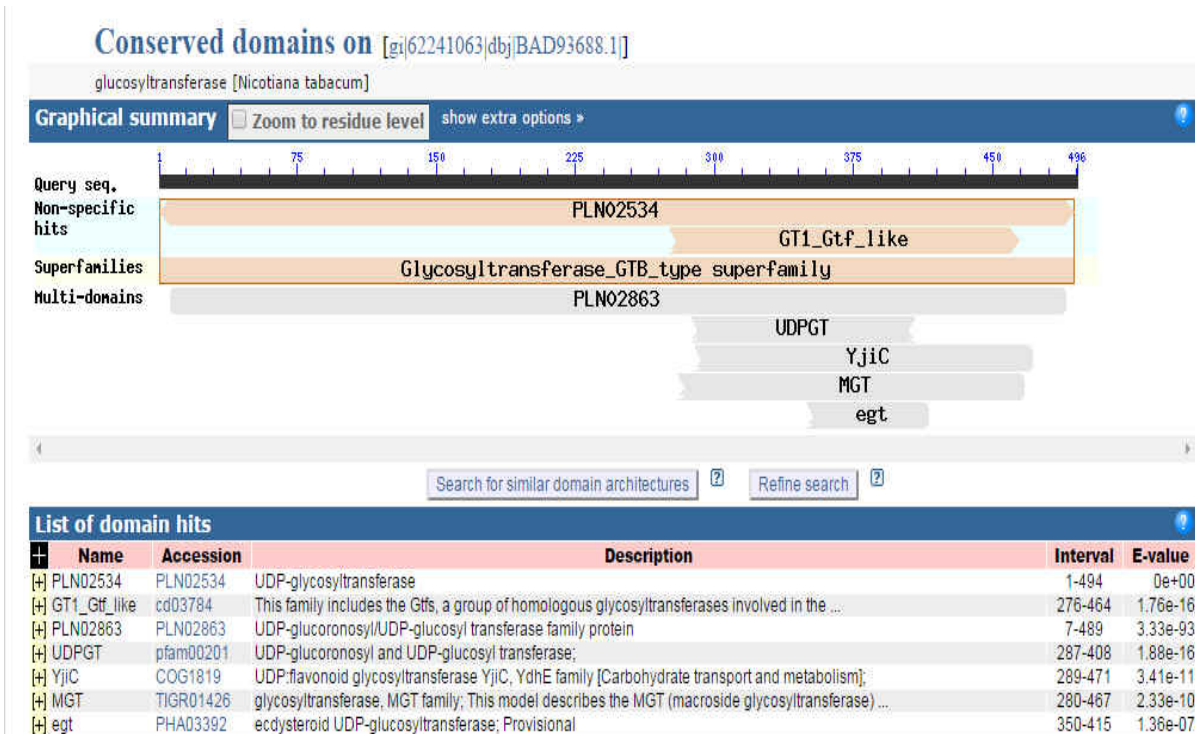


Figure 25: SBIP68 Protein BLAST Query. SBIP68 is a GTB_type protein with putative GT1_Gtf and UDPGT conserved domains amongst others.

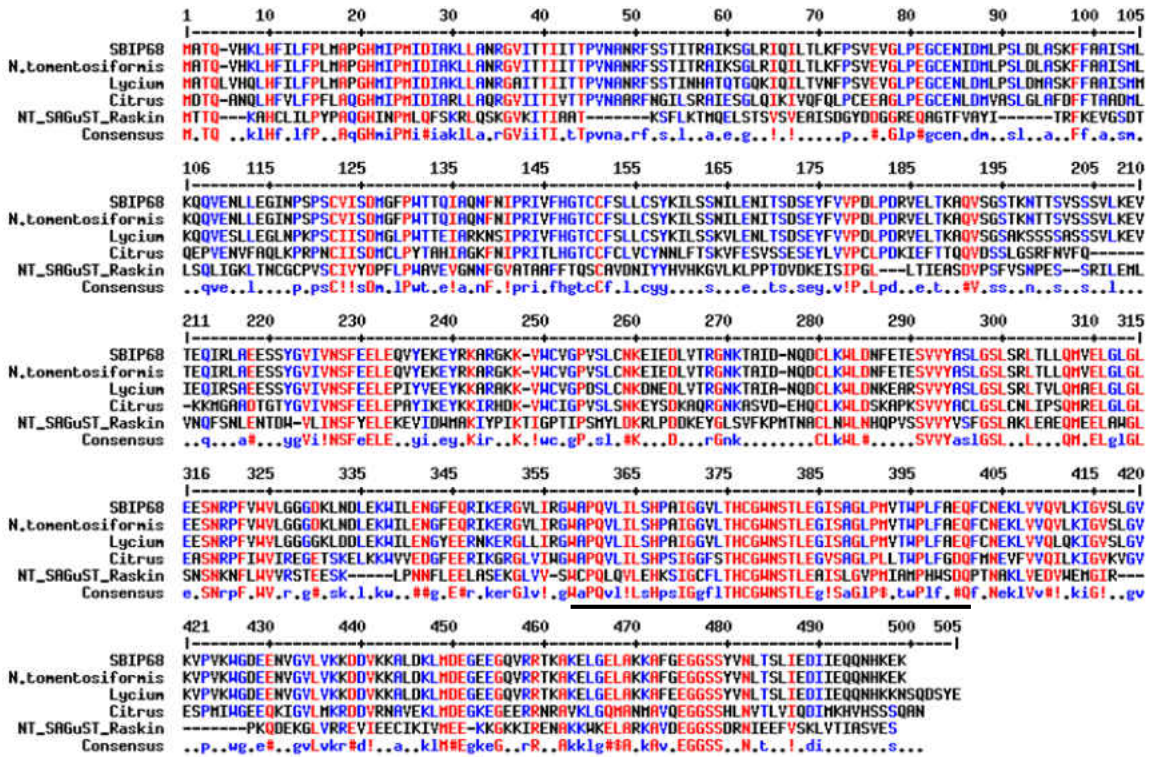


Figure 26: Alignment of SBIP68 with Other Similar Glucosyltransferases. *N. tomentosiformis* putative UDP-glycosyltransferase (NCBI reference sequence: XP_009623864.12014), *Lycium barbarum* putative glucosyltransferase UGT73E5 (GenBank: BAG80535.1), *Citrus paradisi* putative flavonoid UDP-glycosyltransferase 2 (GenBank: AIS39471.1), *Nicotiana tabacum* SA GTase (GenBank: AAF61647.1).

PCR Screening of pET-28a-SBIP68 Bacterial Clones

The pGEMT-SBIP68 (644 & 645) plasmids were restriction digested and the fragments gel purified. The gel purified SBIP68 (644 & 645) were ligated into pET-28a vector digested with the same set of enzymes. The resulting pET-28a-SBIP68 constructs were used to transform competent bacterial cells (BL21(DE3) pLysE) capable of recombinant protein expression. The cells were plated and incubated, after which several clones were tested for presence of the plasmids using colony PCR. The PCR products were analyzed by agarose electrophoresis (Fig. 27).

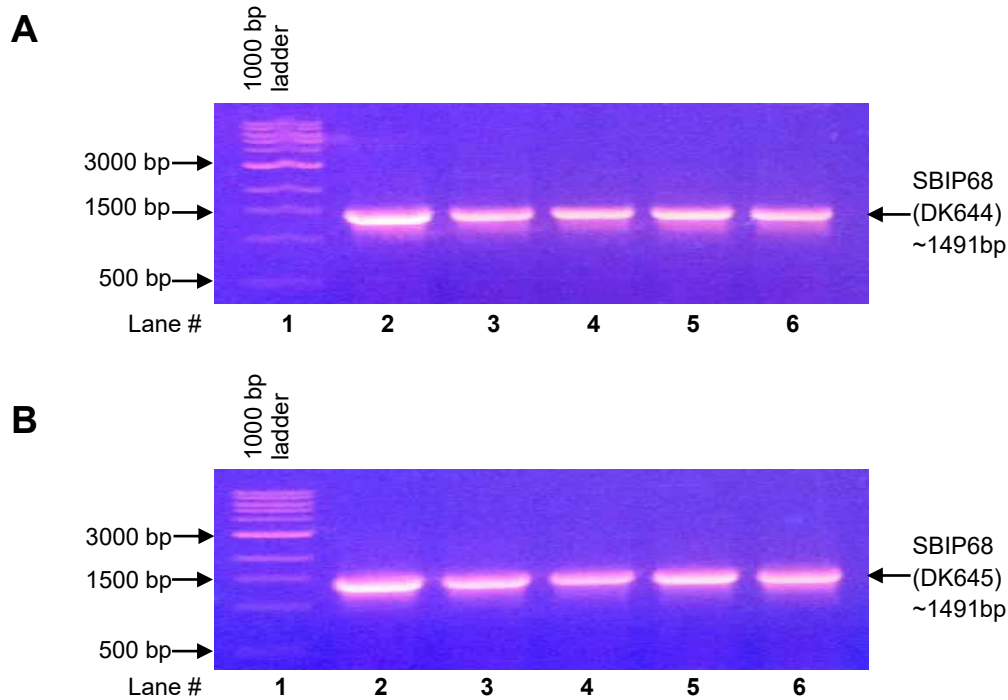


Figure 27: Colony PCR Screening of pET28a-SBIP68 Clones. Agarose gel (0.8%) showing PCR amplified SBIP68. All clones tested were positive for the presence of insert. **A.** Colony PCR of 644, gene specific DK643 forward and DK644 reverse primer were used for PCR. Lane numbers 2, 3, 4, 5, and 6 represent clones 1, 2, 3, 4, and 5, respectively. **B.** Colony PCR of 645, gene specific DK643 forward primer and gene specific DK645 reverse primer were used for PCR. Lane numbers 2, 3, 4, 5, and 6 represent clones 6, 7, 8, 9, and 10, respectively.

Test for Recombinant pET-28a-SBIP68 Protein Expression

Clones which were positive for pET-28a-SBIP68 were used for protein expression. To start the culture, 3 ml of LB with kanamycin were inoculated with a single isolated colony and incubated in a shaker at 37 °C for 2 hours (see materials and methods). Protein expression was induced by adding 1mM IPTG (final concentration) and cultures were further incubated for 3 hours at 37°C. Pellets were collected and processed as previously described. Samples were analyzed by SDS PAGE gel followed

by coomassie blue staining (Fig. 28). It is not clear from the SDS-PAGE analysis which of the expressed proteins are SBIP68 644 (expected size, ~58.5 kDa) or 645 (expected size, ~59.6 kDa).

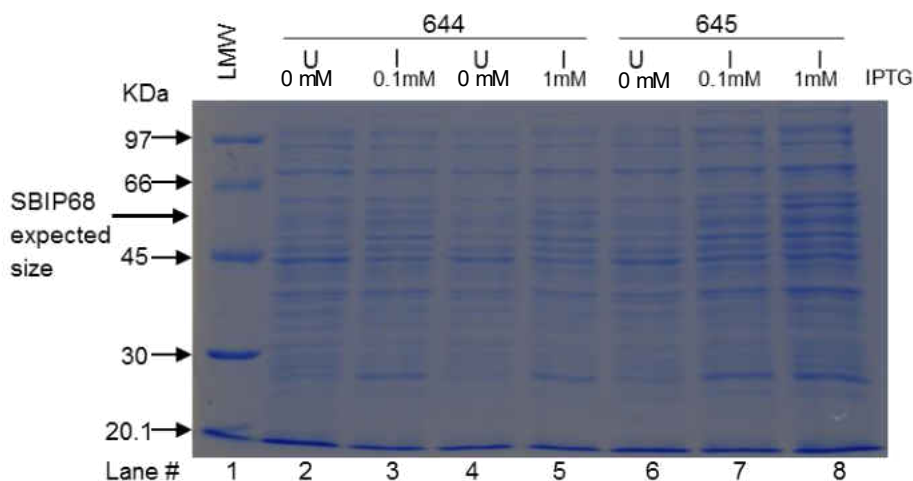


Figure 28: SDS-PAGE of pET-28a-SBIP68 (644 & 645) Expressed in *E. coli*. In lane 1 is the low molecular weight marker, lanes 2 and 4 are pET-28a-SBIP68 (644) from uninduced bacterial cultures. Lanes 3 and 5 contain pET-28a-SBIP68 (644) from 0.1mM and 1mM IPTG induced bacterial cultures respectively. Lane number 6 contains pET-28a-SBIP68 (645) from uninduced bacterial culture, while lane numbers 7 and 8 contain pET-28a-SBIP68 645 from 0.1mM and 1mM IPTG induced bacterial cultures respectively. 'U' in the figure stands for uninduced and 'I' is for induced.

To specifically detect recombinant SBIP68, Western blot analysis using anti-polyhistidine primary antibody was performed (Fig. 29A). Recombinant SBIP68 was highly expressed in IPTG induced cultures (Lane #3, 5, 7, and 9) compared to uninduced cultures (Lane #2, 4, 6, and 8). Recombinant SBIP68 was expressed at higher levels in 645 (lane #2 - 5) compared to 644 (Lane #6 - 9). Low level recombinant protein was also detected in uninduced cultures (lane #2, 3, 6, and 8). The extra bands seen in lane #3, 5, 7, and 9 (Fig. 29A) could be as a result of degradation of SBIP68. It is also possible that there are proteins indigenous to the expression host that have

polyhistidine. To visualize the loaded proteins, the blot was later stained with coomassie blue (Fig. 29B).

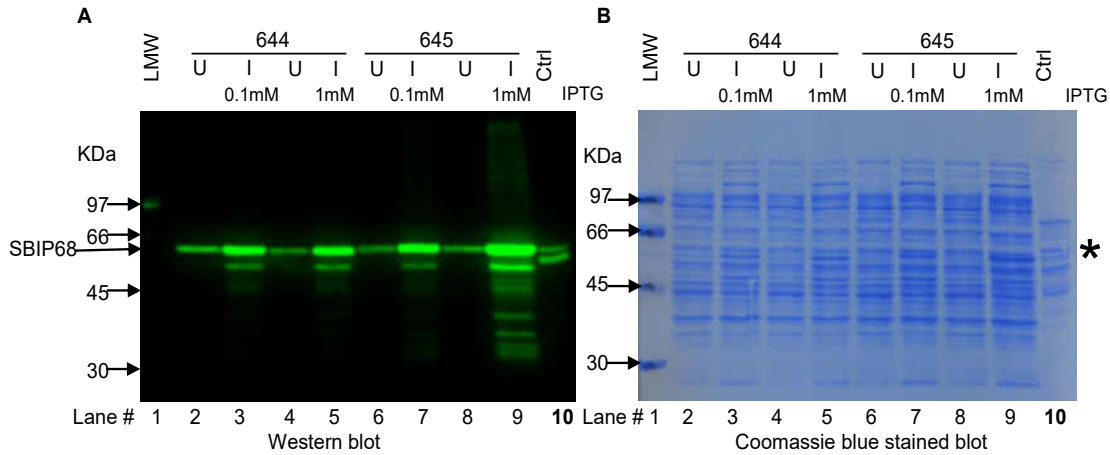


Figure 29: Test for Expression of pET28a-SBIP68 (644) and (645) in *E. coli*. **A.** Western Blot Analysis of pET-28a-SBIP68 (644 & 645) recombinant proteins expression in *E. coli*. Lane 1 shows the low molecular weight marker, lanes 2 and 4 are pET-28a-SBIP68 644 from uninduced bacterial cultures, while lanes 3 and 5 are pET-28a-SBIP68 644 from 0.1mM and 1mM IPTG induced bacterial cultures respectively. Lane numbers 6 and 8 contain pET-28a-SBIP68 645 from uninduced bacterial cultures, while lane numbers 7 and 9 contain pET-28a-SBIP68 645 from 0.1mM and 1mM IPTG induced bacterial cultures respectively. Lane 10 served as a positive control for Western blot. **B.** Corresponding coomassie blue stained blot. The membrane was stained after Western blot analysis. 'U' in the figures stand for uninduced and 'I' for induced. The asterisk indicates SBIP68's expected position on the blot.

Recombinant pET-28a-SBIP68 Protein Solubility Test

A solubility test was performed to verify if SBIP68 was being expressed in the soluble or insoluble protein fractions. pET-28a-SBIP68 (644) and 645 in *E. coli* cells were cultured and the pellets derived following induction with IPTG were processed as described in materials and methods. The supernatants (soluble) and pellet (insoluble) fractions were analyzed by Western blot (Fig. 30A). Western blot analysis revealed that pET-28a-SBIP68 (644) & (645) are both expressed mostly in the insoluble (lane # 3, 5,

7, and 9) form but a small fraction was also expressed in the soluble form (lane # 4, 6, 8, and 10). The extra bands seen in lane # 3, 5, 7, 8, 9, and 10 (Fig. 30A), are either degradation products of SBIP68 and/ or non-specific host proteins. Upon the completion of Western blot, the membrane was stained with coomassie blue (Fig. 30B).

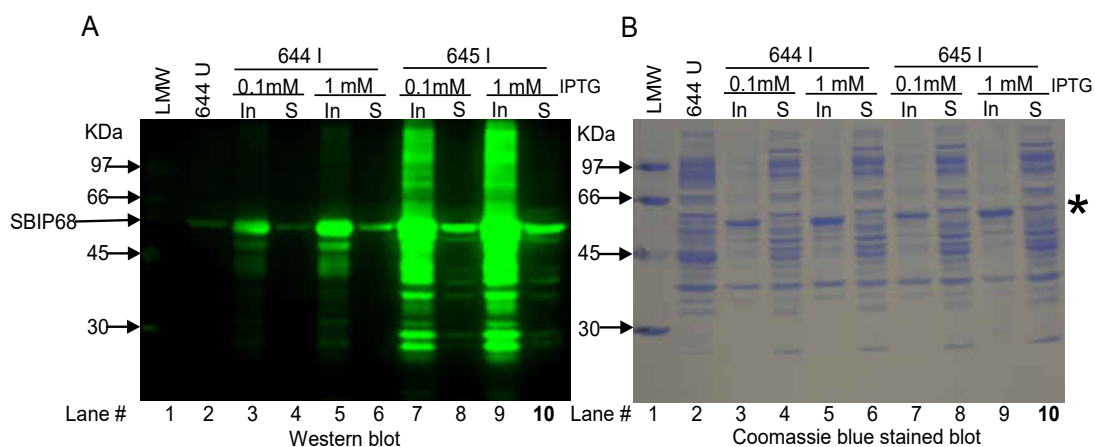


Figure 30: Solubility Test of Expressed pET28a-SBIP68 (644) and (645). **A.** Western blot analysis of 644 & 645 recombinant proteins. Lane#1 shows the low molecular weight marker. Lane#2 is 644 from uninduced bacterial culture. Lanes 3 and 4 consist of insoluble and soluble cell fractions from 0.1mM IPTG induced 644 bacterial culture respectively, while lanes 5 and 6 are insoluble and soluble cell fractions from 1mM IPTG induced 644 bacterial culture respectively. Lanes 7 and 8 contain insoluble and soluble cell fractions from 0.1mM IPTG induced 645 bacterial culture respectively, while lanes 9 and 10 contain insoluble and soluble cell fractions from 1mM IPTG induced 645 bacterial culture respectively. **B.** Corresponding coomassie blue stained blot. The membrane was stained after Western blot analysis. ‘U’ and ‘I’ in the figures stand for uninduced and induced respectively. ‘In’ and ‘S’ represent insoluble and soluble respectively. The asterisk indicates SBIP68’s expected position on the blot.

Optimization of Conditions for Protein Solubility

In a bid to increase the amount of soluble SBIP68 recombinant protein, the conditions for expression were fine-tuned by lowering the incubation temperature for expression to 17 °C and different IPTG concentrations (1 mM, 0.1 mM, and 0.01 mM).

Induction at 37 °C and 1 mM IPTG concentration was also performed simultaneously to serve as a control. pET-28a-SBIP68 (644) and 645 in *E. coli* cells were cultured and protein expression induced with IPTG. The pellets were processed as described in materials and methods. The supernatants (soluble) and pellet (insoluble) fractions from the 17 °C expression (Fig. 31A), and 37 °C expression (Fig. 31C), were analyzed by Western blot. Western blot analysis revealed that there was no significant difference in the amount of soluble pET-28a-SBIP68 (644) & (645) recombinant proteins expressed at the different temperatures (17 °C and 37 °C). The membranes were stained with coomassie blue after Western blot to visualize total protein loaded in the gel (Fig. 31B, and Fig. 31D for 17 °C and 37 °C, respectively).

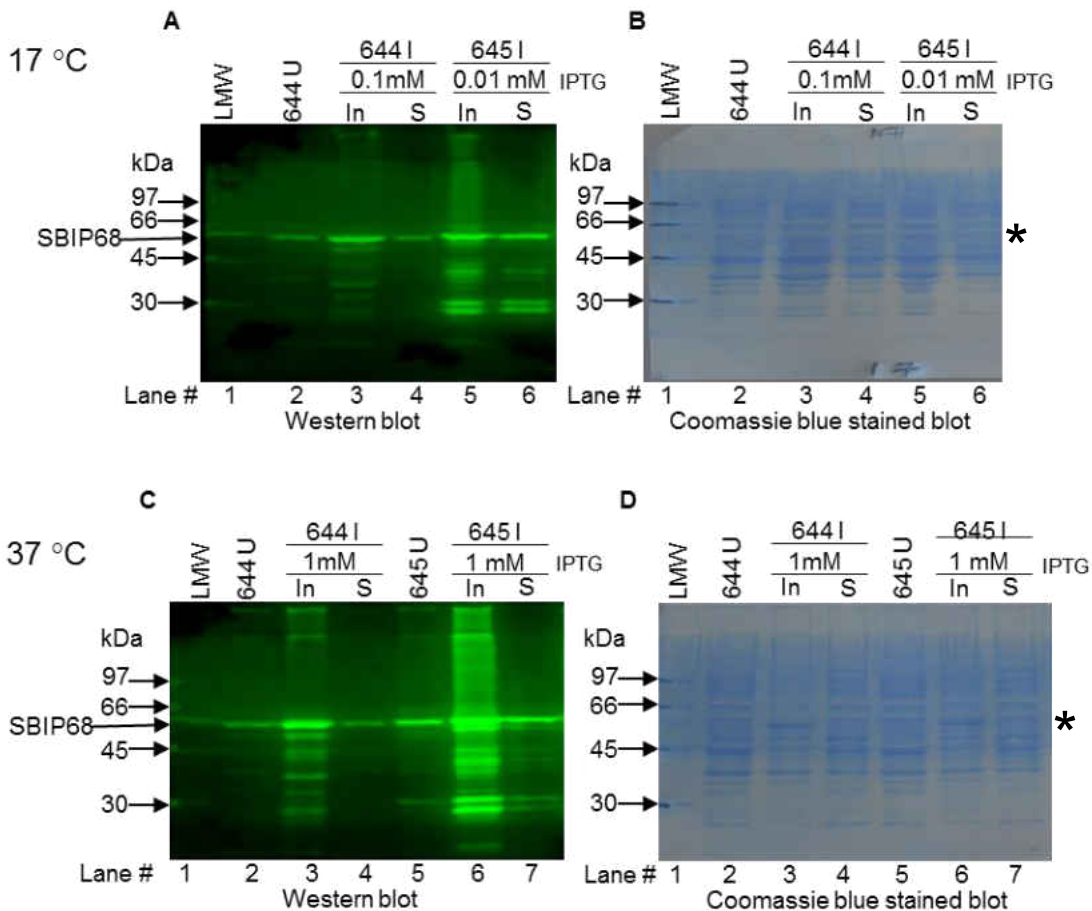


Figure 31: Optimization of Protein Solubility. Solubility Test of Expressed pET28a-SBIP68 (644) and (645). **A.** Western blot analysis of 644 & 645 recombinant protein solubility at 17 °C. Lane one shows the low molecular weight marker. Lane 2 is 644 from uninduced bacterial culture. Lanes 3 and 4 consist of insoluble and soluble cell fractions from 0.1mM IPTG induced 644 bacterial culture respectively, while lanes 5 and 6 are insoluble and soluble cell fractions from 0.01mM IPTG induced 645 bacterial culture respectively. **B.** Corresponding coomassie blue stained blot after Western blot analysis. **C.** Western blot analysis of 644 & 645 recombinant protein solubility at 37 °C. Lane one shows the low molecular weight marker. Lane 2 is 644 from uninduced bacterial culture. Lanes 3 and 4 consist of insoluble and soluble cell fractions from 1mM IPTG induced 644 bacterial culture respectively. Lane 5 is 645 from uninduced bacterial culture while lanes 6 and 7 are insoluble and soluble cell fractions from 1mM IPTG induced 645 bacterial culture respectively. **D.** Coomassie blue stained blot after Western blot analysis. There appears to be no significant difference in the amount of soluble SBIP68 produced at different temperatures. The major difference here is the amount of insoluble protein being produced and this is due to the different concentrations of IPTG used in inducing expression. The asterisks indicate SBIP68's expected position on the blots.

Affinity Purification of Recombinant SBIP68 Protein

To purify the soluble recombinant SBIP68, large scale expression was conducted. Bacterial cell pellets derived from 100 ml cultures from expression at 17 °C and 37 °C were resuspended in 3 ml of 1 x Ni-NTA binding buffer containing PMSF each. The cell lysates were collected and recombinant SBIP68 was purified using a Ni-NTA column. The column was washed with 15 ml of 1 x Ni-NTA wash / binding buffer (containing 15 mM imidazole) at room temperature. Elution of 6xHis-tagged SBIP68 protein was achieved by 1 x Ni-NTA buffer containing 250 mM imidazole. The eluted fractions (1 ml each) were analyzed by Western blot (Fig. 32A, Fig. 32C, Fig. 32E). After Western blot, the membranes were stained with coomassie blue (Fig. 32B, Fig. 32D, Fig. 32F). In lane # 3 of Figures 32A, 32C, and 32E, SBIP68 can be seen in the flow through. This is probably as a result of the presence of 15 mM imidazole in the wash/binding buffer. The pellets were resuspended in the binding buffer before lysis with the French press. In other words, the binding buffer served as the lysis buffer, this was done to minimize non-specific binding by non-target proteins. Another possibility is that the Ni-NTA columns were saturated by the bound protein and could not hold any more (their binding capacity was reached), so the excess proteins eluted in the flow through. A combination of both factors, that is imidazole and binding capacity, could also have been responsible for the elution of SBIP68 in the flow through.

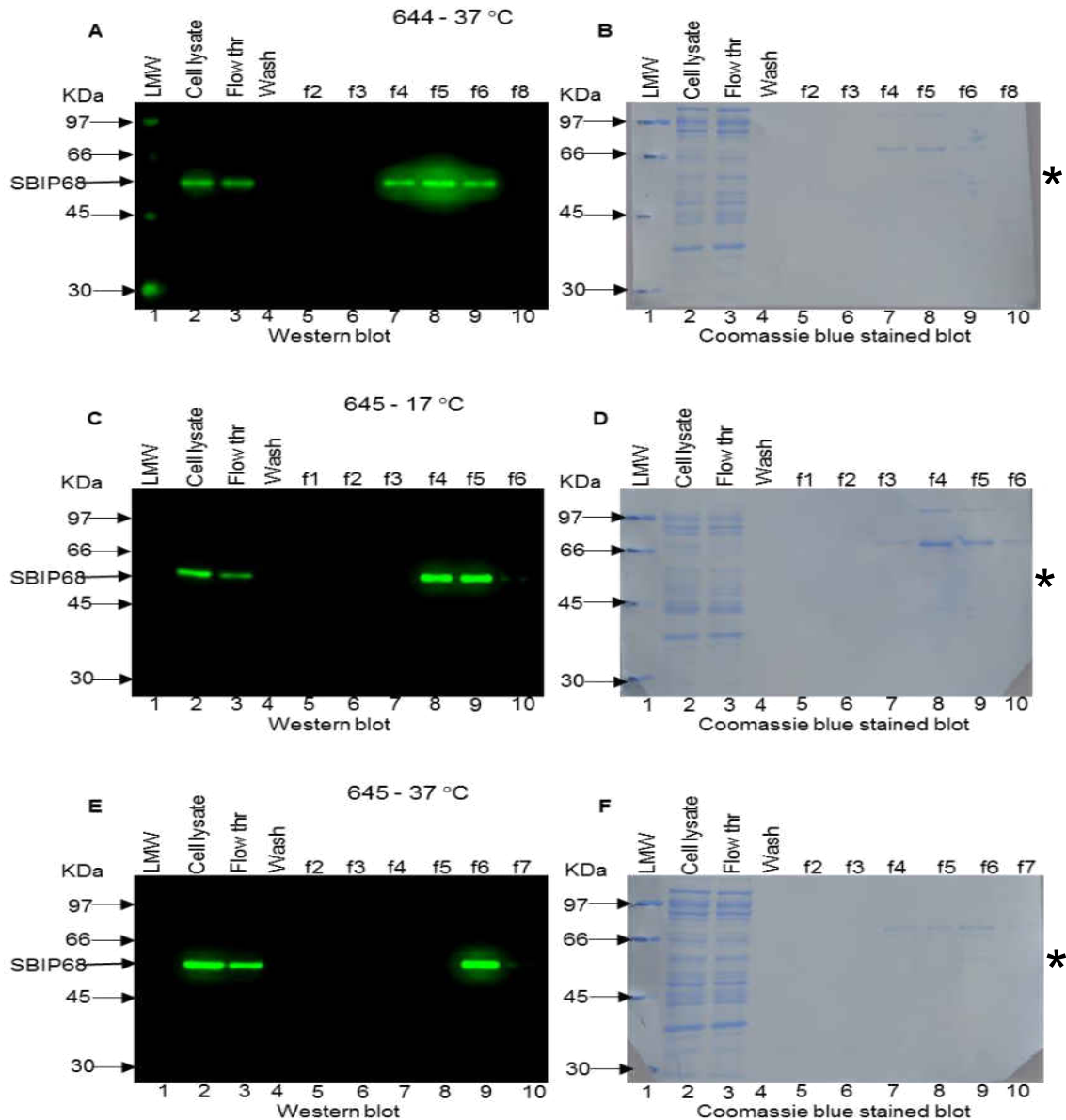


Figure 32 A-F: Ni-NTA Purification of SBIP68 Expressed in *E. coli*. **A.** Western blot analysis of 644 expressed at 37 °C and 1 mM IPTG concentration. In lane 2 is the cell lysate before purification, lane 3 is the flow through and lane 4 wash. Lanes 5 to 10 contain fraction numbers 2, 3, 4, 5, 6, and 8, respectively collected from the purification process. **B.** Corresponding coomassie blue stained blot. **C.** Western blot analysis of 645 expressed at 17 °C and 0.01 mM IPTG concentration. In lane 2 is the cell lysate before purification, lane 3 is the flow through and lane 4 wash. Lanes 5 to 10 contain fraction numbers 1, 2, 3, 4, 5, and 6, respectively. **D.** Corresponding coomassie blue stained blot. **E.** Western blot analysis of 645 expressed at 37 °C and 1 mM IPTG concentration. In lane 2 is the cell lysate before purification, lane 3 is the flow through and lane 4 wash. Lanes 5 to 10 contain fraction numbers 2, 3, 4, 5, 6, and 7, respectively. **F.** Corresponding coomassie blue stained blot. The asterisks indicate SBIP68's expected position on the blots.

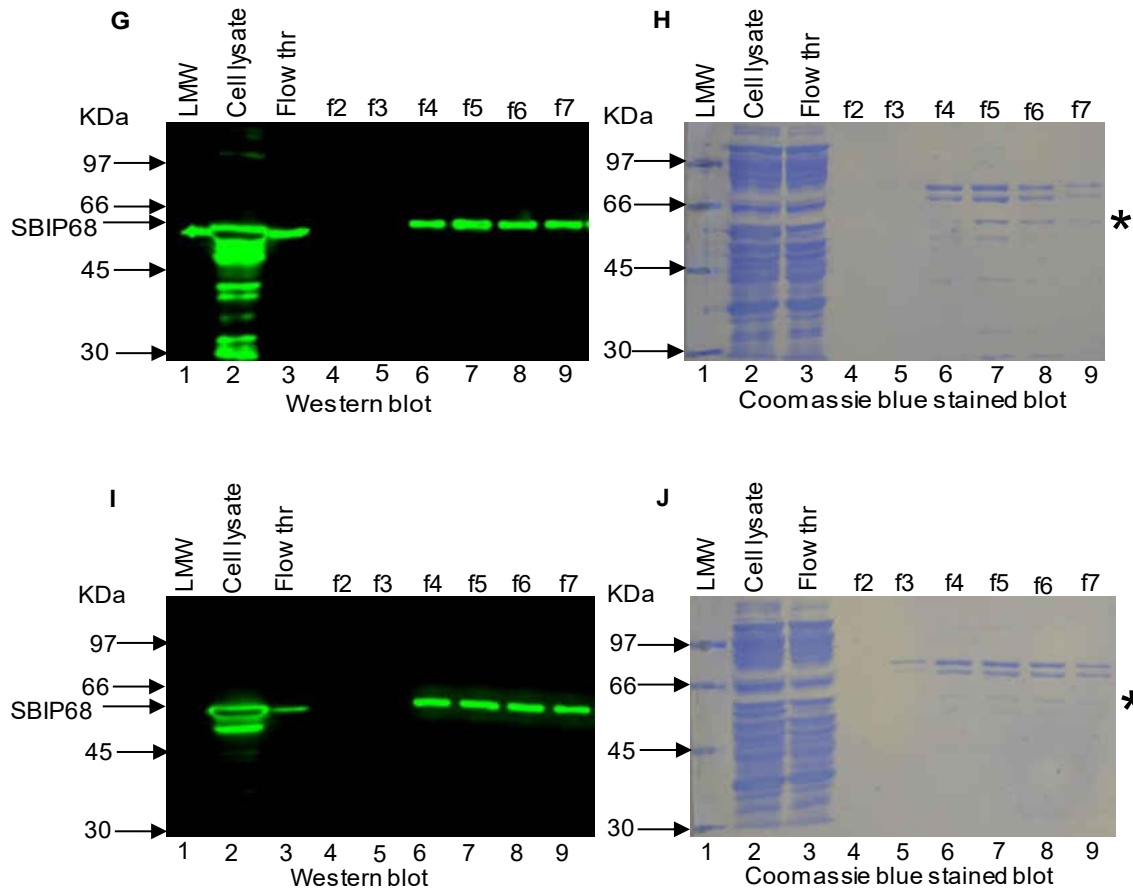


Figure 32 G-J: Ni-NTA Purification of SBIP68 Expressed in *E. coli*. **G.** Western blot analysis of 645 expressed at 37 °C and 0.2 mM IPTG concentration. In lane 2 is the cell lysate before purification, and lane 3 is the flow through. Lanes 4 to 9 contain fraction numbers 2, 3, 4, 5, 6, and 7, respectively collected from the purification process. **H.** Corresponding coomassie blue stained blot. **I.** Western blot analysis of 644 expressed at 37 °C and 0.2 mM IPTG concentration. In lane 2 is the cell lysate before purification, and lane 3 is the flow through. Lanes 4 to 9 contain fraction numbers 2, 3, 4, 5, 6, and 7, respectively collected from the purification process. **J.** Corresponding coomassie blue stained blot. The asterisks indicate SBIP68's expected position on the blots.

HPLC Analysis of Glucosyltransferase Activity Assay Products

After determining that large scale expression of SBIP68 in *E. coli* produced some soluble protein, SBIP68 was again expressed, purified, and used to test enzymatic activity (Fig. 32G, Fig. 32I). HPLC analysis was performed to identify the products of the

glucosyltransferase reactions using purified SBIP68 as described in the materials and methods. The acceptor substrates tested were kaempferol, quercetin, hesperetin, and naringenin (Fig. 33, Fig. 34). Kaempferol, kaempferol 3-O-glucoside, quercetin, quercetin 3-O-glucoside, naringenin, naringenin 7-O-glucoside, and hesperetin were used as standards in the identification of the reaction products.

The cloning and heterologous expression of SBIP68 in *E. coli* (prokaryote) and *P. pastoris* (eukaryote) was performed simultaneously. This was done because there are well known limitations to the expression of functional recombinant proteins with eukaryotic origins in prokaryotic systems, and at the time of cloning there was no idea as to just how much SBIP68 would be expressed in the soluble (functional) form in *E. coli*. As can be seen from the results of the expression of SBIP68 in *E. coli*, a greater percentage of expressed SBIP68 was present in the (non-functional) insoluble form (Figs. 30 and 31).

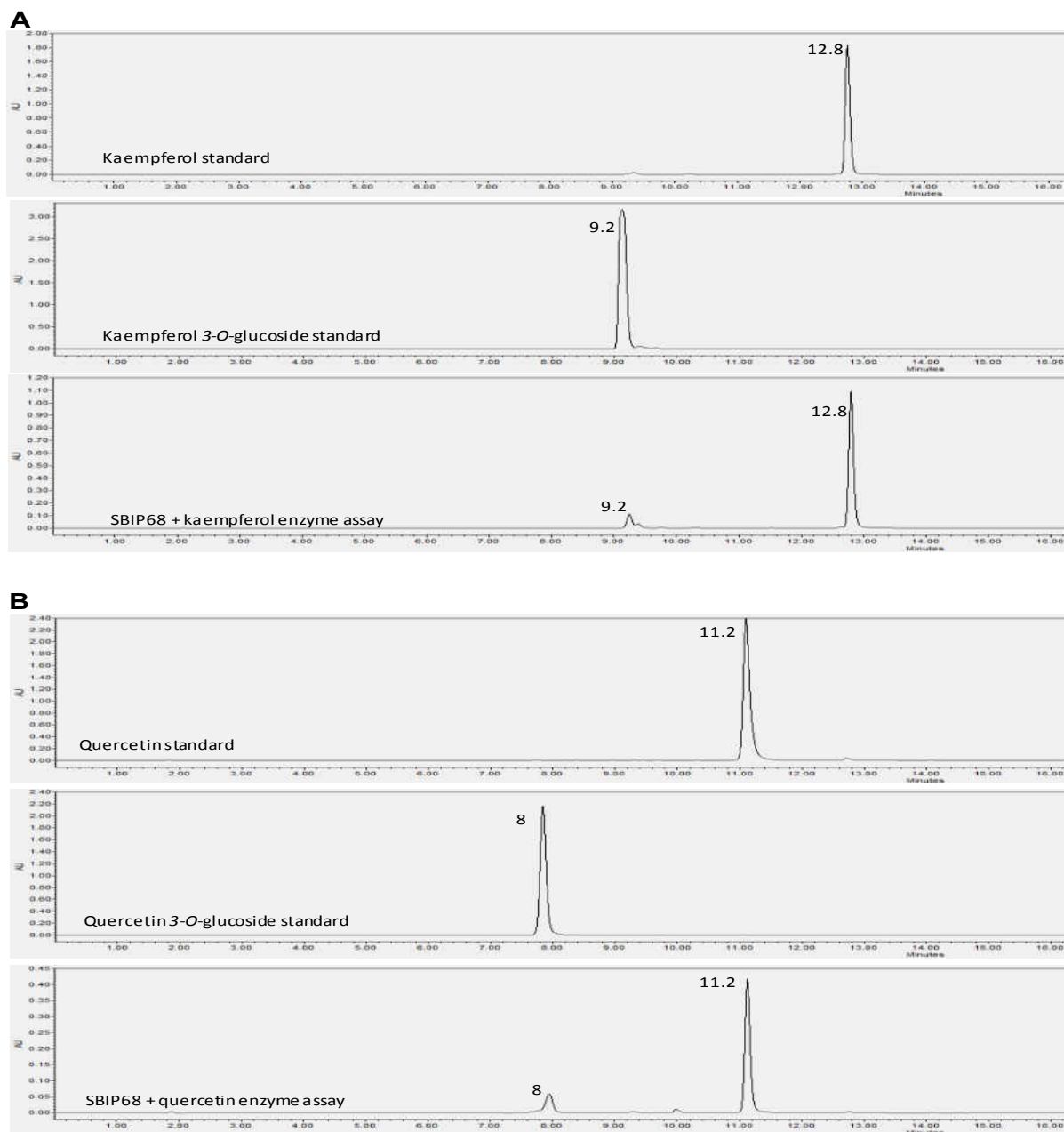


Figure 33 A-B: GT Assay using *E. coli* Expressed SBIP68 (645). **A.** Top panel shows retention time for kaempferol standard at 12.7 minutes, middle panel shows retention time for kaempferol 3-O-glucoside standard at 9.2 minutes. The bottom panel shows the products formed from the reaction with SBIP68-645, kaempferol 3-O-glucoside and kaempferol, with retention times at 9.2 minutes and 12.8 minutes respectively. **B.** Top panel shows retention time for quercetin standard at 11.2 minutes, middle panel shows retention time for quercetin 3-O-glucoside standard at 8 minutes. The bottom panel shows the products formed from the reaction with SBIP68-645, quercetin 3-O-glucoside and quercetin, with retention times at 8 minutes and 11.2 minutes respectively.

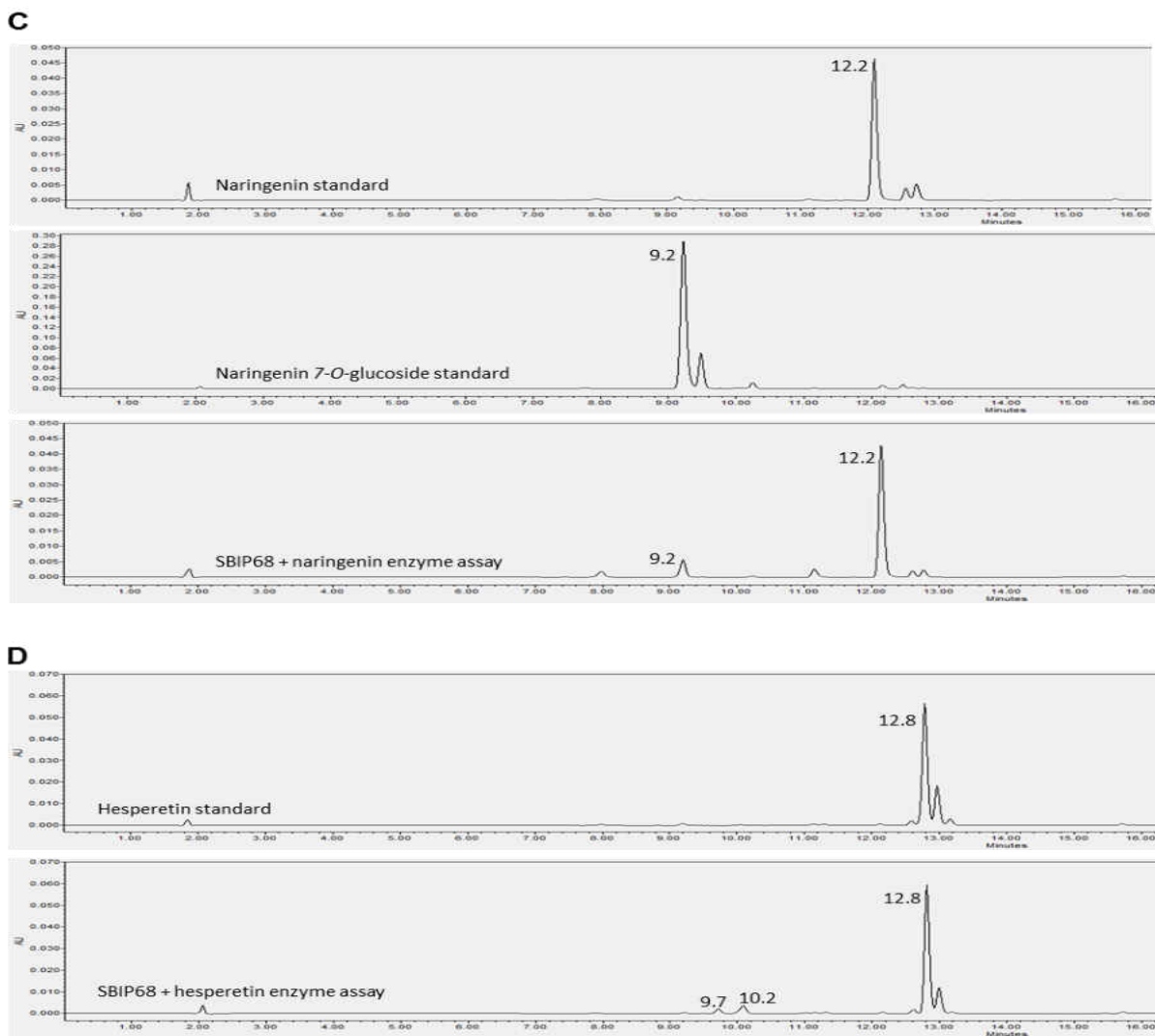


Figure 33 C-D: GT Assay using *E. coli* Expressed SBIP68 (645). **C**. Top panel shows retention time for naringenin standard at 12.2 minutes, middle panel shows retention time for naringenin 7-O-glucoside standard at 9.2 minutes. The bottom panel shows the products formed from the reaction with SBIP68-645, naringenin 7-O-glucoside and naringenin, with retention times at 9.2 minutes and 12.2 minutes respectively. **D**. Top panel shows retention time for hesperetin standard at 12.8 minutes. The bottom panel shows the products formed from the reaction with SBIP68-645, hesperetin glucoside and hesperetin, with retention times at 10.2 minutes and 12.8 minutes respectively. It appears there is a second hesperetin glucoside with a retention time of 9.7 minutes. There were no hesperetin glucoside standards available at the time of this experiment.

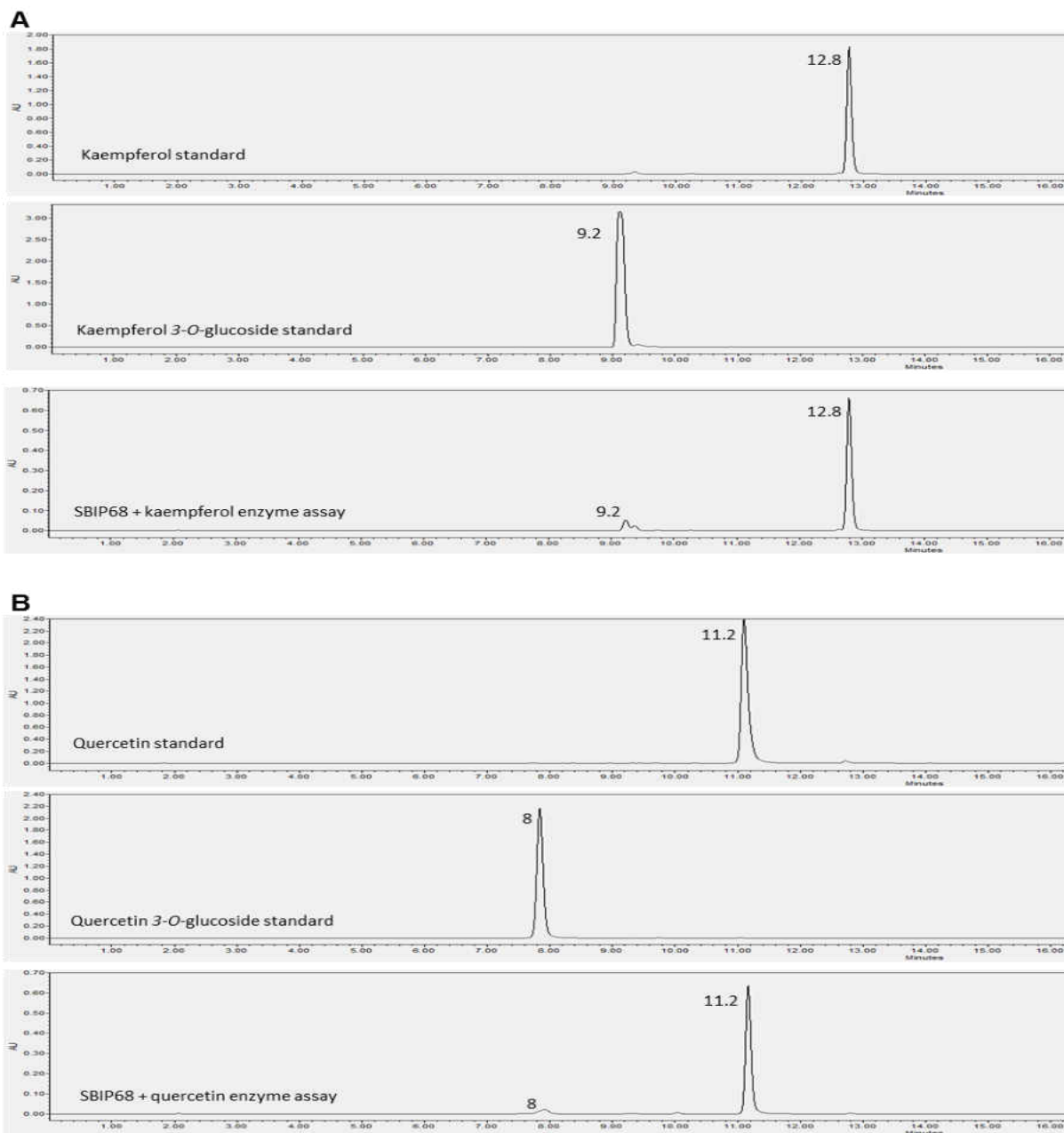


Figure 34 A-B: GT Assay using *E. coli* Expressed SBIP68 (644). **A**. Top panel shows retention time for kaempferol standard at 12.7 minutes, middle panel shows retention time for kaempferol 3-O-glucoside standard at 9.2 minutes. The bottom panel shows the products formed from the reaction with SBIP68-644, kaempferol 3-O-glucoside and kaempferol, with retention times at 9.2 minutes and 12.8 minutes respectively. **B**. Top panel shows retention time for quercetin standard at 11.2 minutes, middle panel shows retention time for quercetin 3-O-glucoside standard at 8 minutes. The bottom panel shows the products formed from the reaction with SBIP68-644, quercetin 3-O-glucoside and quercetin, with retention times at 8 minutes and 11.2 minutes respectively.

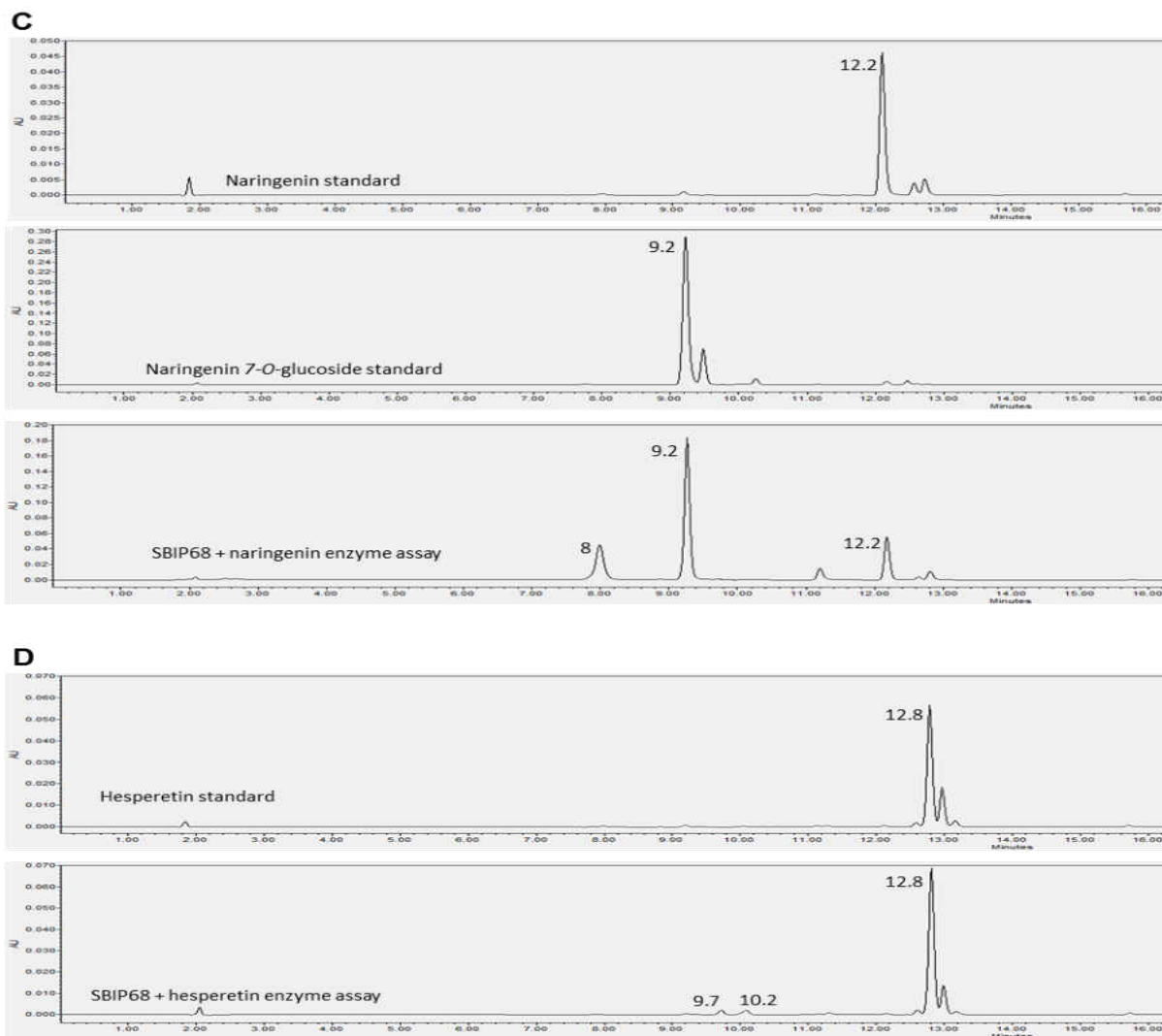


Figure 34 C-D: GT Assay using *E. coli* Expressed SBIP68 (**644**). **C**. Top panel shows retention time for naringenin standard at 12.2 minutes, middle panel shows retention time for naringenin 7-O-glucoside standard at 9.2 minutes. The bottom panel shows the products formed from the reaction with SBIP68-644, naringenin 7-O-glucoside and naringenin, with retention times at 9.2 minutes and 12.2 minutes respectively. **D**. Top panel shows retention time for hesperetin standard at 12.8 minutes. The bottom panel shows the products formed from the reaction with SBIP68-644, hesperetin glucoside and hesperetin, with retention times at 10.2 minutes and 12.8 minutes respectively. It appears there is a second hesperetin glucoside with a retention time of 9.7 minutes. There were no hesperetin glucoside standards available at the time of this experiment.

Cloning and Expression of SBIP68 in *P. pastoris*

PCR Amplification of *SBIP68* with Modified Ends for Cloning into pPICZA

For cloning full length *SBIP68* into *P. pastoris*, primers were synthesized and used for PCR amplification. The pGEMT-SBIP68 plasmid (Clone# C2) was used as a template for PCR, while DK639 and DK640 primers were used for amplification. Figure 35 below shows an ethidium bromide stained agarose gel of the PCR products.

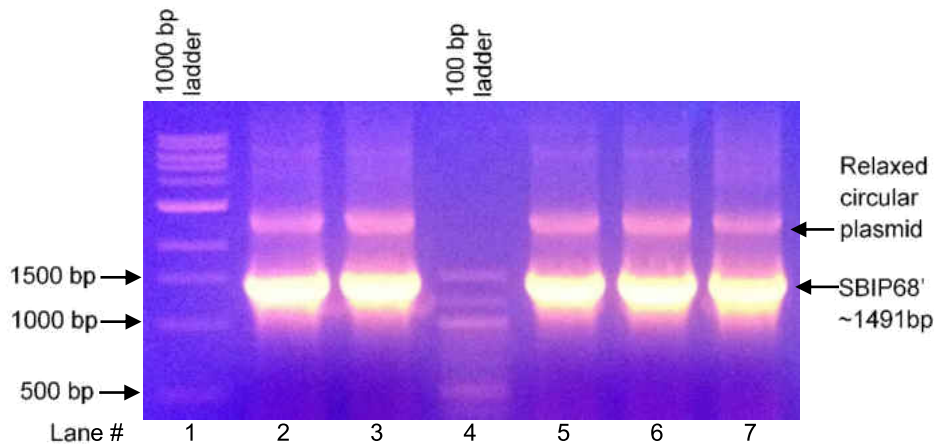


Figure 35: PCR Amplification of *SBIP68* for Cloning into pPICZA. Ethidium bromide stained 0.8 % agarose gel picture of *SBIP68'*. Lane numbers 2, 3, 5, 6, and 7 contain replicates of the same PCR reaction.

The PCR products were gel purified and ligated into pGEMT forming a new set of pGEMT-SBIP68' constructs. Selected clones were tested for presence of the plasmids using colony PCR. M13 forward and reverse primers were used in this PCR amplification. PCR products were analyzed by electrophoresis using a 0.8 % agarose gel (Fig. 36). Size of the amplified product is relatively large due to the amplification of pGEMT fragments on both sides of *SBIP68'*. Several isolated positive colonies (C2, C3, C5, C9, C10, C11, C12, C15, C17, C18) were chosen for plasmid DNA isolation.

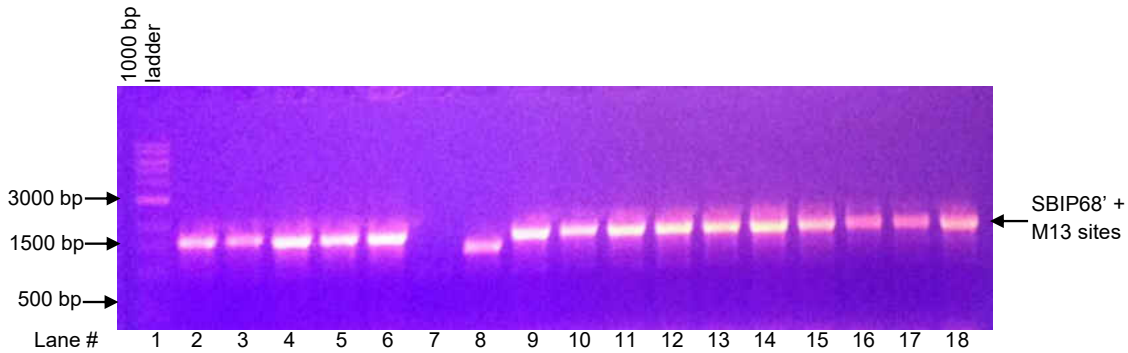


Figure 36: Verification of pGEMT-SBIP68' clones. Ethidium bromide stained 0.8 % agarose gel showing PCR amplified pGEMT-SBIP68'. For PCR amplification pGEMT specific M13 forward and reverse primers were used. Lanes 2 – 18 are representative of individual isolated clones from colonies C2, C3, C4, C5, C6, C7, C8, C9, C10, C11, C12, C13, C14, C15, C16, C17, and C18, respectively. C8 in lane 8 likely did not contain the *SBIP68* insert of interest.

Sequencing of pGEMT-SBIP68' Recombinant Plasmid

The plasmid DNA from several positive clones identified by colony PCR screening (Fig. 36), were used for DNA sequencing. Ten clones (C2, C3, C5, C9, C10, C11, C12, C15, C17, C18) were sequenced, of these, two of them (C11, and C18) were a 100 % match to the pGEMT-SBIP68 used as template for PCR. The only difference being the new restriction enzyme sites introduced for cloning into pPICZA by the new primers. The other eight clones (C2, C3, C5, C9, C10, C12, C15, C17), showed greater than 90 % identity (not shown) to the pGEMT-SBIP68 used as template for PCR. Figure 37 shows the sequence alignment of the new pGEMT-SBIP68' clones (C11 and C18) and the original pGEMT-SBIP68 from which they were derived. The different restriction enzyme sites between pGEMT-SBIP68 and pGEMT-SBIP68' can also be seen highlighted in boxes.

```

ref      ---GGATCCATGGCAACTCAAGTGCACAACTTCATTTCATACTATTCCCTTTAATGGCT
C11     CTCGAGGTCATGGCAACTCAAGTGCACAACTTCATTTCATACTATTCCCTTTAATGGCT
C18     CTCGAGGTCATGGCAACTCAAGTGCACAACTTCATTTCATACTATTCCCTTTAATGGCT
          *
ref      CCAGGCCACATGATTCCCTATGATAGACATAGCTAAACTTCTAGCAAATCGCGGTGTCATT
C11     CCAGGCCACATGATTCCCTATGATAGACATAGCTAAACTTCTAGCAAATCGCGGTGTCATT
C18     CCAGGCCACATGATTCCCTATGATAGACATAGCTAAACTTCTAGCAAATCGCGGTGTCATT
          *
ref      ACCACTATCATCACCCTCCAGTAAACGCAATCGTTTCAGTTCAACAATTACTCGTGCC
C11     ACCACTATCATCACCCTCCAGTAAACGCAATCGTTTCAGTTCAACAATTACTCGTGCC
C18     ACCACTATCATCACCCTCCAGTAAACGCAATCGTTTCAGTTCAACAATTACTCGTGCC
          *
ref      ATAAAATCCGGTCTAAGAAATCCAAATTCCTTACACTCAAATTTCCAAGGTAGAAAGTAGGA
C11     ATAAAATCCGGTCTAAGAAATCCAAATTCCTTACACTCAAATTTCCAAGGTAGAAAGTAGGA
C18     ATAAAATCCGGTCTAAGAAATCCAAATTCCTTACACTCAAATTTCCAAGGTAGAAAGTAGGA
          *
ref      TTACCAGAAGGTTGCGAAAATATTGACATGCTTCCTTCTCTGACTTGGCTTCAAAGTTT
C11     TTACCAGAAGGTTGCGAAAATATTGACATGCTTCCTTCTCTGACTTGGCTTCAAAGTTT
C18     TTACCAGAAGGTTGCGAAAATATTGACATGCTTCCTTCTCTGACTTGGCTTCAAAGTTT
          *
ref      TTTGCTGCAATTAGTATGCTGAAACAACAAGTTGAAAATCTCTTAGAAGGAATAAATCCA
C11     TTTGCTGCAATTAGTATGCTGAAACAACAAGTTGAAAATCTCTTAGAAGGAATAAATCCA
C18     TTTGCTGCAATTAGTATGCTGAAACAACAAGTTGAAAATCTCTTAGAAGGAATAAATCCA
          *
ref      AGTCCAAGTTGTGTTATTTTTCAGATATGGGATTTCTTGGACTACTCAAATGCACAAAAT
C11     AGTCCAAGTTGTGTTATTTTTCAGATATGGGATTTCTTGGACTACTCAAATGCACAAAAT
C18     AGTCCAAGTTGTGTTATTTTTCAGATATGGGATTTCTTGGACTACTCAAATGCACAAAAT
          *
ref      TTTAATATCCCAAGAATTGTTTTTCATGGTACTTGTGTTTCTCACTTTTATGTTTCCTAT
C11     TTTAATATCCCAAGAATTGTTTTTCATGGTACTTGTGTTTCTCACTTTTATGTTTCCTAT
C18     TTTAATATCCCAAGAATTGTTTTTCATGGTACTTGTGTTTCTCACTTTTATGTTTCCTAT
          *
ref      AAAAATACTTCTCCAACATTCCTTGAAAATATAACCTCAGATTCAGAGTATTTTGTGTT
C11     AAAAATACTTCTCCAACATTCCTTGAAAATATAACCTCAGATTCAGAGTATTTTGTGTT
C18     AAAAATACTTCTCCAACATTCCTTGAAAATATAACCTCAGATTCAGAGTATTTTGTGTT
          *
ref      CCTGATTTACCCGATAGAGTCGAACTAACGAAAGCTCAGGTTTCAGGATCGACGAAAAAT
C11     CCTGATTTACCCGATAGAGTCGAACTAACGAAAGCTCAGGTTTCAGGATCGACGAAAAAT
C18     CCTGATTTACCCGATAGAGTCGAACTAACGAAAGCTCAGGTTTCAGGATCGACGAAAAAT
          *
ref      ACTACTTCTGTTAGTTCCTTCTGTATTGAAAGAAGTTACTGAGCAAATCAGATTAGCCGAG
C11     ACTACTTCTGTTAGTTCCTTCTGTATTGAAAGAAGTTACTGAGCAAATCAGATTAGCCGAG
C18     ACTACTTCTGTTAGTTCCTTCTGTATTGAAAGAAGTTACTGAGCAAATCAGATTAGCCGAG
          *
ref      GAATCATCATATGGTGTAATTGTTAATAGTTTTGAGGAGTTGGAGCAAGTGTATGAGAAA
C11     GAATCATCATATGGTGTAATTGTTAATAGTTTTGAGGAGTTGGAGCAAGTGTATGAGAAA
C18     GAATCATCATATGGTGTAATTGTTAATAGTTTTGAGGAGTTGGAGCAAGTGTATGAGAAA
          *
ref      GAATATAGGAAAAGCTAGAGGGAAAAAAGTTTGGTGTGTTGGTCCTGTTTCTTTGTGTAAT
C11     GAATATAGGAAAAGCTAGAGGGAAAAAAGTTTGGTGTGTTGGTCCTGTTTCTTTGTGTAAT
C18     GAATATAGGAAAAGCTAGAGGGAAAAAAGTTTGGTGTGTTGGTCCTGTTTCTTTGTGTAAT
          *
ref      AAGGAAATGAAGATTTGGTTACAAGGGGTAATAAACTGCAATTGATAATCAAGATTGC
C11     AAGGAAATGAAGATTTGGTTACAAGGGGTAATAAACTGCAATTGATAATCAAGATTGC
C18     AAGGAAATGAAGATTTGGTTACAAGGGGTAATAAACTGCAATTGATAATCAAGATTGC
          *
ref      TTGAAATGGTTAGATAAATTTGAAACAGAATCTGTGGTTTATGCAAGTCTTGAAGTTTA
C11     TTGAAATGGTTAGATAAATTTGAAACAGAATCTGTGGTTTATGCAAGTCTTGAAGTTTA
C18     TTGAAATGGTTAGATAAATTTGAAACAGAATCTGTGGTTTATGCAAGTCTTGAAGTTTA
          *

```

Figure 37 (continued on next page)

```

ref      TCTCGTTTGACATTATTGCAAATGGTGGAACTTGGTCTTGGTTTAGAAGAGTCAAATAGG
C11     TCTCGTTTGACATTATTGCAAATGGTGGAACTTGGTCTTGGTTTAGAAGAGTCAAATAGG
C18     TCTCGTTTGACATTATTGCAAATGGTGGAACTTGGTCTTGGTTTAGAAGAGTCAAATAGG
*****

ref      CCTTTTGTATGGGTATTAGGAGGAGGTGATAAATTAATGATTTAGAGAAATGGATTCTT
C11     CCTTTTGTATGGGTATTAGGAGGAGGTGATAAATTAATGATTTAGAGAAATGGATTCTT
C18     CCTTTTGTATGGGTATTAGGAGGAGGTGATAAATTAATGATTTAGAGAAATGGATTCTT
*****

ref      GAGAATGGATTTGAGCAAAGAATTAAGAAAAGAGGAGTTTGGATTAGAGGATGGGCTCCT
C11     GAGAATGGATTTGAGCAAAGAATTAAGAAAAGAGGAGTTTGGATTAGAGGATGGGCTCCT
C18     GAGAATGGATTTGAGCAAAGAATTAAGAAAAGAGGAGTTTGGATTAGAGGATGGGCTCCT
*****

ref      CAAGTGCCTTATACTTTCACACCCTGCAATTGGTGGAGTATTGACTCATTGCGGATGGAAT
C11     CAAGTGCCTTATACTTTCACACCCTGCAATTGGTGGAGTATTGACTCATTGCGGATGGAAT
C18     CAAGTGCCTTATACTTTCACACCCTGCAATTGGTGGAGTATTGACTCATTGCGGATGGAAT
*****

ref      TCTACATTGGAAGGTATTTTCAGCAGGATTACCAATGGTAACATGGCCACTATTTGCTGAG
C11     TCTACATTGGAAGGTATTTTCAGCAGGATTACCAATGGTAACATGGCCACTATTTGCTGAG
C18     TCTACATTGGAAGGTATTTTCAGCAGGATTACCAATGGTAACATGGCCACTATTTGCTGAG
*****

ref      CAATTTTGC AATGAGAAGTTAGTAGTCCAAGTCTAAAAATGGAGTGAGCCTAGGTGTG
C11     CAATTTTGC AATGAGAAGTTAGTAGTCCAAGTCTAAAAATGGAGTGAGCCTAGGTGTG
C18     CAATTTTGC AATGAGAAGTTAGTAGTCCAAGTCTAAAAATGGAGTGAGCCTAGGTGTG
*****

ref      AAGGTGCCTGTCAAATGGGGAGATGAGGAAAATGTTGGAGTTTGGTAAAAAAGGATGAT
C11     AAGGTGCCTGTCAAATGGGGAGATGAGGAAAATGTTGGAGTTTGGTAAAAAAGGATGAT
C18     AAGGTGCCTGTCAAATGGGGAGATGAGGAAAATGTTGGAGTTTGGTAAAAAAGGATGAT
*****

ref      GTTAAGAAAGCATTAGACAACTAATGGATGAAGGAGAAGAAGGACAAGTAAGAAGAACA
C11     GTTAAGAAAGCATTAGACAACTAATGGATGAAGGAGAAGAAGGACAAGTAAGAAGAACA
C18     GTTAAGAAAGCATTAGACAACTAATGGATGAAGGAGAAGAAGGACAAGTAAGAAGAACA
*****

ref      AAAGCAAAGAGTTAGGAGAATTGGCTAAAAAGGCATTTGGAGAAGGTGGTTCTTCTTAT
C11     AAAGCAAAGAGTTAGGAGAATTGGCTAAAAAGGCATTTGGAGAAGGTGGTTCTTCTTAT
C18     AAAGCAAAGAGTTAGGAGAATTGGCTAAAAAGGCATTTGGAGAAGGTGGTTCTTCTTAT
*****

ref      GTTAACTTAAACATCTCTGATTGAAGACATCATTGAGCAACAAAATCACAAGGAAAAA
C11     GTTAACTTAAACATCTCTGATTGAAGACATCATTGAGCAACAAAATCACAAGGAAAAA
C18     GTTAACTTAAACATCTCTGATTGAAGACATCATTGAGCAACAAAATCACAAGGAAAAA
*****

ref      GAG
C11     CCC
C18     CCC

```

Figure 37: Alignment of Cloned *SBIP68'* in pGEMT with Reference Gene. The sequences match perfectly except for the new restriction enzyme sites at 5' (Xho 1) and 3' (Apa 1) ends of pGEMT-SBIP68'. The restriction enzyme sites are highlighted in boxes.

PCR Screening of pPICZA-SBIP68' Transformed Bacterial Clones

The positive clones (pGEMT-SBIP68') were digested with restriction enzymes (Xho 1 and Apa 1) and ligated into pPICZA digested with same set of enzymes as described in material and methods. The ligated pPICZA-SBIP68' products were used to transform competent bacterial cells. Selected clones were tested for presence of the pPICZA-SBIP68' plasmid by colony PCR using the vector specific 5' AOX1 (DK 641) forward and 3' AOX1 (DK 642) reverse primers. Figure 39 shows the agarose gel electrophoresis of the PCR amplified products.

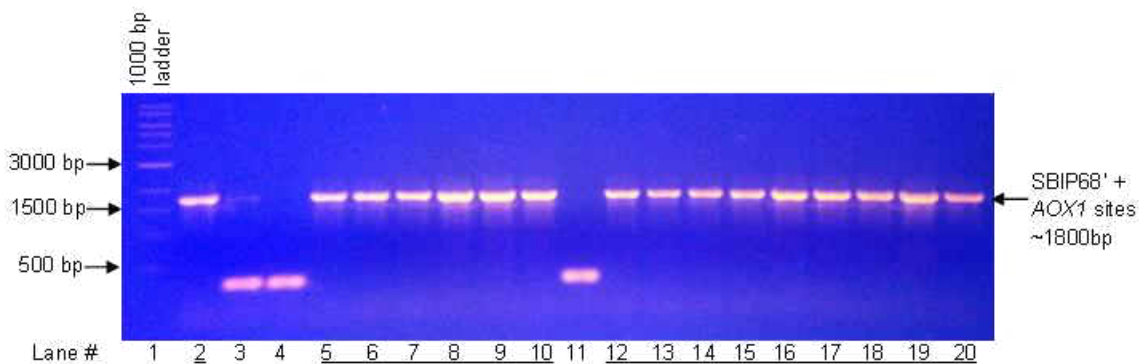


Figure 38: Colony PCR to Verify Presence of *SBIP68'* in pPICZA Plasmid. Colony PCR was performed using pPICZA specific AOX1 primers. Ethidium bromide stained 0.8 % Agarose gel picture of pPICZA-SBIP68'. Lanes 2 – 20 are representative of individual clones C1, C2, C3, C4, C5, C6, C7, C8, C9, C10, C11, C15, C16, C17, C18, C23, C26, C28, and C30, respectively. Positive clones have been underlined.

Sequencing of pPICZA-SBIP68' Recombinant Clones

Clones that tested positive in colony PCR analyses were used for plasmid DNA isolation. Plasmid DNA samples were sent for sequencing. Sequencing was important to ensure that the SBIP68 gene (in the recombinant pPICZA-SBIP68' plasmid) was in-

frame with the rest of the plasmid. This would ensure that the stop codon, fusion tags and other sequences necessary for expression and purification of the protein are in place. Fifteen clones were sequenced, out of which fourteen showed 100 % identity to the reference (expected sequence), and one sequence showed 99 % identity with a single nucleotide difference. Figure 39 shows one of the sequenced clones (C4) as a representative of the clones that showed 100 % identity to the reference (expected) sequence, together with the reference sequence. Figure 40 shows the translated amino acid sequence. The c-myc epitope and 6xHis-tag necessary for detection and purification of the recombinant SBIP68' protein are shown in blue and red respectively (Fig. 40).

```

ref      TCGGATCGGTACCTCGAGGTCATGGCAACTCAAGTGCACAAACTTCATTTTCATACTATTC
C4      TCGGATCGGTACCTCGAGGTCATGGCAACTCAAGTGCACAAACTTCATTTTCATACTATTC
*****
ref      CCTTTAATGGCTCCAGGCCACATGATTCCCTATGATAGACATAGCTAAACTTCTAGCAAAT
C4      CCTTTAATGGCTCCAGGCCACATGATTCCCTATGATAGACATAGCTAAACTTCTAGCAAAT
*****
ref      CGCGGTGTCATTACCACTATCATCACCCTCCAGTAAACGCCAATCGTTTCAGTTCAACA
C4      CGCGGTGTCATTACCACTATCATCACCCTCCAGTAAACGCCAATCGTTTCAGTTCAACA
*****
ref      ATTACTCGTGCCATAAAAATCCGGTCTAAGAATCCAAATTCTTACACTCAAATTTCCAAGT
C4      ATTACTCGTGCCATAAAAATCCGGTCTAAGAATCCAAATTCTTACACTCAAATTTCCAAGT
*****
ref      GTAGAAGTAGGATTACCAGAAGGTTGCGAAAATATTGACATGCTTCCTTCTCTTGACTTG
C4      GTAGAAGTAGGATTACCAGAAGGTTGCGAAAATATTGACATGCTTCCTTCTCTTGACTTG
*****
ref      GCTTCAAAGTTTTTTGCTGCAATTAGTATGCTGAAACAACAAGTTGAAAATCTCTTAGAA
C4      GCTTCAAAGTTTTTTGCTGCAATTAGTATGCTGAAACAACAAGTTGAAAATCTCTTAGAA
*****
ref      GGAATAAATCCAAGTCCAAGTTGTGTTATTTTCAGATATGGGATTTTCCTTGGACTACTCAA
C4      GGAATAAATCCAAGTCCAAGTTGTGTTATTTTCAGATATGGGATTTTCCTTGGACTACTCAA
*****
ref      ATTGCACAAAATTTTAATATCCCAAGAATTGTTTTTCATGGTACTTGTTGTTTCTCACTT
C4      ATTGCACAAAATTTTAATATCCCAAGAATTGTTTTTCATGGTACTTGTTGTTTCTCACTT
*****
ref      TTATGTTCCCTATAAAAATACTTTCCCTCCAACATTCTTGAAAATATAACCTCAGATTCAGAG
C4      TTATGTTCCCTATAAAAATACTTTCCCTCCAACATTCTTGAAAATATAACCTCAGATTCAGAG
*****
ref      TATTTTGTTGTTTCTGATTTACCCGATAGAGTCGAACTAACGAAAGCTCAGGTTTCAGGA
C4      TATTTTGTTGTTTCTGATTTACCCGATAGAGTCGAACTAACGAAAGCTCAGGTTTCAGGA
*****

```

Figure 39 (continued on next page)

```

ref      TCGACGAAAAATACTACTTCTGTTAGTTCTTCTGTATTGAAAGAAGTTACTGAGCAAATC
C4      TCGACGAAAAATACTACTTCTGTTAGTTCTTCTGTATTGAAAGAAGTTACTGAGCAAATC
*****
ref      AGATTAGCCGAGGAATCATCATATGGTGTAAATTGTTAATAGTTTTGAGGAGTTGGAGCAA
C4      AGATTAGCCGAGGAATCATCATATGGTGTAAATTGTTAATAGTTTTGAGGAGTTGGAGCAA
*****
ref      GTGTATGAGAAAGAATATAGGAAAGCTAGAGGGAAAAAAGTTTGGTGTGTTGGTCCTGTT
C4      GTGTATGAGAAAGAATATAGGAAAGCTAGAGGGAAAAAAGTTTGGTGTGTTGGTCCTGTT
*****
ref      TCTTTGTGTAATAAGGAAATTGAAGATTTGGTTACAAGGGGTAATAAAACTGCAATTGAT
C4      TCTTTGTGTAATAAGGAAATTGAAGATTTGGTTACAAGGGGTAATAAAACTGCAATTGAT
*****
ref      AATCAAGATTGCTTGAAATGGTTAGATAAATTTGAAACAGAATCTGTGGTTTATGCAAGT
C4      AATCAAGATTGCTTGAAATGGTTAGATAAATTTGAAACAGAATCTGTGGTTTATGCAAGT
*****
ref      CTTGGAAGTTTATCTCGTTTGACATTATTGCAAATGGTGGAACTTGGTCTTGGTTTAGAA
C4      CTTGGAAGTTTATCTCGTTTGACATTATTGCAAATGGTGGAACTTGGTCTTGGTTTAGAA
*****
ref      GAGTCAAATAGGCCTTTTGTATGGGTATTAGGAGGAGGTGATAAATTAATGATTTAGAG
C4      GAGTCAAATAGGCCTTTTGTATGGGTATTAGGAGGAGGTGATAAATTAATGATTTAGAG
*****
ref      AAATGGATTCTTGAGAATGGATTTGAGCAAAGAATTAAGAAAGAGGAGTTTTGATTAGA
C4      AAATGGATTCTTGAGAATGGATTTGAGCAAAGAATTAAGAAAGAGGAGTTTTGATTAGA
*****
ref      GGATGGGCTCCTCAAGTGCTTATACTTTACACCCTGCAATTGGTGGAGTATTGACTCAT
C4      GGATGGGCTCCTCAAGTGCTTATACTTTACACCCTGCAATTGGTGGAGTATTGACTCAT
*****
ref      TGCGGATGGAATTCTACATTGGAAGGTATTTGAGCAGGATTACCAATGGTAACATGGCCA
C4      TGCGGATGGAATTCTACATTGGAAGGTATTTGAGCAGGATTACCAATGGTAACATGGCCA
*****
ref      CTATTTGCTGAGCAATTTTGAATGAGAAGTTAGTAGTCCAAGTGCTAAAAAATTGGAGTG
C4      CTATTTGCTGAGCAATTTTGAATGAGAAGTTAGTAGTCCAAGTGCTAAAAAATTGGAGTG
*****
ref      AGCCTAGGTGTGAAGGTGCCTGTCAAATGGGGAGATGAGGAAAATGTTGGAGTTTTGGTA
C4      AGCCTAGGTGTGAAGGTGCCTGTCAAATGGGGAGATGAGGAAAATGTTGGAGTTTTGGTA
*****
ref      AAAAAGGATGATGTTAAGAAAGCATTAGACAAACTAATGGATGAAGGAGAAGAAGGACAA
C4      AAAAAGGATGATGTTAAGAAAGCATTAGACAAACTAATGGATGAAGGAGAAGAAGGACAA
*****
ref      GTAAGAAGAACAAAAGCAAAAGAGTTAGGAGAATTGGCTAAAAAGGCATTTGGAGAAGGT
C4      GTAAGAAGAACAAAAGCAAAAGAGTTAGGAGAATTGGCTAAAAAGGCATTTGGAGAAGGT
*****
ref      GGTTCTTCTTATGTAACTTAACATCTCTGATTGAAGACATCATTGAGCAACAAAATCAC
C4      GGTTCTTCTTATGTAACTTAACATCTCTGATTGAAGACATCATTGAGCAACAAAATCAC
*****
ref      AAGGAAAAAGGGCCCGAACAAAACACTCATCTCAGAAGAGGATCTGAATAGCGCCGTCGAC
C4      AAGGAAAAAGGGCCCGAACAAAACACTCATCTCAGAAGAGGATCTGAATAGCGCCGTCGAC
*****
ref      CATCATCATCATCATCATTGAGTTTTAGCCTTA
C4      CATCATCATCATCATCATTGAGTTTTAGCCTTA
*****

```

Figure 39: Nucleotide Sequence Alignment of Cloned *SBIP68'* in pPICZA. C4 is a pPICZA-*SBIP68'* clone, and ref is the reference sequence. The reference sequence was derived from a combination of the *SBIP68* and pPICZA sequences. The underlined nucleotides are part of the pPICZA vector, which include the c-myc and 6xHis tag coding sequences.

MATQVHKLHFILFPLMAPGHMIPMIDIAKLLANRGVITTTIITTPVNANRFSSTITRAIKSGLRIQIL
 TLKFPSVEVGLPEGCENIDMLPSLDLASKFFAAISMLKQQVENLLEGINPSPSCVISDMGFPWTTQI
 AQNFNIPRIVFHGTCCFSL LCSYKILSSNILENITSDSEYFVVPDLPDRVELTKAQVSGSTKNTTSV
 SSSVLKEVTEQIRLAEESSYGVI VNSFEELEQVYEKEYRKARGKKVWCVGPVSLCNKEIEDLVTRGN
 KTAIDNQDCLKWLDNFETESV VYASLGSL SRLTLLQMV ELGLGLEESNRPFVWVLGGGDKLNDLEKW
 ILENGFEQRIKERGVLIRGWAPQVLILSHPAIGGVLTHCGWNSTLEGISAGLPMVTWPLFAEQFCNE
 KLVVQVLKIGVSLGVKVPVKWGDEENVGVLVKKDDVKKALDKLMDEGEEGQVRRTKAKELGELAKKA
 FEGEGSSYVNLTSLIEDIIEQQNHKEKGPEQKLISEEDLNSAVDHHHHHH Stop

Figure 40: Amino Acid Sequence of pPICZA-SBIP68' Clone # C4. Underlined and highlighted in blue and red are the c-myc epitope and the 6xHis-tag for detection and purification of the recombinant protein respectively.

Transformation of pPICZA-SBIP68' Plasmid DNA into *Pichia pastoris*

For transforming *P. pastoris*, both linear and circular plasmids can be used. However it is desirable to linearize the plasmid before using it to transform *P. Pastoris*. Linearized plasmids are believed to produce more stable transformants. Figure 41 shows the picture of a 0.8 % agarose gel with both linearized (~4800 bp) and circular pPICZA-SBIP68' plasmids. The restriction enzyme Pme I was used in linearization.

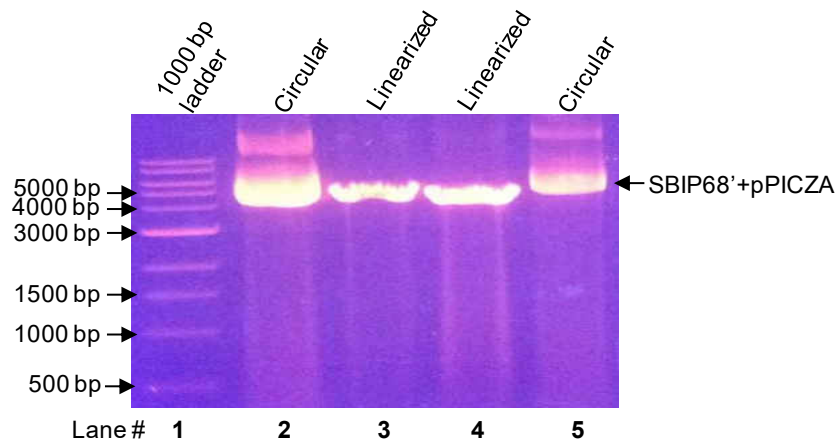


Figure 41: Agarose Gel Electrophoresis of pPICZA-SBIP68' Plasmid DNA. Ethidium bromide stained 0.8 % gel shows circular (uncut) and linearized pPICZA-SBIP68' plasmid DNAs. In lanes 2 and 4 are uncut circular plasmids while lanes 3 and 5 are plasmids that have been cut using the enzyme Pme I, making them linear.

Competent *Pichia pastoris* strain X-33 Mut⁺ cells were prepared for electroporation. Both linearized and circular pPICZA-SBIP68' DNAs were used in two separate transformation reactions. The transformed cells were plated on YPDS/zeocin plates.

Screening of *P. pastoris* Clones

Selected clones after 3.5 days were verified by colony PCR for successful incorporation of SBIP68' into the *P. pastoris* genome. PCR was performed using 5' AOX1 (DK 641) forward primer, and 3' AOX1 (DK 642) reverse primer. The result of the colony PCR is shown in Fig. 42. In this picture (Fig. 42), two distinct bands are noticeable. *P. pastoris* has an AOX1 gene in its genome which is ~2.2 kb.

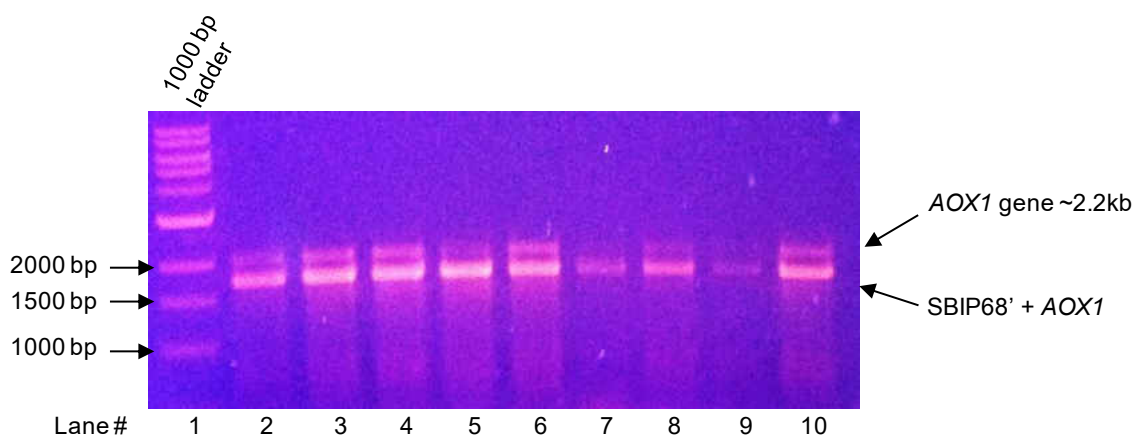


Figure 42: Agarose Gel Showing Colony PCR of *P. pastoris* Clones. The upper band is the AOX1 gene (2.2 Kb) native to *P. pastoris* while the lower band (1.8 Kb) is a combination of the SBIP68' gene (~1.5 kb) and the AOX1 sites (325 bp) of the pPICZA-SBIP68' construct used to transform *P. pastoris*.

The pPICZA plasmid also has 5' and 3' AOX1 priming sites, and the SBIP68' gene is actually cloned in between the 5' and 3' AOX1 priming sites of the pPICZA plasmid. The 5' and 3' AOX1 primers used in PCR therefore amplified both the AOX1

native to *P. pastoris* and the *AOX1* sites (and everything in between which includes SBIP68') introduced by the plasmid. The lower of the two bands in the picture is ~1.8 kb and comprises the SBIP68' gene (~1.5 kb) and the *AOX1* sites of the plasmid (325 bp)

Expression of Recombinant SBIP68' in *Pichia pastoris*

Pichia-SBIP68' was initially grown in BMGY medium to generate biomass and later transferred during log-phase growth to BMMY medium for the recombinant protein expression. Samples were taken regularly at various time points (0, 24, 48, and 72 hr) to determine the optimal recombinant SBIP68' protein expression. The collected *Pichia* samples were centrifuged and the supernatants discarded. Pellets were stored at -80°C until ready for analyses. The pellets were resuspended in breaking buffer and lysed as described in the materials and methods section. A Western blot analysis was performed to specifically detect expression of recombinant SBIP68' (Fig. 43A).

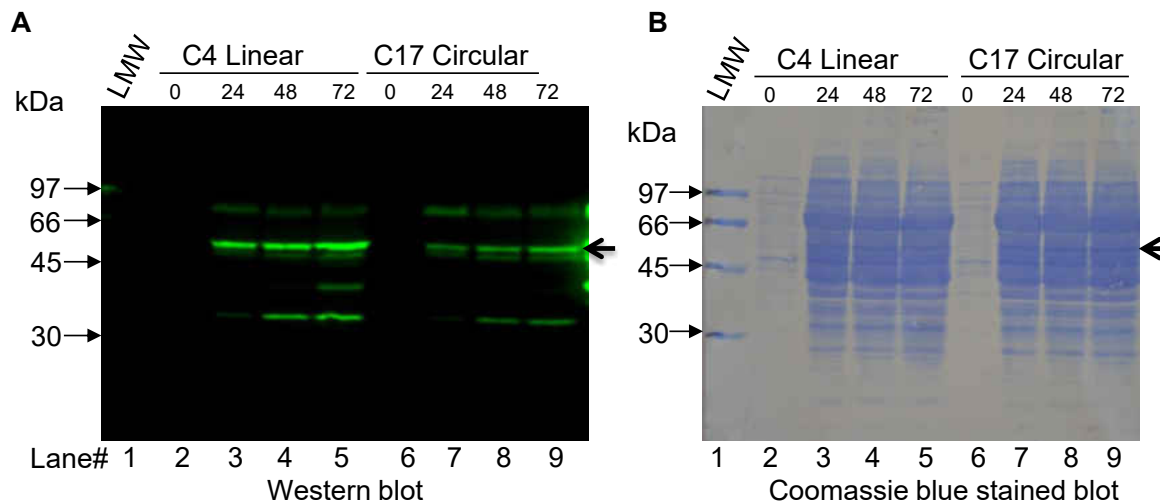


Figure 43: Recombinant SBIP68' expression in *P. pastoris*. Both linear (Colony 4 or C4) and circular (Colony 17 or C17) pPICZA-SBIP68' DNA's were used to transform *P. pastoris* and both transformant have been analyzed for expression of the recombinant protein. **A.** Western blot analysis of SBIP68' recombinant protein (57.6 kDa) expression in *P. Pastoris*. In lanes 2, 3, 4, and 5 are 0 hr, 24 hr, 48 hr, and 72 hr time point expression samples derived from C4. In lanes 6, 7, 8, and 9 are 0 hr, 24 hr, 48 hr, and 72 hr time point expression samples derived from C17. **B.** Corresponding coomassie blue stained blot. The membrane was stained after Western blot analysis.

Due to the presence of multiple bands (other than SBIP68') in Figure 43A, a second expression was performed in which samples were collected at earlier time points (6 hr, 12 hr, 24 hr) following induction with methanol. An uninduced sample (SBIP68' in BMGY) was also maintained. These put together would help in determining if some of the extra immunopositive bands seen in Figure 43A were due to degradation of SBIP68' over time, or these are other proteins present in the expression system. The result of the uninduced sample and the shorter time points are shown in Figure 44A.

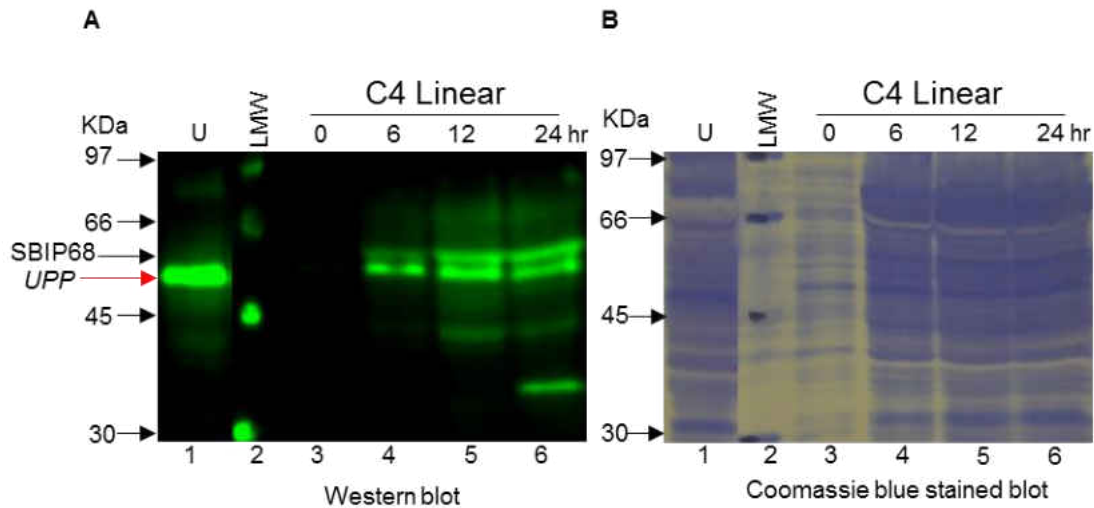


Figure 44: Time Course Expression of Recombinant SBIP68'. Linear pPICZA-SBIP68' DNA transformed colony C4 was used. **A.** Western blot analysis of SBIP68' recombinant protein (57.6 kDa) expression in *P. Pastoris*. In lane 1 is an uninduced sample (C4 in BMGY), lane 2 the low molecular weight ladder, lanes 3, 4, 5, and 6 are 0 hr, 6 hr, 12 hr, and 24 hr time point expression samples derived from C4. U stands for uninduced, and UPP means unidentified *Pichia* protein. **B.** Corresponding coomassie blue stained blot. The membrane was stained after Western blot analysis.

It can be deduced from the Western blot in Figure 44A that the bright band (UPP) directly below SBIP68' in lanes 4, 5, and 6 is not a degradation product of SBIP68' as it is seen to be strongly expressed in the uninduced sample in lane 1. The lowest band (just above 30 kDa) in lane 6 (24 hr) is likely a degradation product of SBIP68' due to proteases present in the expression host. This band is not seen in the 12 hr and 6 hr time points, the amount of SBIP68' in the 24 hr time point (lane 6) also appears to be less than the amount of SBIP68' in the 12 hr time point (lane 5). It may be desirable to express SBIP68' for no longer than 12 hours for subsequent applications. This will reduce the extent of degradation and also gives less room for other undesirable proteins

to be expressed to a great extent. It will also result in better purification of SBIP68' with less non-specific bands.

Large Scale Expression and Purification of Recombinant SBIP68' Protein

Approximately 500 ml culture of *Pichia*-SBIP68' in BMMY media was used for large scale expression. After 96 hrs of induction, the cell pellets were harvested and pellets were saved at – 80 °C until they were processed for purification of recombinant protein. To lyse *Pichia* cells, a French press was utilized. The cell lysate was collected and the recombinant SBIP68' was purified using a Ni-NTA column. The bound 6xHis-tagged SBIP68' protein was eluted with 150 mM imidazole in 1 x Ni-NTA elution buffer at 4 °C. The eluted samples were collected as 1 ml fractions, and the fractions with the highest concentration of proteins were pooled and concentrated before testing the enzyme for activity. Figure 45A shows a Western blot analysis of selected fractions after purification.

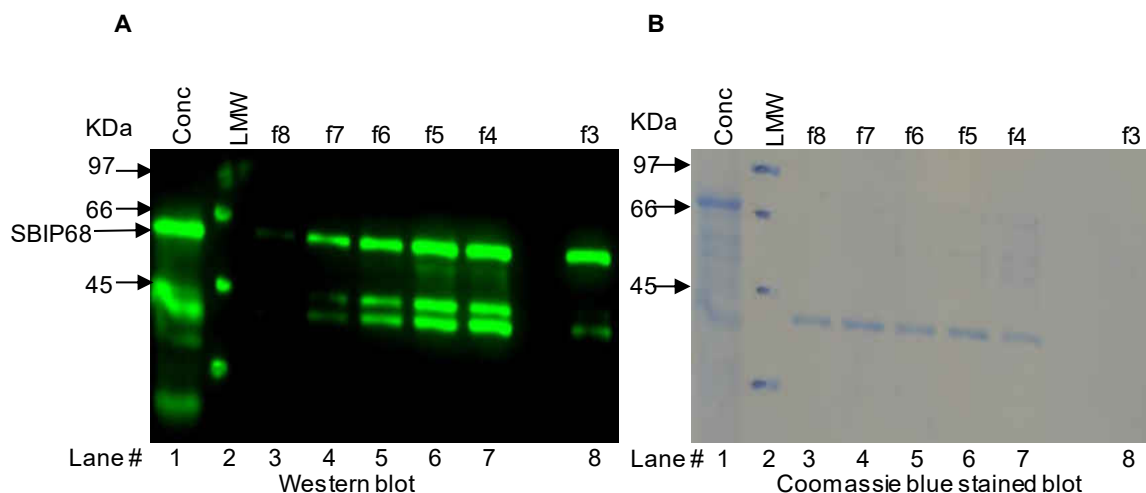


Figure 45: Ni-NTA Affinity Chromatography Purification of SBIP68'. **A.** Western Blot Analysis of SBIP68' recombinant protein present in *P. pastoris*. In lane 1 is the concentrated sample, lane 2 the low molecular weight ladder. Lanes 3 to 8 contain fraction numbers 8, 7, 6, 5, 4, and 3, respectively, collected from the purification process. **B.** Corresponding coomassie blue stained blot. The membrane was stained after Western blot analysis.

Purification of recombinant SBIP68' using Anion Exchange Chromatography

In an attempt to optimize the purification of SBIP68', a new batch of 200 ml (96 hr induction) culture of *Pichia*-SBIP68' was used. Initial purification was achieved by Ni-NTA column using AKTA purifier 10 (Fig. 46). Fractions 7 to 13 containing SBIP68' were pooled, desalted, and purified on a Mono-Q anion exchange column using AKTA purifier 10 (Figure 47-48). Bound proteins were eluted with a linear gradient of 0-500 mM NaCl in potassium phosphate buffer pH 7.5. Western blot analysis was performed on the eluted fractions to detect SBIP68' (Fig. 48).

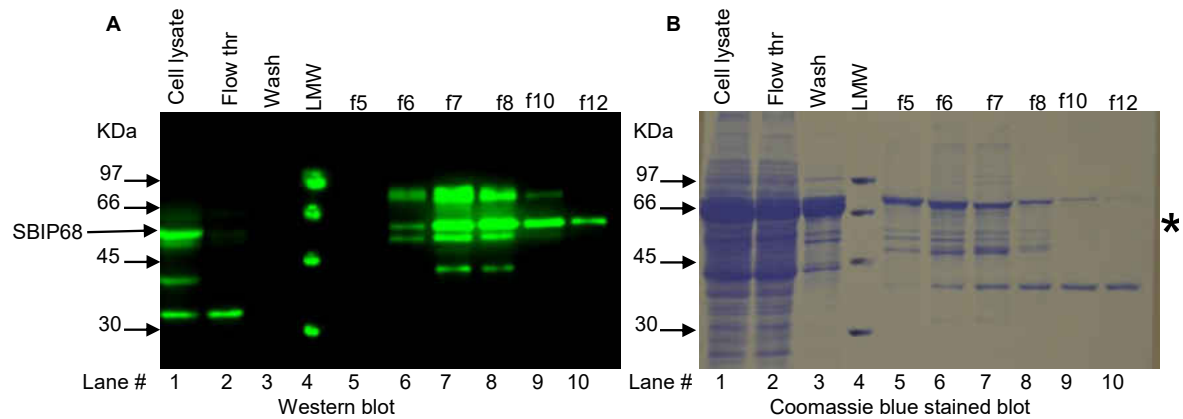


Figure 46: Ni-NTA Affinity Chromatography Purification of SBIP68'. **A.** Western Blot analysis of SBIP68' recombinant protein present in *P. pastoris*. In lane 1 is the cell lysate before purification, lane 2 is the flow through, and lane 3 the wash. Lane 4 contains the low molecular weight ladder. Lane numbers 5 to 10 contain fractions 5, 6, 7, 8, 10, and 12 respectively. The extra bands seen to coelute with SBIP68' in fractions 7 and 8 are likely *Pichia* proteins with polyhistidine-like sequences and therefore bind to the column. Expression of SBIP68' at shorter time points should minimize the appearance of some of the bands as previously demonstrated. **B.** Corresponding coomassie blue stained blot. The membrane was stained after Western blot analysis. The asterisk indicates SBIP68's expected position on the blot.

Coomassie blue staining of the blots (Fig. 48B and Fig. 48D) revealed that proteins other than SBIP68' were still present in the eluted fractions and that SBIP68' was not the major protein present in the samples. One of the major contaminating protein (~40 kDa) was eluted in earlier fractions. One option to further purify SBIP68' will be to perform size-exclusion chromatography.

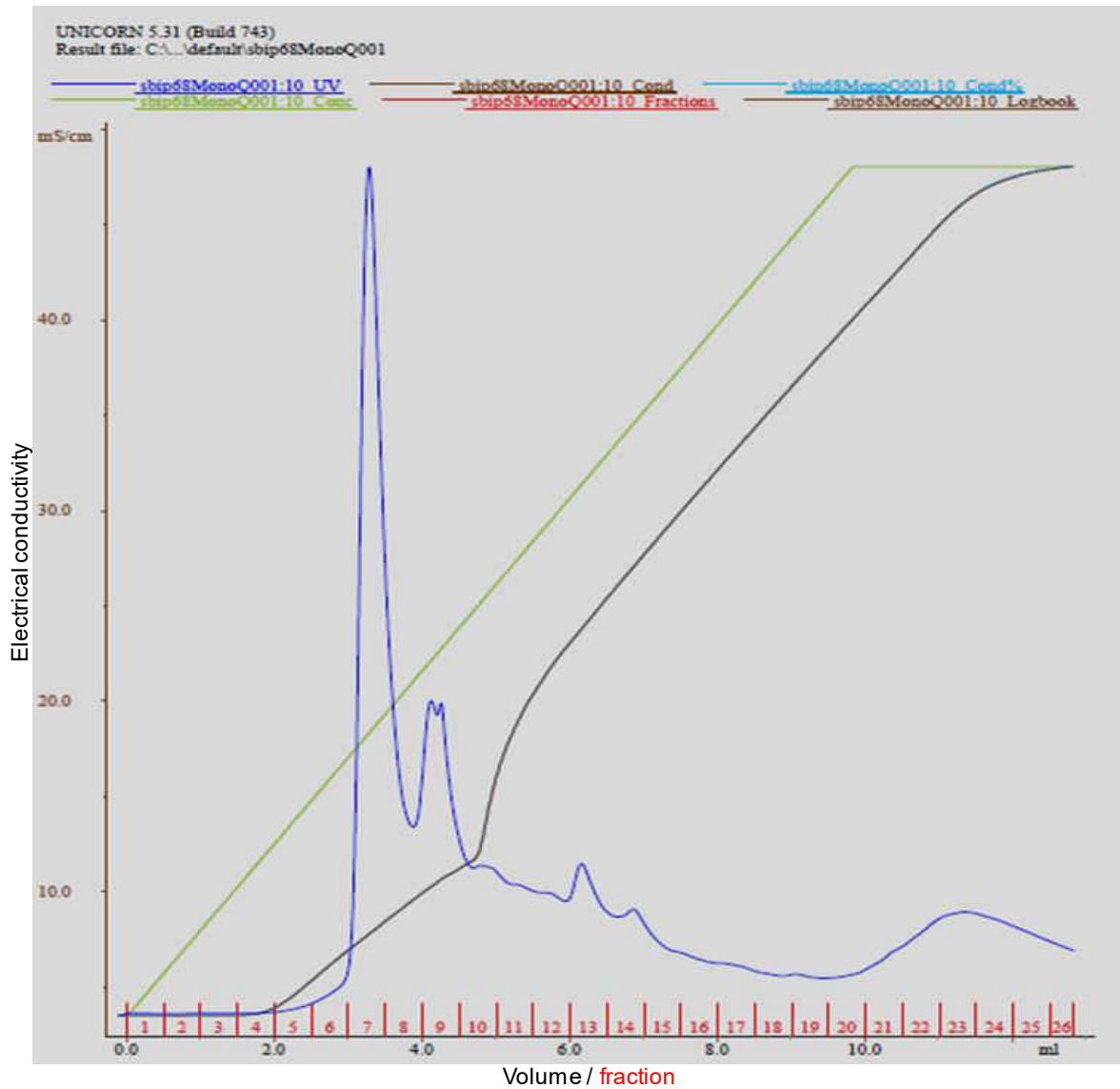


Figure 47: Chromatogram Showing Purification of SBIP68' on MonoQ Column. The vertical axis represents electrical conductivity; the horizontal axis represents the volume of eluted sample. The red lines on the horizontal axis represent the eluted (0.5 ml) fractions. The blue line represents the absorbance of the protein sample at 280 nm, the green line represents the salt concentration, and the dark brown line represents salt conductivity.

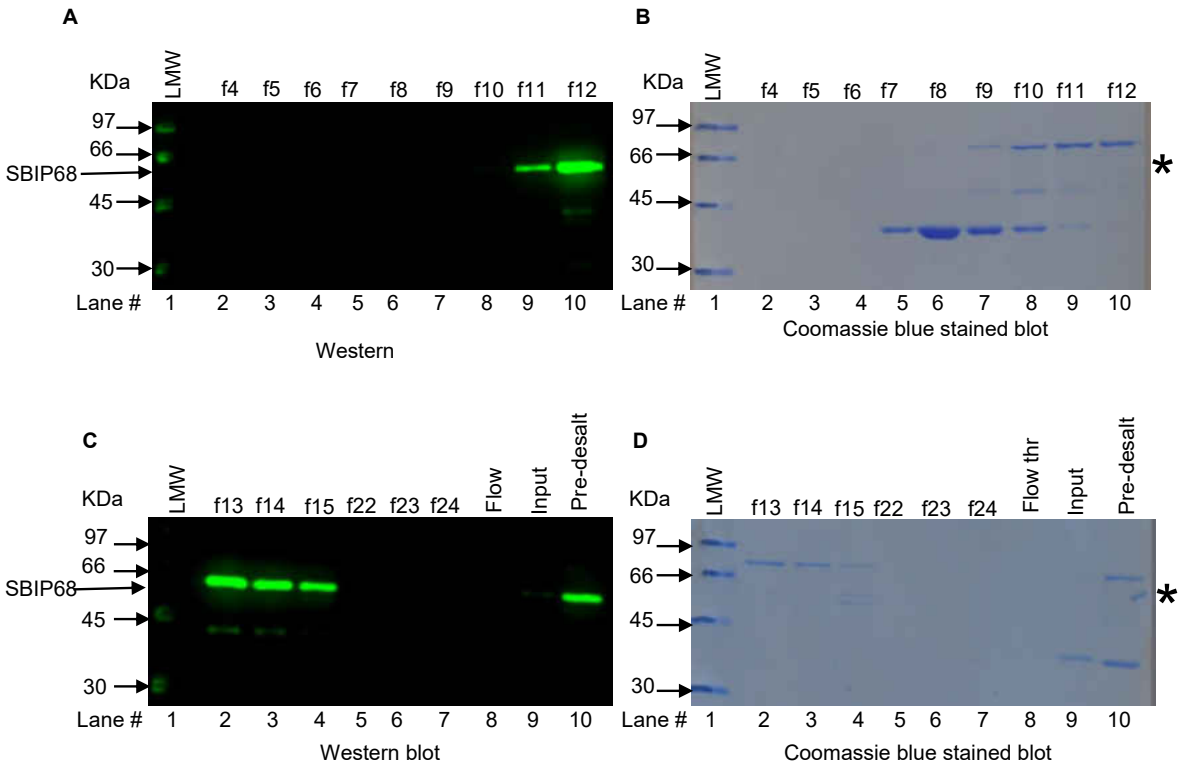


Figure 48: MonoQ Anion Exchange Chromatography Purification of SBIP68'. **A.** Western Blot Analysis of SBIP68' recombinant protein. Lanes 2 to 10 represent fractions 4, 5, 6, 7, 8, 9, 10, 11, and 12 derived from MonoQ anion exchange chromatography. **B.** Corresponding coomassie blue stained blot of **A.** **C.** Lanes 2 to 7 represent fractions 13, 14, 15, 22, 23, and 24 derived from MonoQ anion exchange chromatography. Lanes 8, 9, and 10 represent the flow-through, the input (Ni-NTA purified, desalted sample), and the undesalted sample respectively. **D.** Corresponding coomassie blue stained blot of **C.** The asterisks indicate SBIP68's expected position on the blots.

Analysis of Glucosyltransferase Activity of SBIP68' using Radioactive Method

A radioactive assay was performed to test for glucosyltransferase activity of purified recombinant SBIP68 as described in the materials and methods section (McIntosh et al., 1990). UDP-[U- ^{14}C] glucose was the donor substrate while a total of 14 different aglycones were each used as potential acceptor substrates. The incorporation of ^{14}C glucose (CPM, counts per minute) for each of the substrates tested is represented in Table 2 below. SBIP68' showed highest activity with kaempferol.

Figure 49 and Table 2 show the relative activity (kaempferol was considered 100%) for each substrate tested. Two independent reactions were performed for each substrate tested and the average of the values are also shown (Table 2). This radioactive assay method was developed for the detection of flavonoid glucosides that are soluble in ethyl acetate (see materials and methods), and may not be suitable for testing glucosyltransferase activity with salicylic acid and other simple phenols, as the solubility of their glucosides in ethyl acetate could not be ascertained at the time of this experiment.

Table 2: Activity Screening of SBIP68' using UDP-¹⁴C-glucose

Substrate	Cpm/rxn 1	Cpm/rxn 2	Average cpm/rxn	% Relative activity
Kaempferol	7599	7467	7533	100
Quercetin	5326	5674	5500	73
Hesperetin	4295	4909	4602	61
Naringenin	4277	4208	4243	56
Gossypetin	2051	2067	2059	27
4-acetone-7 Hydroxy-6-methoxy-Isoflavone	1325	1263	1294	17
Luteolin	1171	1221	1196	16
Apigenin	991	966	979	13
Fisetin	565	462	514	7
MeSA	269	244	257	3
Benzoic acid	260	234	247	3
Azelaic acid	216	257	237	3
Salicylic acid	235	232	234	3
p-hydroxybenzoic acid	217	192	205	3
Blank	59	47	53	1

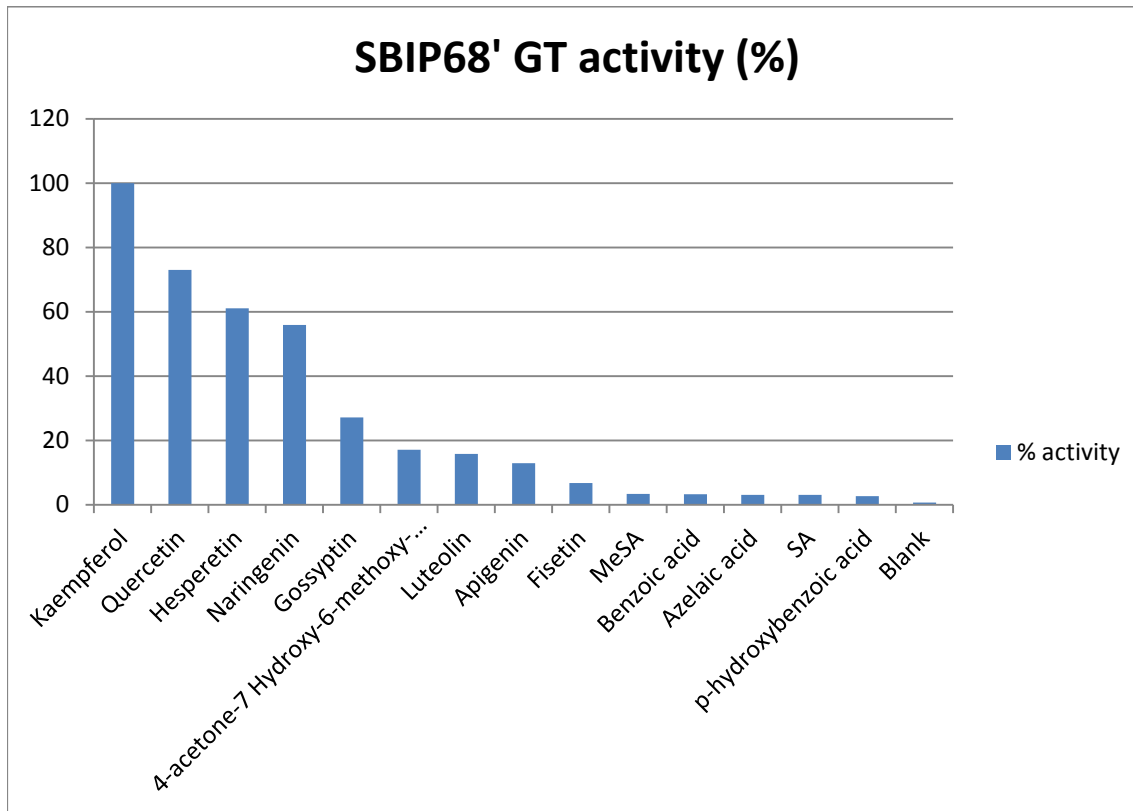


Figure 49: Relative Activity of SBIP68' with Different Potential Acceptor Substrates. Radioactive UDP glucose was used as the donor substrate. The CPM for each reaction was measured with a scintillation counter. All reactions were in duplicates and the average was taken.

Analysis of Glucosyltransferase Activity using HPLC

An HPLC based method (Owens and McIntosh, 2009) was used to identify the products formed from five different reactions involving kaempferol, quercetin, naringenin, hesperetin, and salicylic acid as acceptor substrates (Fig. 50). The glucosyltransferase reaction using purified SBIP68' was performed as described in the materials and methods. HPLC grade kaempferol 3-O-glucoside, kaempferol, quercetin, quercetin 3-O-glucoside, naringenin, naringenin 7-O-glucoside, hesperetin, and salicylic acid were also used as standards in the identification of the reaction products.

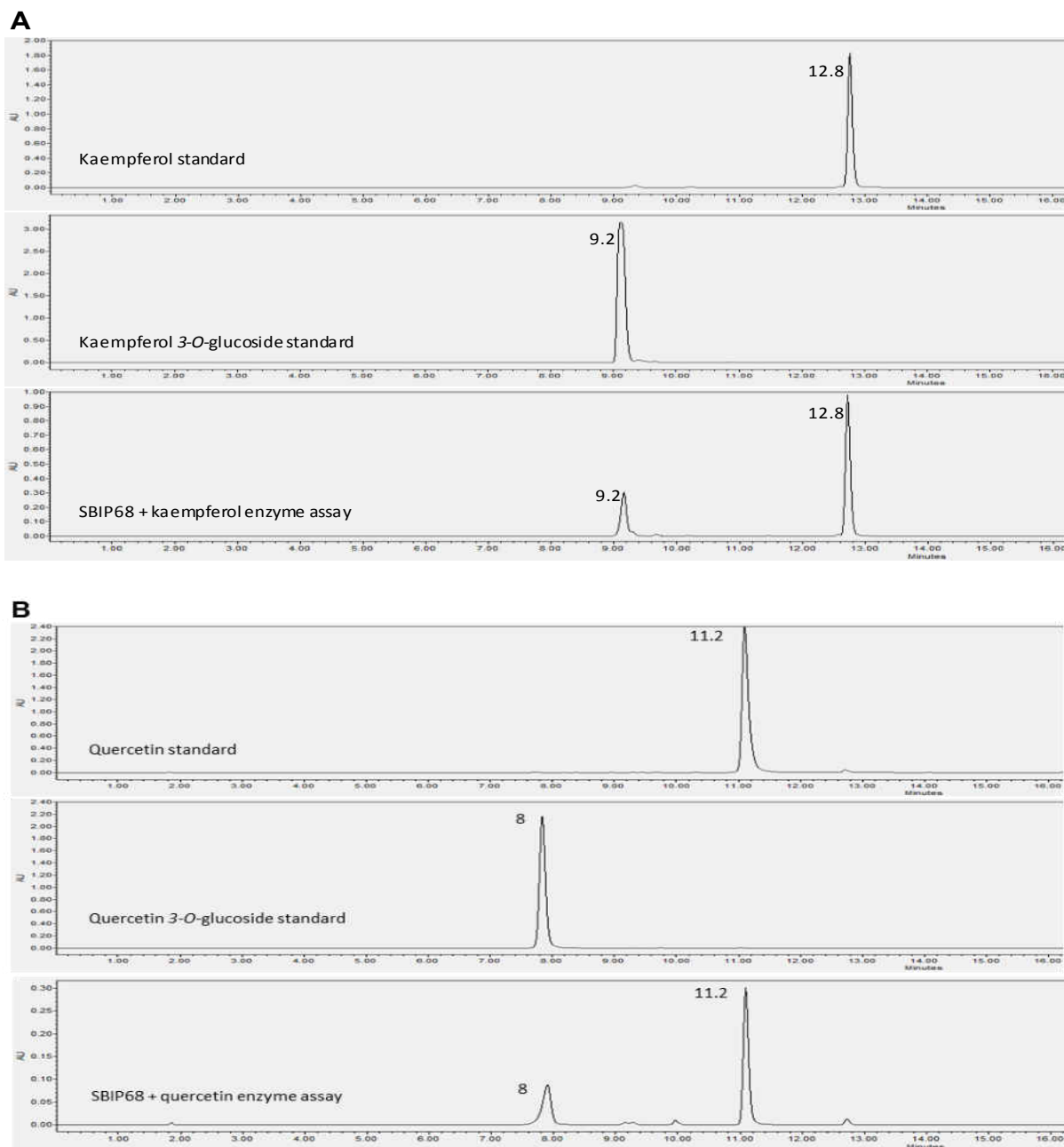


Figure 50 A-B: Identification of Reaction Products by HPLC. **A.** Top panel shows retention time for kaempferol standard at 12.7 minutes, middle panel shows retention time for kaempferol 3-O-glucoside standard at 9.2 minutes. The bottom panel shows the products formed from the reaction with SBIP68, kaempferol 3-O-glucoside and kaempferol, with retention times at 9.2 minutes and 12.8 minutes respectively. **B.** Top panel shows retention time for quercetin standard at 11.2 minutes, middle panel shows retention time for quercetin 3-O-glucoside standard at 8 minutes. The bottom panel shows the products formed from the reaction with SBIP68, quercetin 3-O-glucoside and quercetin, with retention times at 8 minutes and 11.2 minutes respectively.

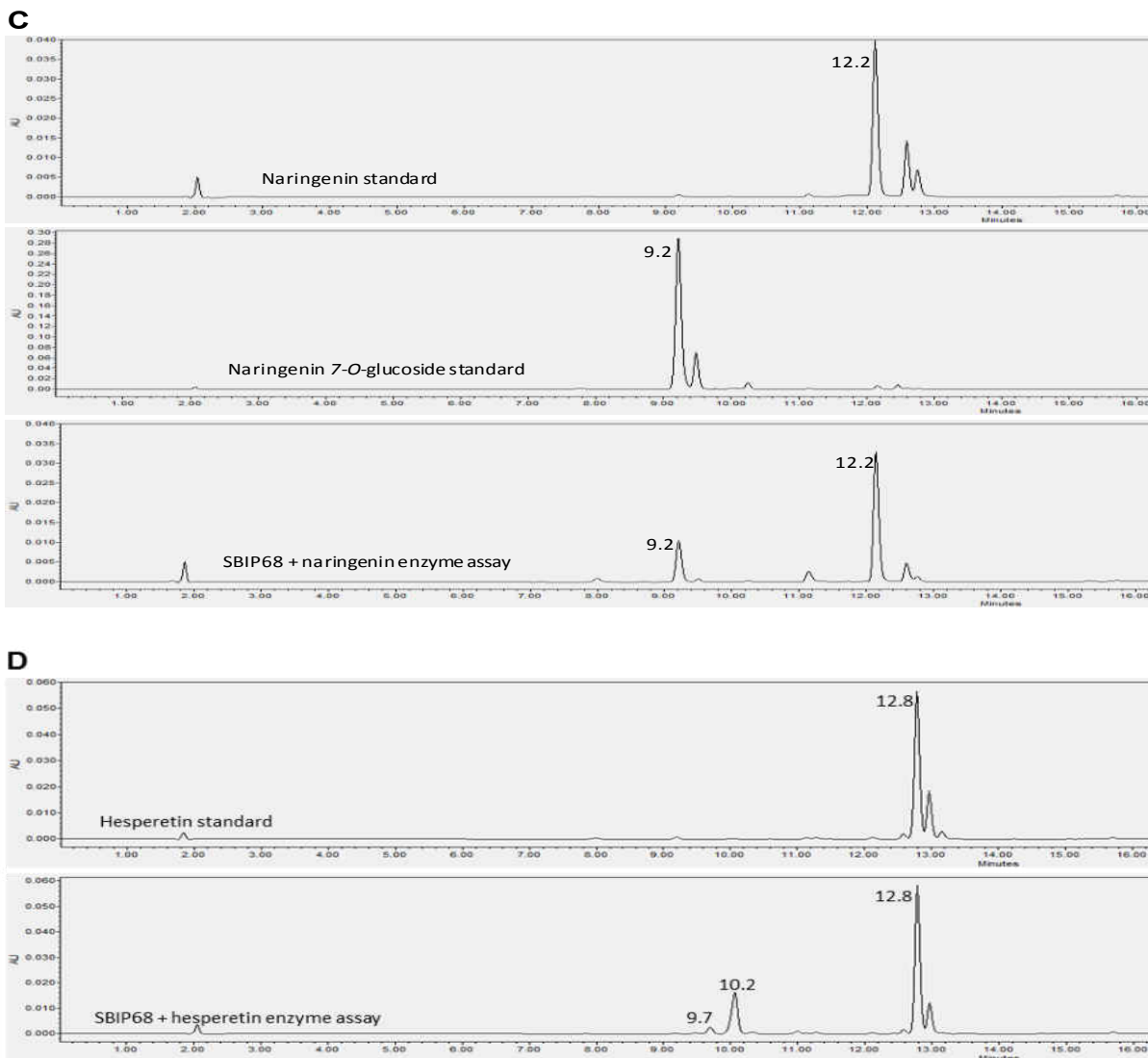


Figure 50 C-D: Identification of Reaction Products by HPLC. **C.** Top panel shows retention time for naringenin standard at 12.2 minutes, middle panel shows retention time for naringenin 7-O-glucoside standard at 9.2 minutes. The bottom panel shows the products formed from the reaction with SBIP68, naringenin 7-O-glucoside and naringenin, with retention times at 9.2 minutes and 12.2 minutes respectively. **D.** Top panel shows retention time for hesperetin standard at 12.8 minutes. The bottom panel shows the products formed from the reaction with SBIP68, hesperetin glucoside and hesperetin, with retention times at 10.2 minutes and 12.8 minutes respectively. It appears there is a second hesperetin glucoside with a retention time of 9.7 minutes. There were no hesperetin glucoside standards available at the time of this experiment.

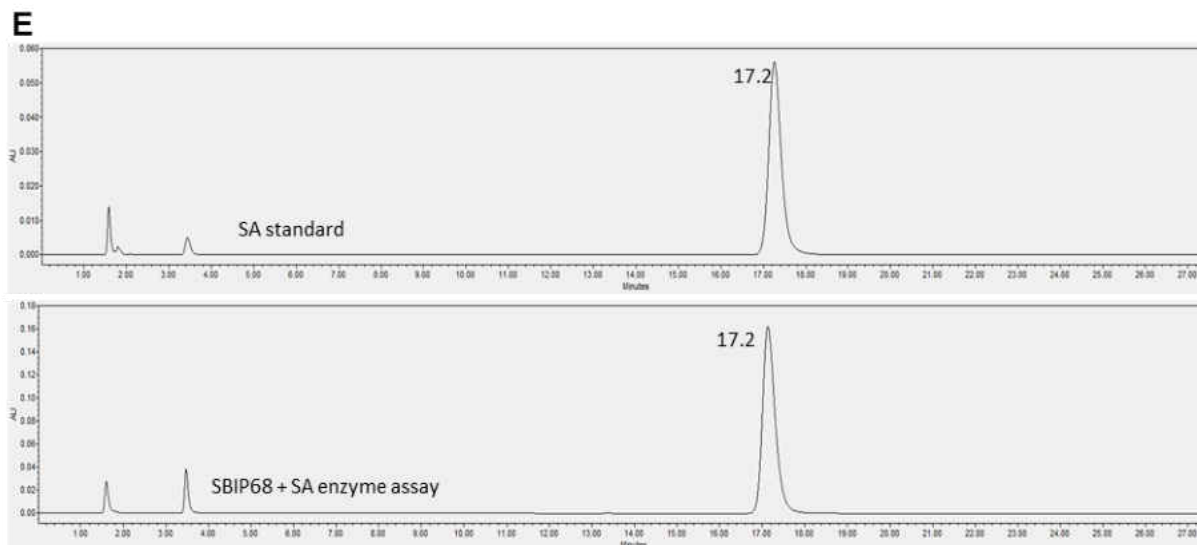


Figure 50 E: Identification of Reaction Products by HPLC. **E**. Top panel shows retention time for salicylic acid standard at 17.2 minutes. The bottom panel shows the product(s) from the SBIP68 reaction involving salicylic acid as a potential acceptor substrate. SA is seen to have a retention time of 17.2 minutes, no SA glucosides are observed. There were no salicylic acid glucoside standards available at the time of this experiment.

CHAPTER 4

DISCUSSION

Salicylic acid is a well-established signal molecule when it comes to defense responses in plants (Chen et al., 2009). The exogenous application of SA has been known to induce the expression of plant pathogenesis-related genes (Ward et al., 1991), and disease resistance (White, 1979). SA is not only involved in inducing hypersensitive response in infected areas of the plant but also systemic acquired resistance (SAR) in uninfected and distal parts (Malamy et al., 1990; Yalpani et al., 1991; Yalpani et al., 1993). The majority of the SA produced by plants undergoes glucosylation and/or methylation (Rivas-San Vicente and Plasencia, 2011). Glucosylation of SA at the hydroxyl group produces SA 2-O- β -D-glucoside (SAG), while glucosylation at the carboxyl group produces the SA glucose ester in large and minute amounts respectively (Rivas-San Vicente and Plasencia, 2011). SA glucosyltransferases are responsible for these glucosylation reactions which are induced upon the application of SA or during response to pathogen attack in tobacco and *Arabidopsis* (Lee and Raskin, 1999; Song, 2006). SAG stored in the vacuole may serve as an inactive form of SA capable of releasing free SA when required (Dean and Mills, 2004; Dean et al., 2005).

The methylation of SA by SA carboxyl methyltransferase produces methyl salicylate (MeSA), a volatile SA derivative that plays a crucial role serving as a long distance signal during systemic acquired resistance in tobacco and *Arabidopsis* (Shulaev et al., 1997; Chen et al., 2003; Park et al., 2007; Vlot et al., 2008). Tobacco SABP2 is the enzyme responsible for converting the volatile methyl salicylate into

salicylic acid in the distal parts of the plant to induce SAR (Park et al., 2007; Tripathi et al., 2010). An improved knowledge of SABP2 functionality would be a great achievement in the quest to understand how plants respond to stress. In a bid to achieve this, a yeast two-hybrid screening was performed with tobacco SABP2 as a bait and total expressed tobacco leaf proteins as prey. This led to the identification of several interacting proteins including SBIP68. Computational analysis revealed that SBIP68 belongs to the Family 1 of plant GTs (UGT), and it has the C-terminal PSPG signature motif characteristic of this group. The PSPG box is predicted to be involved in the binding of the UDP moiety of the sugar-donor substrate in the glycosylation reaction (Hughes and Hughes, 1994).

As mentioned previously, SABP2 has high affinity for salicylic acid and is important for the induction of SAR in the event of a pathogen attack (Kumar and Klessig, 2003). Since SBIP68 possessed the characteristics of a potential glucosyltransferase as determined by bioinformatics, and it interacts with SABP2, it is logical to hypothesize that SBIP68 might be a UGT involved in the glucosylation of salicylic acid during plant stress signaling.

UGTs have been known to participate in the detoxification of metabolites produced by plant-pathogens (Schweiger et al., 2013), or detoxification of harmful compounds including herbicides (Kreuz et al., 1996). They also enhance the solubility of low molecular weight compounds in water (Hrazdina, 1988), and are involved in the regulation of the action of essential compounds like indole acetic acid and cytokinins (Dixon et al., 1989; Szerszen et al., 1994).

As previously mentioned, a number of glucosyltransferases have been found to glucosylate salicylic acid, and their expression has been induced by SA. In *Oryza sativa*, probenazole (an agrochemical) induced the expression of OsSGT1, a UDP-glucose:SA glucosyltransferase involved in catalyzing the conversion of SA into SA O- β -glucoside (SAG) (Umemura et al., 2009). RNAi silencing of *OsSGT1* was observed to reduce to a large extent, the probenazole-dependent resistance to blast disease (Umemura et al., 2009). This strengthens the suggestion that OsSGT1 is a key player in the development of chemically induced disease resistance in rice (Umemura et al., 2009). OsSGT1 may be involved in the SA signaling pathway by inducing the up-regulation of SAG in rice (Umemura et al., 2009).

In tobacco plants possessing the 'N' resistance protein, bacterial or viral pathogens were observed to induce tobacco UDP-glucose:salicylic acid glucosyltransferase (SA GTase) mRNA expression (Lee and Raskin, 1999). This observed induction of SA GTase mRNA expression corresponded to an increase in endogenous SA found in the inoculated tissue (Lee and Raskin, 1999). Also, treatment of plant with SA was found to activate SA GTase mRNA expression, implying that induction of the SA GTase gene is through the SA-mediated signal transduction mechanism (Lee and Raskin, 1999).

The aim of the present study was to determine what role SBIP68 plays in tobacco and more importantly what kind of relationship exists between SBIP68 and SABP2. To gain more insight into the role of SBIP68, it was cloned, expressed and characterized functionally *in vitro*.

In silico subcellular localization analysis using various computer software predicted SBIP68 to be either present in the cytoplasm, or targeted to the endoplasmic reticulum membrane (Fig. 14 and 16), or may be transported (Fig. 15) to some other organelle where it exerts its effect. Protein BLAST analyses revealed that SBIP68 has a GTB topology, one of two protein topologies found in nucleotide-sugar-dependent glycosyltransferases (Marchler-Bauer et al., 2015). GTB proteins are known to have N and C terminal domains that are distinct each possessing a typical Rossmann fold (Marchler-Bauer et al., 2015). Both domains exhibit high structural homology even though they have very little sequence homology (Marchler-Bauer et al., 2015). Separating both domains is a large cleft which contains the catalytic center and allows a high degree of flexibility (Marchler-Bauer et al., 2015). SBIP68 was also shown to possess a putative GT1_Gtf_like conserved protein domain (Marchler-Bauer et al., 2015). Gtfs are a group of homologous glycosyltransferases that are involved in the last steps of the biosynthesis of vancomycin and related chloroeremomycin (Marchler-Bauer et al., 2015). They catalyze the transfer of sugars from activated NDP-sugar donors to the heptapeptide core of vancomycin group of antibiotics (Marchler-Bauer et al., 2015). In contrast, SBIP68 has a PSPG motif (Fig. 26) characteristic of plant GT's which binds the sugar donor substrate (Hughes and Hughes, 1994).

SBIP68 was cloned and expressed in *E. coli*. Solubility results revealed that recombinant SBIP68 in *E. coli* were mostly expressed in the insoluble form, and only a minor fraction was present in the soluble form (Fig. 30). The construct with C-terminal 6xHis tag (pET-28a-SBIP68-645) seemed to be better expressed in the soluble form compared to one with N-terminal 6xHis tag (pET-28a-SBIP68-644) (Fig. 30). There are

certain limitations to expression of recombinant proteins in a prokaryotic system such as *E. coli*, one of which is the formation of densely packed denatured proteins in the form of particles referred to as inclusion bodies (Singh and Panda, 2005). They occur as a stress response upon the high level expression of recombinant proteins (Sorensen and Mortenson, 2005) and they do not have a defined structure (Carrio et al., 2000). Formation of inclusion bodies in recombinant systems could be reduced by altering certain expression conditions including but not limited to temperature, rate of expression, and target protein engineering (Jonasson et al., 2002). In an attempt to produce more soluble SBIP68 recombinant protein, the amount of IPTG used in inducing expression, the expression temperature, and the duration of time used in expression were altered. The altering of these parameters, did not bring about significant improvement in the amount of soluble SBIP68 recombinant protein that was being produced (Fig. 31). The affinity purified soluble protein, however, showed glucosyltransferase activity when tested using four flavonoid acceptor substrates and UDP-glucose (Fig. 33, Fig. 34).

SBIP68 was also cloned into the pPICZA (a yeast expression) plasmid to be expressed in *P. pastoris*, a eukaryotic system. Some important characteristics that make yeast cells desirable for protein expression include the ability to proper protein folding and post-translational modifications because they are eukaryotes (Mattanovich et al., 2012). Presently, *Saccharomyces cerevisiae*, *Hansenula polymorpha*, and *Pichia pastoris* are being used in the large scale expression of heterologous proteins. These appear to be the most promising yeast strains at the moment (Mattanovich et al., 2012). *P. pastoris* is a methylotrophic yeast capable of growing on simple, inexpensive medium

and is appropriate for small as well as large scale heterologous expression of proteins (Daly and Hearn, 2005). It has two alcohol oxidase genes, *AOX1* and *AOX2*, whose promoters are methanol inducible (Daly and Hearn, 2005). Usually, the gene for the heterologous protein to be expressed is placed under the control of the *AOX1* promoter, which is strongly induced by methanol. Molecular manipulations like gene targeting, high efficiency of DNA transformation, and cloning for the purpose of functional complementation are similar to those obtainable with *S. cerevisiae* (Cereghino and Cregg, 2000). In addition to the above, *P. pastoris* has the ability to integrate heterologous DNA into the host chromosome easily, has promoters that are very tightly controlled, and is capable of generating more posttranslational modifications, making it preferable to *S. cerevisiae* (Yesilirmak and Sayers, 2009).

Cloning of SBIP68 into the pPICZA vector resulted in the formation of the pPICZA-SBIP68' construct which was used to transform *P. pastoris*. Because pPICZA has the *AOX1* promoter, and SBIP68 had been cloned behind this promoter, expression of the SBIP68 gene was made possible by induction of the *AOX1* promoter with methanol. Recombinant SBIP68 had a c-myc epitope as well as a C-terminal 6xHistidine tag which facilitated identification and purification, respectively. The *Pichia pastoris* expression system proved to be a preferable alternative to *E. coli* system in the expression of SBIP68 as a large proportion of the protein was present in the soluble form. Time point expression studies showed that the amount of SBIP68 produced from 0 – 96 hours continued to increase, however, after about 6 hours of induction, what appears to be a degradation product of SBIP68 starts to form and some other unwanted host proteins started accumulating (Figs. 43 and 44). Expression of SBIP68 for more

than 6 hours but no longer than 12 hours may be best as this may reduce the extent of degradation seen in 24 hour and above time points and also reduces the chances of expression of some of the non-specific proteins that appear during detection by Western blot analysis and also bind to the column during purification (Fig. 45).

Recombinant SBIP68 from *Pichia pastoris* was purified by affinity chromatography using Ni-NTA. Purification with Ni-NTA got rid of most but not all of the unwanted host proteins (Fig. 45). Ni-NTA purified samples were subsequently purified using anion exchange chromatography. Anion exchange chromatography further purified to a great extent, still several unwanted proteins co-purified as was visualized by coomassie blue staining (Fig. 48). It may be desirable to perform a purification using size-exclusion chromatography or other available chromatography matrix.

Based on our hypothesis of SBIP68 being a salicylic acid GT, and bioinformatics analysis predicting it to be a flavonoid GT, the purified SBIP68 was screened for GT activity with fourteen potential acceptor substrates using UDP-glucose as the sugar donor substrate. The acceptor substrates tested included a number of flavonoids, simple phenolics, and azelaic acid, a compound known to induce the accumulation of salicylic acid in plants after infection (Jung et al., 2009; Everts, 2011).

In testing the recombinant enzyme for glucosyltransferase activity, a radioactive assay (McIntosh et al., 1990) involving radiolabeled UDP-glucose, was employed. Recombinant SBIP68 glucosylated flavonols (kaempferol, quercetin, gossypetin, fisetin), flavanones (hesperetin, naringenin), flavones (apigenin, luteolin,), and isoflavones (4-acetone-7 Hydroxy-6-methoxy-isoflavone), displaying broad substrate specificity. SBIP68 barely showed activity in the reactions involving azelaic acid and the simple

phenolic compounds benzoic acid, salicylic acid, p-hydroxybenzoic acid, and MeSA, as acceptor substrates. Of the fourteen substrates tested, the reaction with kaempferol had the highest activity with 7,533 cpm, and quercetin was next with 5,500 cpm. Reactions involving hesperetin, naringenin, gossypetin, 4-acetone-7 hydroxy-6-methoxy-isoflavone, luteolin, apigenin, fisetin, methyl salicylic acid, benzoic acid, azelaic acid, and salicylic acid had 4602 cpm, 4243 cpm, 2059 cpm, 1294 cpm, 1196 cpm, 979 cpm, 514 cpm, 257 cpm, 247 cpm, 237 cpm, and 234 cpm respectively. The reaction with p-hydroxybenzoic acid had the lowest with 200 cpm (Fig. 49 and Table 2). Because the radioactive method was developed for detecting flavonoid glucosides that are soluble in the organic ester ethyl acetate (see materials and methods), this method may not be suitable for testing glucosyltransferase activity with salicylic acid and other simple phenols as the solubility of their glucosides in ethyl acetate could not be ascertained.

An HPLC based method (Owens and McIntosh, 2009) was used to identify the products formed from separate reactions involving kaempferol, quercetin, naringenin, hesperetin and salicylic acid as acceptor substrates (Fig. 33, Fig. 34, Fig. 50). Kaempferol, kaempferol 3-O-glucoside, quercetin, quercetin 3-O-glucoside, naringenin, naringenin 7-O-glucoside, hesperetin, and salicylic acid were also used as standards in an attempt to identify the products formed from the reactions with each of the acceptor substrates, there were no hesperetin glucoside and salicylic acid glucoside standards available at the time of the experiment. These reactions, when analyzed by HPLC, had distinct peaks for substrate and products formed. The reactions involving kaempferol as acceptor substrate had retention times of 9.2 minutes and 12.8 minutes for kaempferol-3-O-glucoside and kaempferol, respectively (Fig. 33A, Fig. 34A, Fig. 50A). The reaction

with quercetin had retention times of 8 minutes and 11.2 minutes for quercetin 3-O-glucoside and quercetin, respectively (Fig. 33B, Fig. 34B, Fig. 50B). The reaction involving naringenin as acceptor substrate had retention times of 9.2 minutes and 12.2 minutes for naringenin-7-O-glucoside and naringenin, respectively (Fig. 33C, Fig. 34C, Fig. 50C). The reaction with hesperetin had retention times of 9.7 minutes, 10.2 minutes, and 12.8 minutes for two unidentified hesperetin glucosides and hesperetin, respectively (Fig. 33D, Fig. 34D, Fig. 50D), while that with salicylic acid only showed a retention time for salicylic acid at 17.2 minutes (Fig. 50E). These results suggest that SBIP68 is a UDP-glucose: flavonoid glucosyltransferase, and probably not a salicylic acid glucosyltransferase.

Flavonoids are secondary metabolites synthesized by plants with known biological activities, they are involved in the interactions of plants with other organisms as well as their environment (Mierziak et al., 2014). Flavonoids undergo modification reactions such as methylation and glycosylation by methyltransferases and glucosyltransferases respectively (Mierziak et al., 2014). These reactions are known to alter their reactivity, solubility, and stability (Mierziak et al., 2014). Due to their diverse chemical structures and variety arising from the attached substituent groups, flavonoids have various important roles in plants, the most significant of which is UV protection (Treutter, 2005; Mierziak et al., 2014). They are involved in plant protection against both abiotic and biotic stresses, and they also maintain a redox state in cells arising from their antioxidative properties (Mierziak et al., 2014). Fat-soluble flavonoids could distort microbial membranes, alter their fluidity and damage the respiratory chain (Haraguchi et al., 1998; Mishra et al., 2009). The B ring of flavonoids are capable of intercalating or

forming hydrogen bonds with the stacking of nucleic acid bases causing an inhibition of DNA and RNA synthesis in bacteria and also enhance the activity of DNA gyrase (Wu et al., 2013). This feature is also considered to be the basis of their antiviral properties, as they are known to inhibit viral polymerase enzymes and bind to the nucleic acids or capsid proteins viruses (Selway, 1986). Flavonols (quercetin, kaempferol, myricetin) have also been shown to strongly promote pollen germination frequency, pollen development, and pollen tube growth in cultures of tobacco (*Nicotiana tabacum L.*) immature pollen *in vitro* (Ylstra et al., 1992). Low concentrations of these flavonols produced the best results, indicative of a signaling function (Ylstra et al., 1992).

Cucumber mosaic virus containing satellite RNA (CMV sat) which causes catastrophic necrotic tomato disease and is capable of infecting *Arabidopsis* was used in an experiment involving three groups of *Arabidopsis* plants; control plants which were untreated, wounded plants which were treated with buffer, and infected plants which were treated with CMV sat (Likić et al., 2014). As mentioned earlier, flavonoids participate in the detoxification of ROS in plants after wounding (León et al., 2001; Apel and Hirt, 2004). A decrease in kaempferol aglycone levels observed in the treated plants confirmed a putative role for kaempferol in the detoxification of ROS (Likić et al., 2014). Also, based on a model suggesting that H₂O₂ induces SA accumulation (Summermatter et al., 1995), detoxification of ROS by kaempferol and quercetin would inhibit the accumulation of SA in inoculated leaves (Likić et al., 2014). Observed changes in the concentrations of kaempferol and SA during the first four time points after inoculation with CMVsat were in accordance with the model (Likić et al., 2014). Significantly smaller concentrations of kaempferol present in the upper leaves of all

CMVsat infected plants as compared to the controls also indicated an important role for kaempferol in defense responses induced by CMVsat (Likić et al., 2014). Results from the experiment indicate a plausible regulatory function of kaempferol as a part of a proposed kaempferol-indole acetic acid dependent defense response where the systemic spread of CMVsat is curtailed through the joint action of kaempferol and IAA (Likić et al., 2014). This response is believed to be activated prior to the activation of well known salicylic acid defense response (Likić et al., 2014).

Quercetin is known to induce resistance in response to infection by virulent strain *Pseudomonas syringae* pv. *tomato* DC3000 (*Pst*) in *Arabidopsis*, via H₂O₂ burst and the involvement of SA and non-pathogenesis related 1 (NPR1) (Jia et al., 2010). Defense responses such as callose deposition, H₂O₂ burst, cell death, *pathogenesis-related 1* (PR1) and *Phenylalanine ammonia-lyase 1* (*PAL1*) gene expression were observed in quercetin-pretreated *Pst*-inoculated *Arabidopsis* Col-0 and a strong defense response against virulent *Pst* was found to occur in quercetin-pretreated *Arabidopsis* (Jia et al., 2010). In the presence of the enzyme catalase however, the anti-pathogenic effects of quercetin on virulent *Pst* in *Arabidopsis* was observed to disappear (Jia et al., 2010). This suggests that H₂O₂ is also important in the defense response against *Pst* (Jia et al., 2010). Quercetin was shown to have no beneficial effect on pathogen-free leaves in *Arabidopsis*, indicating that pathogen challenge is necessary to induce the defense responses observed to occur in quercetin-pretreated *Arabidopsis* (Jia et al., 2010).

Two new isoflavones and seven other known isoflavones were isolated from the stems and roots of *Nicotiana tabacum* and their anti-tobacco mosaic virus (anti-TMV) activities were evaluated using the half-leaf method (Yan et al., 2010; Chena et al.,

2012). Two of the tested isoflavones, licoisoflavone and 6-hydroxy-7,3',4',5'-tetramethoxy-isoflavone showed high (48.4%) anti-TMV activity and moderate (22.2%) anti-TMV activity respectively by inhibiting replication of the virus (Chena et al., 2012). The other seven compounds, 7-hydroxy-6,3',4',5'-tetramethoxy-isoflavone, irigenin, genistein, glycitein, 8-hydroxyglycitein, 2',4',5',6,7-pentamethoxyisoflavone, and 2',3',4',6,7-pentamethoxy isoflavone, all displayed weak (< 10%) anti-TMV activities (Chena et al., 2012). Ningnanmycin, a commercial product used in controlling plant diseases showed 33% inhibition rate and served as a positive control (Chena et al., 2012).

Under natural conditions, most flavonoids are present in form of their respective glycosides (Bohm, 1998; Forkmann and Heller, 1999). Glycosylation is one key mechanism that functions in regulating the storage and bioactivity of phytochemicals and the detoxification of xenobiotics in plants (Mackenzie et al., 1997; Bowles et al., 2005). Flavonoids are most commonly glycosylated by UGTs with one sugar group or more (Harborne and Baxter, 1999), and glucose happens to be the most common sugar found in naturally occurring flavonoid glycosides (Noguchi et al., 2009). Certain plants however, possess characteristic flavonoids in conjugation with specific sugars as their specialized metabolites (Noguchi et al., 2009).

UGT707B1 a glucosyltransferase found in the cytoplasm and the nucleus of stigma and tepal cells of *Crocus sativus* (saffron) is absent in the tepals of certain species (Trapero et al., 2012). Analysis of the glucosylated flavonoids present in the tepals of *Crocus* revealed two main flavonoid compounds present in saffron, these are kaempferol-3-O- β -D-glucopyranosyl-(1-2)- β -D-glucopyranoside and quercetin-3-O- β -D-

glucopyranosyl-(1-2)- β -D-glucopyranoside (Trapero et al., 2012). Both of these flavonoid glucosides were not found in the tepals of *Crocus* species that did not express UGT707B1 (Trapero et al., 2012). Transgenic *Arabidopsis* plants constitutively expressing UGT707B1 under the control of the cauliflower mosaic virus 35S promoter showed a number of phenotypic changes similar to those observed in previously described lines in which flavonoid levels had been altered (Trapero et al., 2012). The plants displayed thicker stems, hyponastic leaves, delay in flowering, and a lesser amount of trichomes (Trapero et al., 2012). Flavonoid levels present in extracts of the transgenic plants varied in their flavonol content as compared to wild-type plants (Trapero et al., 2012). Extracts obtained from the stems and flowers showed an increase in 3-sophoroside flavonol glucosides (Trapero et al., 2012). A new flavonol compound not found in *Arabidopsis* ecotype col-0 wild-type plants was found in all the tissues and this was identified to be kaempferol-3-O-sophoroside-7-O-rhamnoside (Trapero et al., 2012). All of these put together indicate that UGT707B1 is involved in the biosynthesis of flavonol-3-O-sophorosides and that the overexpression of a flavonoid glucosyltransferase could bring about significant changes in flavonoid homeostasis in a plant (Trapero et al., 2012).

UGT73A10 (49 % similarity to SBIP68) a glycosyltransferase cloned from Chinese wolfberry (*Lycium barbarum* L.) was heterologously expressed in *E. coli* and found to show outstanding regiospecific glucosyltransferase activity towards flavan-3-ols (e.g., (+)-catechin and epigallocatechin gallate), which are known to occur rarely in nature as glucosides (Noguchi et al., 2008). UGT73A10 showed high specificity for the donor substrate UDP-glucose and displayed broad acceptor substrate specificity with

the highest preference for naringenin (Noguchi et al., 2008). The enzyme glucosylated the 7 hydroxyl position of naringenin and was shown to be phylogenetically related to flavonoid 7-O-glucosyltransferases (Noguchi et al., 2008). UGT73A10 displayed high glucosyltransferase activity, up to 83% glucosyl transfer to (+)-catechin was observed. Spectroscopic analyses revealed that the transfer product was 4'-O- β -D-glucopyranoside, and not the 7-O- β -D-glucoside, of (+)-catechin (Noguchi et al., 2008). Stability studies also revealed that this glucoside product had better stability than (+)-catechin when subjected to alkaline conditions and high temperatures (Noguchi et al., 2008). The glucosylation of flavonoids by SBIP68 may serve to maintain flavonoid homeostasis in tobacco as well as play a protective role in the plant during abiotic or biotic stress conditions (Fig. 51).

As part of an ongoing project intended to elucidate the SA defense pathway in plants, and the SA-SABP2 relationship in tobacco, this research aimed at characterizing functionally the role of SBIP68 as a glucosyltransferase in the SA-SABP2 interaction. Recombinant SBIP68 activity screening performed with fourteen potential acceptor substrates and UDP-glucose as the donor substrate revealed SBIP68 to have broad substrate specificity, glucosylating flavonols, flavanones, and isoflavones. Kaempferol, quercetin, and naringenin appeared to be the preferred substrates, however, further experiments will have to be performed to determine SBIP68's substrate of choice. HPLC analysis and comparison with available commercial standards confirmed the formed glucosides from the reactions with kaempferol, quercetin, and naringenin, to be kaempferol 3-O-glucoside, quercetin 3-O-glucoside, and naringenin 7-O-glucoside, respectively.

Results from this study, as well as information available in the database indicate that SBIP68 is a UDP-glucose: flavonoid glucosyltransferase with broad substrate specificity. As earlier mentioned, flavonoids may be involved in plants defense against

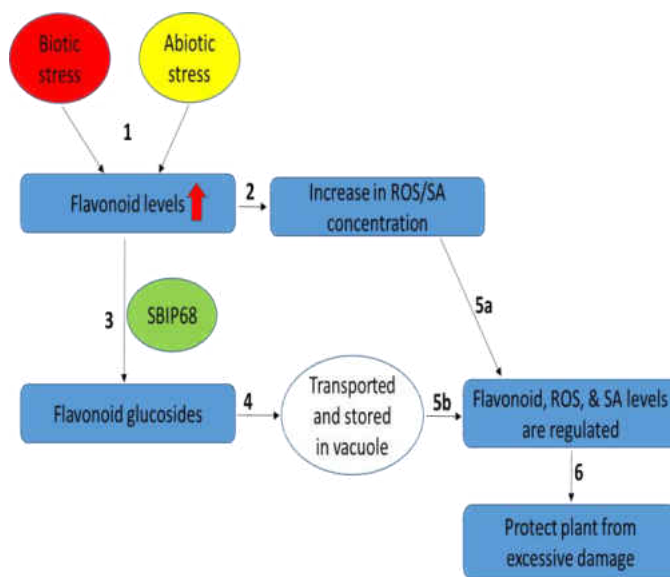


Figure 51: Model Suggesting SBIP68 Function *in planta*. SBIP68 may serve to maintain flavonoid homeostasis in tobacco plants during abiotic or biotic stress conditions, and consequently prevent excessive to the plants.

pathogens and most flavonoids occur naturally in their glycosylated forms. Glycosylation of flavonoids may function in regulating their storage and bioactivity (Fig. 51).

The reactions with azelaic acid, benzoic acid, and MeSA have to be repeated and optimized, and the reaction products analyzed in order to determine if SBIP68 is involved in the glucosylation of any of these. Bacterial infections lead to an increased accumulation of azelaic acid, which is known to confer local and systemic resistance against the pathogen *Pseudomonas syringae* in plants. It is required for the accumulation of salicylic acid and systemic immunity upon pathogen infection (Jung et al., 2009). Methyl salicylate (MeSA) is the *in planta* substrate of SABP2. SABP2 converts MeSA into SA, a requirement for the onset of systemic acquired resistance

(SAR) in systemic tissues (Park et al., 2007). Infection of tobacco (*Nicotiana tabacum* cv Samsun NN) plants with TMV or elicitation of tobacco cell suspensions with β -megaspermin brings about a rapid *de novo* synthesis and accumulation of a conjugated form of benzoic acid, benzoyl-glucose, which is a likely involved in the biosynthesis of SA (Chong et al., 2001).

This entire experiment was performed *in vitro*, and as a result we do not have information regarding the substrates of SBIP68 *in planta*. What we do know from this study is that SBIP68 is a glucosyltransferase. This information will be used in attempts to determine SBIP68's natural substrates and its role *in planta*, and more significantly its interaction with SABP2 and its role in the SA induced defense pathway, if any.

Future Directions

The characterization of SBIP68 is only a piece of the puzzle intended at deciphering the SA pathway in tobacco. Based on what is known about the glucosylation of salicylic acid, and available information indicating that SBIP68 is a glucosyltransferase that interacts with SABP2, it was proposed that SBIP68 is likely involved in the glucosylation of salicylic acid. Based on the results obtained in this study using *in vitro* enzyme assay, recombinant SBIP68 failed to glucosylate salicylic acid, but several potential flavonoid substrates were identified. Further experiments should be performed to determine SBIP68's most preferred substrate, as well as various kinetic studies to determine its rate of glucosylation, effect of temperature, pH, metal ions, etc. To study the effect of SABP2's interaction with SBIP68, the glucosyltransferase activity assay with flavonoid substrates should be conducted in the presence of SABP2.

To further study the role of SBIP68 in plant defense, transgenic plants either silenced in SBIP68 expression or overexpressing SBIP68 should be generated and used. These SBIP68 transgenic plants could be used for a range of experiments including challenging with viral pathogens such as tobacco mosaic virus (TMV) or bacterial plant pathogens such as *Pseudomonas syringae*. The results from all these proposed experiments is likely to help in understanding the role of SBIP68 in tobacco plants, and determine if it is involved in defense against pathogens.

REFERENCES

- Agrios GN. 1988. Plant pathology. Third edition. Academic Press, London.
- Alberts B, Johnson A, Lewis J, Raff M, Roberts K, Walter P. 2003. Molecular biology of the cell. 4th edn. Ann Bot 91(3):401.
- Apel K and Hirt H. 2004. Reactive oxygen species: metabolism, oxidative stress, and signal transduction. Annual Review of Plant Biology 55:373–399.
- Ausubel FM. 2005. Are innate immune signaling pathways in plants and animals conserved? Nat Immunol 6(10):973-9.
- Bashan Y. 1998. Azospirillum plant growth promoting strains are nonpathogenic on tomato, pepper, cotton, and wheat. Can J Microbiol 44:168-174.
- Bechthold A, Berger U, Heide L. 1991. Partial purification, properties, and kinetic studies of UDP-glucose:p-hydroxybenzoate glucosyltransferase from cell cultures of *Lithospermum erythrorhizon*. Arch Biochem Biophys 288(1):39-47.
- Ben-Tal Y and Cleland CF. 1982. Uptake and metabolism of [¹⁴C] salicylic acid in *Lemna gibba* G3. Plant Physiol 70: 291–296.
- Benbrook CM, Groth E, Halloran JM, Hansen MK, Marquardt S. 1996. Pest management at the crossroads. Consumers Union, New York.
- Bent AF and Mackey D. 2007. Elicitors, effectors, and R genes: the new paradigm and a lifetime supply of questions. Annu Rev Phytopathol 45:399-436.
- Bent AF, Innes RW, Ecker JR, Staskawicz BJ. 1992. Disease development in ethylene-insensitive arabidopsis thaliana infected with virulent and avirulent pseudomonas and xanthomonas pathogens. Mol Plant Microbe Interact 5:372-378.
- Bhat WW, Dhar N, Razdan S, Rana S, Mehra R, Nargotra A, Dhar RS, Ashraf N, Vishwakarma R, Lattoo SK. 2013. Molecular characterization of UGT94F2 and UGT86C4, two glycosyltransferases from *Picrorhiza kurrooa*: comparative structural insight and evaluation of substrate recognition. PLoS One 8(9):e73804.
- Blount JW, Dixon RA, Paiva NL. 1992. Stress responses in alfalfa (*Medicago sativa* L.) XVI. Antifungal activity of medicarpin and its biosynthetic precursors; implications for the genetic manipulation of stress metabolites. Physiol Mol Plant Pathol 41:333–349.
- Bohm B. 1998. Introduction of flavonoids. Harwood Academic Publishers, Singapore.

- Borsani O, Valpuesta V, Botella A. 2001. Evidence for a role of salicylic acid in the oxidative damage generated by NaCl and osmotic stress in arabidopsis seedlings. *Plant Physiol* 126(3):1024-30.
- Bowles D, Isayenkova J, Lim E-K, Poppenberger B. 2005. Glycosyltransferases: Managers of small molecules. *Curr Opin Plant Biol* 8:254–263.
- Brown AE and Surgeoner R. 1991. Enhancement of plant growth by zygorrhynchus moelleri. *Ann Appl Biol* 118(1):39-46.
- Burr TJ, Schroth MN, and Suslow T. 1978. Increased potato yields by treatment of seed pieces with specific strains of pseudomonas fluorescens and p. putida. *Phytopathology* 68:1377-1383.
- Calhelha RC, Andrade JV, Ferreira IC, Estevinho LM. 2006. Toxicity effects of fungicide residues on the wine-producing process. *Food Microbiol* 23(4):393-8.
- Carrio MM, Cubarsi R, Villaverde A. 2000. Fine architecture of bacterial inclusion bodies. *FEBS Lett* 471(1):7-11.
- Catinot J, Buchala A, Abou-Mansour E, Metraux JP. 2008. Salicylic acid production in response to biotic and abiotic stress depends on isochorismate in nicotiana benthamiana. *FEBS Lett* 582(4):473-8.
- Cereghino JL and Cregg JM. 2000. Heterologous protein expression in the methylotrophic yeast pichia pastoris. *FEMS Microbiol Rev* 24(1):45-66.
- Chen F, D'Auria JC, Tholl D, Ross JR, Gershenzon J, Noel JP, Pichersky E. 2003. An arabidopsis thaliana gene for methylsalicylate biosynthesis, identified by a biochemical genomics approach, has a role in defense. *The Plant Journal* 36:577-588.
- Chen Z, Zheng Z, Huang J, Lai Z, Fan G. 2009. Biosynthesis of salicylic acid in plants. *Plant Signal Behav* 4(6):493–496.
- Chena Z, Tana J, Yanga G, Miao M, Chena Y, Li T. 2012. Isoflavones from the roots and stems of nicotiana tabacum and their anti-tobacco mosaic virus activities. *Phytochemistry Letters* 5(2):233–235.
- Chini A, Grant JJ, Seki M, Shinozaki K, Loake GJ. 2004. Drought tolerance established by enhanced expression of the CCI-NBS-LRR gene, ADR1, requires salicylic acid, EDS1 and ABI1. *Plant J* 38(5):810-22.
- Chinnusamy V, Schumaker K, Zhu JK. 2004. Molecular genetic perspectives on cross-talk and specificity in abiotic stress signalling in plants. *J Exp Bot* 55(395):225-36.

- Chisholm ST, Coaker G, Day B, Staskawicz BJ. 2006. Host–microbe interactions: shaping the evolution of the plant immune response. *Cell* 124(4):803-14.
- Chong J, Pierrel M-A, Atanassova R, Werck-Reichhart D, Fritig B, Saindrenan P. 2001. Free and conjugated benzoic acid in tobacco plants and cell cultures. Induced accumulation upon elicitation of defense responses and role as salicylic acid precursors. *Plant Physiology* 125(1):318-328.
- Chou CH and Patrick ZA. 1976. Identification and phytotoxic activity of compounds produced during decomposition of corn and rye residues in soil. *J Chem Ecol* 2: 369-387.
- Cooper JB, Chen JA, Varner JE. 1984. The glycoprotein component of plant cell wall. In: Dugger WM and Bartnicki-Garcia S, eds. *Structure, function and biosynthesis of plant cell walls*. American Society of Plant Physiologist: 75-88
- Creelman RA and Mullet JE. 1995. Jasmonic acid distribution and action in plants: regulation during development and response to biotic and abiotic stress. *Proc Natl Acad Sci* 92(10):4114–4119.
- Creelman RA and Mullet JE. 1997. Oligosaccharins, Brassinolides, and Jasmonates: Nontraditional Regulators of Plant Growth, Development, and Gene Expression. *Plant Cell* 9(7): 1211–1223.
- Cregg JM, Barringer KJ, Hessler AY, Madden KR. 1985. *Pichia pastoris* as a host system for transformations. *Mol Cell Biol* 5(12):3376–3385.
- Cregg JM, Madden KR, Barringer KJ, Thill GP, Stillman CA. 1989. Functional characterization of two alcohol oxidase genes from the yeast *Pichia pastoris*. *Mol Cell Biol* 9:1316–1323.
- Dai GH, Nicole M, Andary C, Martinez C, Bresson E, Boher B, Daniel JF, Geiger JP. 1996. Flavonoids accumulate in cell walls, middle lamellae and callose-rich papillae during an incompatible interaction between *Xanthomonas campestris* pv. *malvacearum* and cotton. *Physiol Mol Plant Pathol* 49:285–306.
- Daly R and Hearn MT. 2005. Expression of heterologous proteins in *pichia pastoris*: a useful experimental tool in protein engineering and production". *J Mol Recognit* 18(2):119–38.
- Dangl JL and Jones JD. 2001. Plant pathogens and integrated defence responses to infection. *Nature* 411(6839):826-33.

- De Waard MA, Georgopoulos SG, Hollomon DW, Ishii H, Leroux P, Ragsdale NN, Schwinn FJ. 1993. Chemical control of plant diseases: problems and prospects. *Annu Rev Phytopathol* 31:403-21.
- Dean JV and Mills JD. 2004. Uptake of salicylic acid 2-O- β -D-glucose into soybean tonoplast vesicles by an ATP-binding cassette transporter-type mechanism. *Physiologia Plantarum* 120:603-612.
- Dean JV, Mohammed LA, Fitzpatrick T. 2005. The formation, vacuolar localization, and tonoplast transport of salicylic acid glucose conjugates in tobacco cell suspension cultures. *Planta* 221:287-296.
- Dernoeden PH and McIntosh MS. 1991. Disease enhancement and kentucky bluegrass quality as influenced by fungicides. *Agron J* 83:322-326.
- Devaiah SP, Owens DK, Sibhatu MB, Roy Sarkar T, Strong CL, Mallampalli VKPS, Asiago J, Cooke J, Kaiser S, Lin Z, Wamuch A, Hayford D, Williams BE, Loftis P, Berhow M, Pike LM, McIntosh CA. Isolation, recombinant expression, and biochemical characterization of putative secondary product glucosyltransferase clones from *Citrus paradisi*. Unpublished.
- Dixon SC, Martin RC, Mok MC, Shaw G, Mok DW. 1989. Zeatin glycosylation enzymes in phaseolus: isolation of O-glucosyltransferase from p. lunatus and comparison to O-xylosyltransferase from p. vulgaris. *Plant Physiol* 90(4):1316-21.
- Du H and Klessig DF. 1997. Identification of a soluble, high-affinity salicylic acid-binding protein in tobacco. *Plant Physiol* 113:1319-27
- Duke SO, Menn JJ, Plimmer JR. 1993. Challenges of pest control with enhanced toxicological and environmental safety. In: Duke SO, Menn JJ, Plimmer JR, eds. *Pest Control with Enhanced Environmental Safety*. American Chemical Society: 1-13.
- Ecker JR, and Davis RW 1987. Plant defense genes are regulated by ethylene (stress responses/plant hormone/wounding/RNA bedlot analysis). *Proc Natl Acad Sci* 84:5202-5206.
- Ecobichon DJ, Davies JE, Doull J, Ehrich M, Joy R, McMillan D, MacPhail R, Reiter LW, Slikker W Jr, Tilson H. 1990. Neurotoxic effects of pesticides. *Advances in Modern Environmental Toxicology* 18:131-199.
- Elmholt S 1991. Side effects of propiconazole (Tilt 250 EC) on non-target soil fungi in a field trial compared with natural stress effects. *Microb Ecol* 22(1):99-108.

- Elskus AA. 2014. Toxicity, sublethal effects, and potential modes of action of select fungicides on freshwater fish and invertebrates: U.S. Geological Survey Open-File Report 2012–1213, 42 p.
- Emmert EA, Handelsman J. 1999. Biocontrol of plant disease: a (Gram-) positive perspective. *FEMS Microbiol Lett* 171(1):1-9.
- Enyedi AJ and Raskin I. 1993. Induction of UDP-glucose:salicylic acid glucosyltransferase activity in tobacco mosaic virus-inoculated tobacco (*Nicotiana tabacum*) leaves. *Plant Physiol* 101:1375-1380.
- Enyedi AJ, Yalpani N, Silverman P, Raskin I. 1992. Localization, conjugation, and function of salicylic acid in tobacco during the hypersensitive reaction to tobacco mosaic virus. *Proc Natl Acad Sci USA* 89:2480-2484.
- Everts S. 2011. Vegetative warfare. *Chemical & Engineering News* 89(5):53–55.
- FAO/UNEP/WHO. 2004. Pesticide poisoning: information for advocacy and action. Geneva, UNEP.
- Felton GW and Dahlman DL 1984. Nontarget effects of a fungicide: Toxicity of Maneb to the parasitoid microplitis croceipes (Hymenoptera: Braconidae). *J Econ Entomol* 77:842-850.
- Foote RH, Schermerhorn EC, Simkin ME. 1986. Measurement of semen quality, fertility, and reproductive hormones to assess dibromochloropropane (DBCP) effects in live rabbits. *Fundam Appl Toxicol* 6(4):628-37.
- Forkmann G and Heller W. 1999. Biosynthesis of flavonoids. Pages 713–748. In: *Comprehensive Natural Products Chemistry*. Elsevier, Amsterdam.
- Forouhar F, Yang Y, Kumar D, Chen Y, Fridman E, Park SW, Chiang Y, Acton TB, Montelione GT, Pichersky E, Klessig DF, Tong L. 2005. Structural and biochemical studies identify tobacco SABP2 as a methyl salicylate esterase and implicate it in plant innate immunity. *Proc Natl Acad Sci* 102(5):1773-8.
- Freeman JL, Garcia D, Kim D, Hopf AM, Salt DE. 2005. Constitutively elevated salicylic acid signals glutathione-mediated nickel tolerance in thlaspi nickel hyperaccumulators. *Plant Physiol* 137(3):1082-91.
- Fukuchi-Mizutani M, Okuhara H, Fukui Y, Nakao M, Katsumoto Y, Yonekura-Sakakibara K, Kusumi T, Hase T, Tanaka Y. 2003. Biochemical and molecular characterization of a novel UDP-glucose:anthocyanin 3'-o-glucosyltransferase, a key enzyme for blue anthocyanin biosynthesis, from gentian. *Plant Physiol* 132(3):1652-1663.

- Glass ADM. 1973. Influence of phenolic acids on ion uptake. I. Inhibition of phosphate uptake. *Plant Physiol* 51(6): 1037–1041.
- Goldman L and Tran N. 2002. *Toxics and poverty: the impact of toxic substances on the poor in developing countries*. Washington DC, World Bank.
- Goodman RN and Novacky AJ. 1994. *The Hypersensitive reaction in plants to Pathogens: a resistance phenomenon*. St. Paul, MN: APS Press
- Grasso P. 2002. *Essentials of Pathology for Toxicologists*. CRC Press, Boca Raton, FL.
- Griesser M, Vitzthum F, Fink B, Bellido ML, Raasch C, Munoz-Blanco J, Schwab W. 2008. Multi-substrate flavonol O-glucosyltransferases from strawberry (*Fragaria x ananassa*) achene and receptacle. *Journal of Experimental Botany* 59(10):2611–2625.
- Guy SO, Oplinger ES, Grau CR. 1989. Soybean cultivar response to metalaxyl applied in furrow and as a seed treatment. *Agron J* 81:529-532.
- Haraguchi H, Tanimoto K, Tamura Y, Mizutani K, Kinoshita T. 1998. Mode of antibacterial action of retrochalcones from *Glycyrrhiza inflata*. *Phytochemistry* 48:125–129.
- Harborne JB and Baxter H. 1999. *The Handbook of Natural Flavonoids*. Vol 2, New York.
- Harper JR and Balke NE. 1981. Characterization of the inhibition of K⁺ absorption in oat roots by salicylic acid. *Plant Physiol* 68: 1349-1353.
- Harris AR, Schisler DA, Correll RL, Ryder MH. 1994. Soil bacteria selected for suppression of *Rhizoctonia solani*, and growth promotion, in bedding plants. *Soil Biol Biochem* 26:1249-1255.
- Hayat S and Ahmad A. 2007. *Salicylic acid: A plant hormone*. Springer. Dordrecht. Pp 1-40
- Hiron RW and Wright ST. 1973. The Role of Endogenous Abscisic Acid in the Response of Plants to Stress. *J Exp Bot* 24(4):769-780.
- Hoffman T, Schmidt JS, Zheng X, Bent AF. 1999. Isolation of ethylene insensitive soybean mutants that are altered in pathogen susceptibility and gene-for-gene disease resistance. *Plant Physiol* 119(3):935-50.
- Hoof van Huijsduijnen RA, Van Loon LC, Bol JF. 1986. cDNA cloning of six mRNAs induced by TMV infection of tobacco and a characterization of their translation products. *EMBO J* 5(9):2057-61.

- Hrazdina G. 1988. Purification and properties of a UDP-glucose: flavonoid 3-O-glucosyltransferase from *Hippeastrum* petals. *Biochimica et Biophysica Acta (BBA) - Protein Structure and Molecular Enzymology* 955(3):301-309.
- Hughes J, Hughes MA. 1994. Multiple secondary plant product UDP-glucose glucosyltransferase genes expressed in cassava (*Manihot esculenta crantz*) cotyledons. *DNA Sequence: The Journal of DNA Sequencing and Mapping* 5(1):41-49.
- Hunt M and Ryals J. 1996. Systemic acquired resistance signal transduction. *Crit Rev Plant Sci* 15:583-606.
- Hurt J, Thibodeau S, Hirsh A, Pabo C, Joung J. 2003. Highly specific zinc finger proteins obtained by directed domain shuffling and cell-based selection. *Proc Natl Acad Sci* 100(21):12271–6.
- Jia Z, Zou B, Wang X, Qiu J, Ma H, Gou Z, Song S, Dong H. 2010. Quercetin-induced H₂O₂ mediates the pathogen resistance against *Pseudomonas syringae* pv. *tomato* DC3000 in *Arabidopsis thaliana*. *Biochemical and Biophysical Research Communications* 396:522–527.
- Jonasson P, Liljeqvist S, Nygren PA, Stahl S. 2002. Genetic design for facilitated production and recovery of recombinant proteins in escherichia coli. *Biotechnol Appl Biochem* 35(Pt 2):91-105.
- Jollès P and Muzzarelli RA. 1999. Chitin and chitinases. Basel: Birkhäuser.
- Jones P, Messner B, Nakajima J, Schäffner AR, Saito K. 2003. UGT73C6 and UGT78D1, glycosyltransferases involved in flavonol glycoside biosynthesis in *Arabidopsis thaliana*. *J Biol Chem* 278:43910–43918.
- Joung J, Ramm E, Pabo C. 2000. A bacterial two-hybrid selection system for studying protein-DNA and protein-protein interactions. *Proc Natl Acad Sci* 97(13):7382–7.
- Jung HW, Tschaplinski TJ, Wang L, Glazebrook J, Greenberg JT. 2009. Priming in systemic plant immunity. *Science* 324(5923):89–91.
- Kloepper JW, Leong J, Teintze M, Schroth MN. 1980(a). Enhanced plant growth by siderophores produced by plant growth-promoting rhizobacteria. *Nature* 286:885-886.
- Kloepper JW, Lifshitz R, Zablutowicz RM. 1989. Free-living bacterial inocula for enhancing crop productivity. *Trends Biotechnol* 7:39-44.

- Kloepper JW, Schroth MN, Miller TD. 1980(b). Effects of rhizosphere colonization by plant growth-promoting rhizobacteria on potato plant development and yield. *Phytopathology* 70:1078-1082.
- Kreuz K, Tommasini R, Martinoia E. 1996. Old enzymes for a new job (Herbicide detoxification in plants). *Plant Physiol* 111(2): 349–353.
- Kumar D. 2014. Salicylic acid signaling in disease resistance. *Plant Science*, 228: 127-134.
- Kumar D and Klessig DF. 2003. High-affinity salicylic acid-binding protein 2 is required for plant innate immunity and has salicylic acid-stimulated lipase activity. *Proc Natl Acad Sci* 100:16101–6
- Kunkel BN and Brooks DM. 2002. Cross talk between signaling pathways in pathogen defense. *Curr Opin Plant Biol* 5(4):325-31.
- Lairson LL, Henrissat B, Davies GJ, Withers SG. 2008. Glycosyltransferases: structures, functions, and mechanisms. *Annu Rev Biochem* 77:521-55.
- Lamport DT. 1980. Structure and function of plant glycoproteins. In: *The Biochemistry of Plants*, ed. Preiss, J. (Academic, New York) 3:501-541.
- Langlois-Meurinne M, Gachon CMM, and Saindrenan P. 2005. Pathogen-responsive expression of glycosyltransferase genes UGT73B3 and UGT73B5 is necessary for resistance to *Pseudomonas syringae* pv. tomato in *Arabidopsis*. *Plant Physiol* 139(4):1890–1901.
- Larkindale J, Hall JD, Knight MR, Vierling E. 2005. Heat stress phenotypes of *Arabidopsis* mutants implicate multiple signaling pathways in the acquisition of thermotolerance. *Plant Physiol* 138(2):882-97.
- Larkindale J and Knight MR. 2002. Protection against heat stress-induced oxidative damage in *Arabidopsis* involves calcium, abscisic acid, ethylene, and salicylic acid. *Plant Physiol* 128(2):682-95.
- Lee HI and Raskin I. 1998. Glucosylation of salicylic acid in *Nicotiana tabacum* Cv. Xanthi-nc. *Phytopathology* 88(7):692-7.
- Lee HI and Raskin I. 1999. Purification, cloning and expression of a pathogen inducible udp-glucose:salicylic acid glucosyltransferase from tobacco. *J Biol Chem* 274(51):36637-42.
- León J, Rojo E, Sánchez-Serrano JJ. 2001. Wound signalling in plants. *Journal of Experimental Botany* 52:1–9.

- Likić S, Šola I, Ludwig-Müller J, and Rusak G. 2014. Involvement of kaempferol in the defence response of virus infected *Arabidopsis thaliana*. *Eur J Plant Pathol* 138:257–271.
- Lorenc–Kukula K, Korobczak A, Aksamit–Stachurska A, Kostyń K, Lukaszewicz M, Szopa J. 2004. Glucosyltransferase: the gene arrangement and enzyme function. *Cell Mol Biol Lett* 9:935-946.
- Lotti M. 1988. The delayed polyneuropathy caused by some organophosphorus esters. Pages 247-257. In: CL Galli, L Manzo, PS Spencer, eds. *Recent Advances in Nervous Systems Toxicology*. Plenum, New York.
- Lund ST, Stall RE, Klee HJ. 1998. Ethylene regulates the susceptible response to pathogen infection in tomato. *Plant Cell* 10(3): 371–382.
- Mackenzie PI, Owens IS, Burchell B, Bock KW, Bairoch A, Bélanger A, Fournel-Gigleux S, Green M, Hum DW, Iyanagi T, Lancet D, Louisot P, Magdalou J, Chowdhury JR, Ritter JK, Schachter H, Tephly TR, Tipton KF, Nebert DW. 1997. The UDP glycosyltransferase gene superfamily: Recommended nomenclature update based on evolutionary divergence. *Pharmacogenetics* 7(4):255–269.
- Macri F, Vianello A, Pennazio S. 1986. Salicylate-collapsed membrane potential in pea stem mitochondria. *Physiol Plant* 67: 136-140.
- Malamy J, Carr JP, Klessig DF, Raskin I. 1990. Salicylic acid: a likely endogenous signal in the resistance response of tobacco to viral infection. *Science* 250:1002–1004.
- Malamy J, Hennig J, Klessig DF. 1992. Temperature-dependent induction of salicylic acid conjugates during the resistance response to tobacco mosaic virus infection. *Plant Cell* 4:359-366
- Manohar M, Tian M, Moreau M, Park SW, Choi HW, Fei Z, Giulia F, Klessig DF. 2014. Identification of multiple salicylic acid-binding proteins using two high throughput screens. *Frontiers in Plant Science* 5:777.
- Marchler-Bauer A, Derbyshire MK, Gonzales NR, Lu S, Chitsaz F, Geer LY, Geer RC, He J, Gwadz M, Hurwitz DI, Lanczycki CJ, Lu F, Marchler GH, Song JS, Thanki N, Wang Z, Yamashita RA, Zhang D, Zheng C, Bryant SH. 2015. CDD: NCBI's conserved domain database. *Nucleic Acids Res* 43:D222-6.
- Mattanovich D, Branduardi P, Dato L, Gasser B, Sauer M, Porro D. 2012. Recombinant protein production in yeasts. *Methods Mol Biol* 824:329-58.

- Mauch-Mani B and Mauch F. 2005. The role of abscisic acid in plant-pathogen interactions. *Curr Opin Plant Biol* 8(4):409-14.
- McIntosh CA, Latchinian L, Mansell RL. 1990. Flavanone-specific 7-O-glucosyltransferase activity in *Citrus paradisi* seedlings: Purification and characterization. *Archives of Biochemistry and Biophysics* 282(1):50-57.
- McMullen MP and Lamey HA. 2001. *Plant Diseases Development and Management*. NDSU Extension Service.
- McNeil M, Darvill AG, Fry SC, Albersheim P. 1984. Structure and function of the primary cell walls of higher plants. *Annu Rev Biochem* 53:625-663.
- Metwally A, Finkemeier I, Georgi M, Dietz KJ. 2003. Salicylic acid alleviates the cadmium toxicity in barley seedlings. *Plant Physiol* 132(1):272-81.
- Mierziak J, Kostyn K, Kulma A. 2014. Flavonoids as important molecules of plant interactions with the environment. *Molecules* 19:16240-16265.
- Mishina TE and Zeier J. 2007. Pathogen-associated molecular pattern recognition rather than development of tissue necrosis contributes to bacterial induction of systemic acquired resistance in arabidopsis. *Plant J* 50(3):500-13.
- Mishra AK, Mishra A, Kehri HK, Sharma B, Pandey AK. 2009. Inhibitory activity of Indian spice plant *Cinnamomum zeylanicum* extracts against *Alternaria solani* and *Curvularia lunata*, the pathogenic dematiaceous moulds. *Ann Clin Microbiol Antimicrob* 8:9.
- Morel JB and Dangl JL. 1997. The hypersensitive response and the induction of cell death in plants. *Cell Death Differ* 4(8):671-83.
- Munne-Bosch S and Penuelas J. 2003. Photo- and antioxidative protection, and a role for salicylic acid during drought and recovery in field grown phillyrea angustifolia plants. *Planta* 217(5):758-66 *Planta* 217, 758–766.
- Naoumkina MA, Zhao Q, Gallego-Giraldo L, Dai X, Zhao PX, Dixon RA. 2010. Genome-wide analysis of phenylpropanoid defence pathways. *Mol Plant Pathol* 11:829–846.
- Natl Acad Sci 1987. *Regulating pesticides in food: The Delaney paradox*. Washington: Natl. Acad. Press. 272pp.) Committee on Scientific and Regulatory Issues Underlying Pesticide Use Patterns and Agricultural Innovation (Author), National Research Council (Author), Board on Agriculture (Author)

- Neuenschwander U, Lawton K, Ryals J. 1996. Systemic acquired resistance. In: Stacey G and Keen NT, eds. Plant-microbe Interactions. Vol. 1, (New York: Chapman and Hall), pp. 81-106.
- Noguchi A, Horikawa M, Fukui Y, Fukuchi-Mizutani M, Iuchi-Okada A, Ishiguro M, Kiso Y, Nakayama T, Ono E. 2009. Local differentiation of sugar donor specificity of flavonoid glycosyltransferase in lamiales. *The Plant Cell* 21:1556–1572.
- Noguchi A, Sasaki N, Nakao M, Fukami H, Takahashi S, Nishino T, Nakayama T. 2008. cDNA cloning of glycosyltransferases from Chinese wolfberry (*Lycium barbarum* L.) fruits and enzymatic synthesis of a catechin glucoside using a recombinant enzyme (UGT73A10). *Journal of Molecular Catalysis B: Enzymatic* 55:84–92.
- Norman-Setterblad C, Vidal S, Palva ET. 2000. Interacting signal pathways control defense gene expression in arabidopsis in response to cell wall-degrading enzymes from erwinia carotovora. *Mol Plant Microbe Interact* 13(4):430-438.
- NRC Report. 1996. Ecologically based pest management: new solutions for a new century. 144 pp. Natl Acad Sci Press.
- Ó Gráda C. 2006. Ireland's great famine: interdisciplinary perspectives. University College Dublin Press.
- Ostrowski M, Jakubowska A. 2014. UDP-glycosyltransferases of plant hormones. *Advances In Cell Biology* 4(1):43–60.
- Owens DK and McIntosh CA. 2009. Identification, recombinant expression, and biochemical characterization of a flavonol 3-O-glucosyltransferase clone from *Citrus paradisi*. *Phytochemistry* 70:1382-1391.
- Pal KK and Gardener BM. 2006. Biological control of plant pathogens. The Plant Health Instructor.
- Pareek RP and Gour AC. 1973. Organic acids in the rhizosphere of *Zea mays* and *Phaseolus aureus* plants. *Plant Soil* 39:441–444.
- Park SW, Kaimoyo E, Kumar D, Mosher S, Klessig DF. 2007. Methyl salicylate is a critical mobile signal for plant systemic acquired resistance. *Science* 318(5847):113-6.
- Paro R, Tiboni GM, Buccione R, Rossi G, Cellini V, Canipari R, Cecconi S. 2012. The fungicide mancozeb induces toxic effects on mammalian granulosa cells. *Toxicol Appl Pharmacol* 260(2):155-61.

- Pimentel D, Acquay H, Biltonen M, Rice P, Silva M, Nelson J, Lipner V, Giordano S, Horowitz A, D'Amore M. 1992. Environmental and economic costs of pesticide use. *Bioscience* 42(10):750-760.
- Pimentel D and Burgess M. 2014. Biofuel production using food. *Environ Dev Sustain* 16(1):1-3
- Pimentel D, Lach L, Zuniga R, Morrison D. 2000. Environmental and economic costs associated with non-indigenous species in the United States. *Bioscience* 50:53-65.
- Pimentel D, McLaughlin L, Zepp A, Lakitan B, Kraus T, Kleinman P, Vancini F, Roach WJ, Graap E, Keeton WS, Selig G. 1991. Environmental and economic impacts of reducing u.s. agricultural pesticide use. Pp 679-718. In: D Pimentel, ed. *Handbook on Pest Management in Agriculture*. CRC Press, Boca Raton, FL.
- Plaper A, Golob M, Hafner I, Oblak M, Solmajer T, Jerala R. 2003. Characterization of quercetin binding site on DNA gyrase. *Biochem Biophys Res Commun* 306:530–536.
- Potashnik G, and Yanai-Inbar I. 1987. Dibromochloropropane (DBCP): an 8-year reevaluation of testicular function and re-productive performance. *Fertil Steril* 47:317-323.
- Priest DM, Ambrose SJ, Vaistij FE, Elias L, Higgins GS, Ross ARS, Abrams SR, Bowles DJ. 2006. Use of the glucosyltransferase UGT71B6 to disturb abscisic acid homeostasis in *Arabidopsis thaliana*. *Plant J* 46:492-502.
- Ragsdale NN, Hylin JW, Sisler HD, Witt JM. 1991. Health and environmental factors associated with agricultural use of fungicides. Portion USDA/States Natl Agric Pestic Impact Assess Prog (NAPIP) Fungic Assess Proj 117pp.
- Rangwala T, Bafna A, Maheshwari RS. 2013. Harmful effects of fungicide treatment on wheat (*Triticum aestivum* L.) seedlings. *Int Res J Environment Sci* 2(8):1-5.
- Raskin I, Skubatz H, Tang W, Meeuse BJ. 1990. Salicylic acid levels in thermogenic and non-thermogenic plants. *Ann Bot* 66 (4): 369-373
- Raven PH, Evert RH, Eichhorn SE. 1992. *Biology of Plants* 5th Edition. Worth Publishers, New York.
- Ren N and Timko MP. 2001. AFLP analysis of genetic polymorphism and evolutionary relationships among cultivated and wild *Nicotiana* species. *Genome* 44(4): 559–71.
- Rivas-San Vicente M and Plasencia J. 2011. Salicylic acid beyond defence: its role in plant growth and development. *J Exp Bot* 62(10):3321-3338.

- Roby D, Toppan A, Esquerre-Tugaye MT. 1986. Cell surfaces in plant-microorganism interactions : vi. elicitors of ethylene from colletotrichum lagenarium trigger chitinase activity in melon plants. *Plant Physiol* 81(1):228-33
- Roby D, Toppan A, and Esquerre-Tugaye MT. 1985. Cell surfaces in plant-microorganism interactions : v. elicitors of fungal and of plant origin trigger the synthesis of ethylene and of cell wall hydroxyproline-rich glycoprotein in plants. *Plant Physiol* 77(3):700-4.
- Ross D. 2002. Ireland: History of a Nation: 226.
- Russell PE 1995. Fungicide resistance: occurrence and management. *J Agric Sci* 124:317-323.
- Ryals JA, Neuenschwander UH, Willits MG, Molina A, Steiner H, Hunt MD. 1996. Systemic acquired resistance. *The Plant Cell* 8:1809-1819.
- Schaller A, Stintzi A. 2009. Enzymes in jasmonate biosynthesis - structure, function, regulation. *Phytochemistry* 70(13-14):1532-8.
- Schroeder JI, Kwak JM, Allen GJ. 2001. Guard cell abscisic acid signalling and engineering drought hardiness in plants. *Nature* 410(6826):327-30.
- Schweiger W, Pasquet JC, Nussbaumer T, Paris MP, Wiesenberger G, Macadré C, Ametz C, Berthiller F, Lemmens M, Saindrenan P, Mewes HW, Mayer KF, Dufresne M, Adam G. 2013. Functional characterization of two clusters of *Brachypodium distachyon* UDP-glycosyltransferases encoding putative deoxynivalenol detoxification genes. *Mol Plant Microbe Interact* 26(7):781-92.
- Schwinn FJ. 1992. Significance of fungal pathogens in crop production. *Pestic Outlook* 3:18-25.
- Schwinn FJ, Margot P. 1991. Control with chemicals. In *Advances in Plant Pathology*, ed. D. S. Ingram, P. H. Williams, 7:225-65 . London: Academic. 273 pp.
- Selway JW. 1986. Antiviral activity of flavones and flavans. *Prog Clin Biol Res* 213:521-536.
- Seo M and Koshiba T. 2002. Complex regulation of aba biosynthesis in plants. *Trends in Plant Science* 7(1):41-8.
- Shah J, Chaturvedi R, Chowdhury Z, Venables B, Petros RA. 2014. Signaling by small metabolites in systemic acquired resistance. *Plant J* 79(4):645-58.
- Shigematsu T, Kasugai H, Shibahara T, Nakajima T, Teraoka T. 1978. Chemicals for controlling plant virus diseases and control method. United States Patent 4166846.

- Shimizu T and Kojima M. 1984. Partial purification and characterization of UDPG:t-cinnamate glucosyltransferase in the root of sweet potato, *Ipomoea batatas* Lam. J Biochem 95(1):205-12.
- Shulaev V, Silverman P, Raskin I. 1997. Airborne signalling by methyl salicylate in plant pathogen resistance. Nature 385:718-721.
- Sierro N, Battey JND, Ouadi S, Bakaher N, Bovet L, Willig A, Goepfert S, Peitsch MC, Ivanov NV. 2014. The tobacco genome sequence and its comparison with those of tomato and potato. Nature Communications 5: 3833.
- Singh SM and Panda AK. 2005. Solubilization and refolding of bacterial inclusion body proteins. J Biosci Bioeng 99(4):303-10.
- Song JT. 2006. Induction of a salicylic acid glucosyltransferase, AtSGT1, is an early disease response in arabidopsis thaliana. Mol Cells. 22(2):233-8.
- Sorensen HP and Mortensen KK. 2005. Advanced genetic strategies for recombinant protein expression in escherichia coli. J Biotechnol 115(2):113-28.
- Staswick PE, Yuen GY, Lehman CC. 1998. Jasmonate signaling mutants of arabidopsis are susceptible to the soil fungus pythium irregulare. Plant J 15(6):747-54.
- Summermatter K, Sticher L, Métraux JP. 1995. Systemic responses in *Arabidopsis thaliana* infected and challenged with *Pseudomonas syringae* pv *syringae*. Plant Physiology 108:1379–1385.
- Sun Y, Hrazdina G. 1991. Isolation and characterization of a UDPglucose: flavonol o-glucosyltransferase from illuminated red cabbage (*Brassica oleracea* cv red danish) Seedlings. Plant Physiol 95(2):570-6.
- Swamy PM and Smith B. 1999. Role of abscisic acid in plant stress tolerance. Current Science 76:1220–1227.
- Szerszen JB, Szczyglowski K, Bandurski RS. 1994. iaglu, a gene from zea mays involved in conjugation of growth hormone indole-3-acetic acid. Science 265(5179):1699-701.
- Taiz L and Zeiger E. 2002. Plant Physiology Third Edition, page 306. Sinauer Associates Inc, Sunderland, MA.
- Tanaka S, Hayakawa K, Umetani Y, Tabata M. 1990. Glucosylation of isomeric hydroxybenzoic acids by cell suspension cultures of *Mallotus japonicus*. Phytochemistry 29:1555-1558

- The world health report. 2003. Shaping the future. Geneva, World Health Organization.
- Thomma BP, Eggermont K, Penninckx IA, Mauch-Mani B, Vogelsang R, Cammue BP, Broekaert WF. 1998. Separate jasmonate-dependent and salicylate-dependent defense response pathways in arabidopsis are essential for resistance to distinct microbial pathogens. *Proc Natl Acad Sci* 95(25):15107-11.
- Thomma BP, Eggermont K, Tierens KF, Broekaert WF 1999. Requirement of functional ethylene-insensitive 2 gene for efficient resistance of arabidopsis to infection by botrytis cinerea. *Plant Physiol* 121(4):1093-102.
- Thomas PT and House RV. 1989. Pesticide-induced modulation of the immune system. Pp 94-106. In: NN Ragsdale and RE Menzer, eds. *Carcinogenicity and Pesticides: Principles, Issues, and Relationships*. American Chemical Society, Washington, DC.
- Trapero A, Ahrazem O, Rubio-Moraga A, Jimeno ML, Gómez MD, and Gómez-Gómez L. 2012. Characterization of a glucosyltransferase enzyme involved in the formation of kaempferol and quercetin sophorosides in *Crocus sativus*. *Plant Physiol* 159(4):1335-54.
- Treutter D. 2005. Significance of flavonoids in plant resistance and enhancement of their biosynthesis. *Plant Biol (Stuttg)*7(6):581-91.
- Tripathi D, Jiang Y, Kumar D. 2010. SABP2, a methyl salicylate esterase is required for the systemic acquired resistance induced by acibenzolar-s-methyl in plants. *FEBS Lett* 584:3458–3463.
- Troy TN. 2011. Fast-growing fungicide markets: Farm Chemicals International.
- Turner JG, Ellis C, Devoto A. 2002. The jasmonate signal pathway. *Plant Cell* 14 Suppl: S153-64.
- Turner JT and Backman PA. 1991. Factors relating to peanut yield increases after seed treatment with bacillus subtilis. *Plant Dis* 75:347-353.
- Umemura K, Satou J, Iwata M, Uozumi N, Koga J, Kawano T, Koshihara T, Anzai H, Mitomi M. 2009. Contribution of salicylic acid glucosyltransferase, OsSGT1, to chemically induced disease resistance in rice plants. *The Plant Journal* 57: 463–472.
- Uppalapati SR, Ishiga Y, Wangdi T, Kunkel BN, Anand A, Mysore KS, Bender CL. 2007. The phytotoxin coronatine contributes to pathogen fitness and is required for suppression of salicylic acid accumulation in tomato inoculated with

- Pseudomonas syringae* pv. tomato DC3000. *Mol Plant Microbe Interact* 20(8):955-65.
- van Loon LC, Geraats BP, Linthorst HJ. 2006. Ethylene as a modulator of disease resistance in plants. *Trends Plant Sci* 11(4):184-91.
- Vijayan P, Shockey J, Lévesque CA, Cook RJ, Browse J. 1998. A role for jasmonate in pathogen defense of Arabidopsis. *Proc Natl Acad Sci* 95:7209-7214.
- Vlot AC, Dempsey DA, Klessig DF. 2009. Salicylic acid, a multifaceted hormone to combat disease. *Annu Rev Phytopathol* 47:177-206.
- Vlot AC, Liu PP, Cameron RK, et al. 2008. Identification of likely orthologs of tobacco salicylic acid-binding protein 2 and their role in systemic acquired resistance in Arabidopsis thaliana. *The Plant Journal* 56:445-456.
- Ward ER, Uknes SJ, Williams SC, Dincher SS, Wiederhold DL, Alexander DC, et al. 1991. Coordinate gene activity in response to agents that induce systemic acquired resistance. *Plant Cell* 3:1085–1094.
- White RF. 1979. Acetylsalicylic acid (Aspirin) induces resistance to tobacco mosaic virus in tobacco. *Virology* 99:410–412.
- Wildermuth MC, Dewdney J, Wu G, Ausubel FM. 2001. Isochorismate synthase is required to synthesize salicylic acid for plant defense. *Nature* 414(6863):562-5.
- Wu T, Zang X, He M, Pan S, Xu X. 2013. Structure-activity relationship of flavonoids on their anti-*Escherichia coli* activity and inhibition of DNA gyrase. *J Agric Food Chem* 61:8185–8190.
- Wu Y, Kuzma J, Maréchal E, Graeff R, Lee HC, Foster R, Chua NH. 1997. Abscisic acid signaling through cyclic adp-ribose in plants. *Science* 278(5346):2126-30.
- Xiong L and Zhu JK. 2003. Regulation of abscisic acid biosynthesis. *Plant Physiol* 133(1):29–36.
- Yalpani N, Balke NE, Schulz M. 1992. Induction of UDP-glucose:salicylic acid glucosyltransferase in oat roots. *Plant Physiol* 100:1114-1119.
- Yalpani N, Shulaev V, Raskin I. 1993. Endogenous salicylic acid levels correlate with accumulation of pathogenesis-related proteins and virus resistance in tobacco. *Phytopathol* 83:702–708.
- Yalpani N, Silverman P, Wilson TM, Kleier DA, Raskin I. 1991. Salicylic acid is a systemic signal and an inducer of pathogenesis-related proteins in virus-infected tobacco. *Plant Cell* 3:809–818.

- Yan XH, Chen J, Di YT, Fang X, Dong JH, Sang P, Wang YH, He HP, Zhang ZK, Hao XJ. 2010. Anti-tobacco mosaic virus (TMV) quassinoids from *Brucea javanica* (L.) Merr. *J Agric Food Chem* 58:1572–1577.
- Yang SF and Hoffman NE. 1984. Ethylene biosynthesis and its regulation in higher plants. *Ann Rev Plant Physiol* 35:155-189.
- Yang ZM, Wang J, Wang SH, Xu LL. 2003. Salicylic acid-induced aluminium tolerance by modulation of citrate efflux from roots of cassia tora l. *Planta* 217(1):168-74.
- Yesilirmak F and Sayers Z. 2009. Heterologous expression of plant genes. *International Journal of Plant Genomics* 296482.
- Ylstra B, Touraev A, Moreno RMB, Stoger E, van Tunen AJ, Vicente O, Mol JNM, Heberle-Bors E. 1992. Flavonols stimulate development, germination, and tube growth of tobacco pollen. *Plant Physiol* 100:902-907.
- Young KH. 1998. Yeast two-hybrid: so many interactions, (in) so little time. *Biol Reprod* 58(2):302-11.
- Zhou MY, Gomez-Sanchez CE. 2000. Universal TA cloning. *Curr Issues Mol Biol* 2(1):1-7.

APPENDICES

Appendix A – Abbreviations

SABP2 - Salicylic acid binding protein 2

SBIP68 - SABP2 Interacting Protein-68

HR - Hypersensitive response

SA - Salicylic acid

JA - Jasmonic acid

ET - Ethylene

SAR - Systemic acquired resistance

MeSA - Methyl salicylate

SDS PAGE - Sodium dodecyl sulphate-polyacrylamide gel electrophoresis

TMV - Tobacco mosaic virus

PR - Pathogenesis-related

β ME - Beta mercaptoethanol

*E*F α 1 - Elongation Factor alpha 1

TAE - Tris-Acetate EDTA

KDa - Kilo Dalton

OD - Optical Density

UV - Ultra violet

μ g – micro gram

μ l – micro litre

ml – milli litre

mM – milli Molar

Appendix B – Buffers, Reagents, and Media

0.8 % Agarose Gel

Agarose = 0.40 g

1x TAE Buffer = 50 ml

Dissolve the agarose in the TAE buffer by heating in a microwave for ~ 60 seconds.

Place the mixture in a water bath ~ 60 °C to dissolve the agarose completely.

Add 2.5 µl (10 mg/mL) ethidium bromide

20% APS (Ammonium Persulfate) (1 ml)

Ammonium persulfate = 0.2 g

Water = 1 ml

500X B (0.02% Biotin)

Biotin = 20 mg

Dissolve in 100 ml distilled water

Filter sterilize solution

Store at 4 °C

Breaking Buffer (500 mL)

Monobasic Sodium Phosphate Monohydrate = 3.45 g

EDTA (non-salt) = 145 mg

100 % Glycerol = 25 ml

Dissolve ingredients in 500 mL dH₂O

Add 10µl of 0.1M PMSF per ml of breaking buffer immediately before use

BMGY Medium (1 L)

1% Yeast extract = 10 g

2 % Peptone = 20 g

Dissolve in 700 ml sterile distilled water

Autoclave for 20 min on liquid cycle

Cool to room temperature

Add the following

1M Potassium Phosphate Buffer (pH=6.0) = 100 ml

1M 10X Yeast Nitrogen Base = 100 ml

10X Glycerol = 100 ml

500X Biotin = 2 ml

Store at 4 °C

BMMY Medium (1 L)

Yeast extract = 10 g

Peptone = 20 g

Dissolve in 700 ml distilled water

Autoclave for 20 minutes on liquid cycle

Cool to room temperature

Add the following

1M Potassium Phosphate Buffer (pH=6.0) = 100 ml

1M 10X Yeast Nitrogen Base = 100 ml

10X Methanol = 100 ml

500X Biotin = 2 ml

Store at 4°C

Coomassie brilliant blue destaining solution (1 L)

500 ml distilled water

400 ml methanol

100 ml acetic acid

Coomassie Brilliant Blue staining solution (1 L)

500ml Methanol

100 ml acetic acid

400 ml H₂O

Dissolve 1 g of Coomassie Brilliant Blue in the solution.

10X D (20% Dextrose) (500 ml)

Dextrose (D-glucose) = 100 g

Dissolve in 500 ml distilled water

Autoclave for 15 min on liquid cycle

Store at room temperature

0.1% DEPC (Diethyl Pyrocarbonate) Treated Water (0.1 L)

Diethyl pyrocarbonate = 0.1 ml

Distilled water = 100 ml

Mix the above constituents by pipetting the DEPC into the distilled water, incubate the mixture at 37°C for ~12 hours. Autoclave at 121°C and 15 psi atmospheric pressure for 20 minutes and allow to cool to room temperature.

10X GY (10 % Glycerol) (500 ml)

100 % Glycerol = 50 ml

Add 450 ml distilled water

Sterilize by autoclaving for 20 minutes on liquid cycle

Store at room temperature

LB/ampicillin/IPTG/X-Gal Plates

LB Broth = 2.5 g

Agar = 1.5 g

Make up to 100 ml with distilled water

Sterilize by autoclaving for 20 minutes on liquid cycle

Cool to ~ 50 °C and add 100 µl of ampicillin (100 mg/ml)

Pour plates to solidify

Add 20 µl of 0.5 M IPTG and 40 µl of 20 mg/ml X-Gal to each plate and spread using glass beads

LB Medium (1 L)

LB Broth = 25 g

Make up to 1000 ml with distilled water

Sterilize by autoclaving for 15 minutes on liquid cycle

Store at room temperature

Low Salt LB-Agar Plates (200 mL) with 25mg/l Zeocin

0.5 % Yeast Extract = 1 g

1 % Tryptone = 2 g

1 % Sodium Chloride = 2 g

Dissolve in 150 ml distilled water

Adjust to pH 7.5 with 1M NaOH

Make up volume to 200 ml with distilled water

Add 1.5 % Agar = 3 g

Autoclave for 20 minutes

Allow to cool to ~55 °C

Add 50 µl of filter sterilized zeocin (100 mg/ml)

Pour plates to solidify

Store at 4°C in the dark

Low Salt LB Medium (200 ml) with 25 mg/l Zeocin

0.5 % Yeast Extract = 1 g

1 % Tryptone = 2 g

1 % Sodium Chloride = 2 g

Dissolve in 150 ml distilled water

Adjust to pH 7.5 with 1M NaOH

Make up volume to 200 ml with distilled water

Autoclave for 20 minutes

Allow to cool to room temperature

Add 50 µl filter sterilized zeocin (100 mg/ml)

Store at 4°C in the dark

10X M (5% Methanol) (500 ml)

100 % Methanol = 25 ml

Add 475 ml of distilled water

Filter sterilize

Store at 4 °C

Ni-NTA Binding Buffer (1 L)

Sodium phosphate monobasic (M.W: 137.99 g/mol) = 6.89 g,

final concentration = 50 mM

Sodium chloride (M.W: 58.44 g/mol) = 17.53 g, final concentration = 300 mM

Imidazole (M.W: 68.08) = 0.6808, final concentration = 10 mM

Ni-NTA Elution Buffer (1 L)

Sodium phosphate monobasic (M.W: 137.99 g/mol) = 6.896 g,

final concentration = 50 mM

Sodium chloride (M.W: 58.44 g/mol) = 17.53 g, final concentration = 300 mM

Imidazole (M.W: 68.08) = 17.02 g, final concentration = 250 mM

10X PBS (Phosphate Buffer Saline) (1L)

Sodium Phosphate dibasic (M.W: 141.96 g/mol) = 10 g, final conc. = 70mM

Sodium Phosphate monobasic (M.W: 119.96 g/mol) = 4.1g, final conc.= 30mM

Sodium Chloride (58.44g/mol) = 76 g, final concentration = 1.3M

Dissolve the above listed in 500 ml distilled water, adjust the volume to 1L with distilled water.

1X PBS (1 L)

10X PBS = 100 ml

Distilled water = 900 ml

Mix the above.

1X PBS Plus 3% Tween Twenty (1 L)

10X PBS = 100 ml

Distilled water = 870 ml

Tween twenty = 30 ml

Mix the above.

Ponceau S Stain (0.1 L)

Ponceau S = 0.1 g, final concentration = 0.1%

Acetic acid = 5 ml, final concentration = 5%

Distilled water = 95 ml

1M Potassium Phosphate Buffer (500 ml)

Potassium Phosphate Dibasic = 11.5 g

Potassium Phosphate Monobasic = 59.08 g

Dissolve in 450 ml distilled water (Final pH=6.0)

Allow to cool to room temperature

Make up to 500 ml with distilled water

Sterilize by autoclaving for 20 minutes on liquid cycle

Store at 4 °C

10x SDS-PAGE Running Buffer (1 L)

Tris base (M.W: 121.1 g/mol) = 30 g

Glycine (M.W: 75.07 g/mol) = 144 g

SDS = 10 g

1x SDS-PAGE Running Buffer (1 L)

10x SDS-PAGE Running Buffer = 100 ml

Distilled water = 900 ml

4x SDS-PAGE Separating Gel Buffer (500mL)

Tris base (M.W: 121.1 g/mol) = 90.85 g, final concentration = 1.5M

Adjust pH to 8.8

Add SDS to a final concentration of 0.04% = 0.2 g

4x SDS-PAGE Stacking Gel Buffer (500mL)

Tris base (M.W: 121.1 g/mol) = 30.28 g, final concentration = 0.5M

Adjust pH to 6.8

Add SDS to a final concentration of 0.04% = 0.2 g

3M Sodium Acetate (100 mL)

$\text{CH}_3\text{COONa} \cdot 3\text{H}_2\text{O}$ = 40.82 g

Dissolve in 50 ml dd H_2O

Adjust pH to 5.2 with glacial acetic acid

Adjust volume to 100 ml with dd H_2O

Filter and sterilize by autoclaving

50X TAE (Tris Acetate EDTA) Buffer (500mL)

Tris base (M.W: 121.1 g/mol) = 121.0 g

Glacial acetic acid = 28.55 ml

0.5 M EDTA (pH 8.0) = 50.0 ml

Bring volume up to 500 ml with distilled water

5X TBS (Tris Buffered Saline) Buffer (1L)

NaCl = 40 g

KCl = 1 g

Tris base = 15 g

Dissolve in 900 ml distilled water

Adjust to pH=7.4 with concentrated HCl

Allow the solution to cool to room temperature before final adjustment of pH

Make up to a final volume of 1L with distilled water

Store at room temperature

1X TBS Buffer (1L)

5X TBS Buffer = 100 ml

Distilled water= 400 ml

Western Blotting Blocking Buffer 1(100 ml)

Fat-free Milk Powder = 5 g

1X TBS= 100 ml

Add 100 μ l of 20% Sodium azide

Western Blotting Blocking Buffer 2 (100 ml)

1X PBS buffer = 100 ml

Fat-free Milk Powder = 1 g

BSA = 3 g

10x Western Blotting Transfer Buffer (1L)

Tris base (M.W: 121.1 g/mol) = 30.3 g, final concentration = 125 mM

Glycine (M.W: 75.07 g/mol) = 72.06 g, final concentration = 960 mM

Dissolve in 500 ml distilled water and make up to 1000 ml.

1x Western Blotting Transfer Buffer (1L)

10x Western blotting transfer buffer = 100 ml

100% methanol = 100 ml

Cold distilled water = 800 ml

10X YNB (500 ml)

Yeast nitrogen base (YNB) = 17 g

Ammonium sulfate = 50 g

Dissolve in 500 ml distilled water

Heat slightly to dissolve completely

Filter sterilize solution and store at 4 °C

YPD (Yeast extract Peptone Dextrose) Medium (200 ml)

1 % Yeast Extract = 2 g

2 %Peptone = 4 g

Dissolve in 180 ml distilled water

Autoclave for 20 minutes

Cool to room temperature

Add 20 ml of 10X D (final concentration = 2%)

YPD Medium with Zeocin (200 ml)

Prepare YPD medium as above

Add 200 µl of filter sterilized Zeocin (100 mg/ml)

Store in the dark at 4 °C

YPD Plate with Zeocin (200 ml)

1 % Yeast Extract = 2 g

2 % Peptone = 4 g

Dissolve in 180 ml distilled water

Add 2 % Agar = 4 g

Autoclave for 20 minutes

Cool to ~ 55°C

Add the following

10X D = 20 ml (final concentration = 2%)

Zeocin (100 mg/ml) = 200µl

Mix properly by swirling

Pour medium into plate to solidify

Store plates in the dark at 4 °C

YPDS Plates with Zeocin (200 ml)

1 % Yeast Extract = 2 g

2 % Peptone = 4 g

Sorbitol = 36.44 g

Dissolve in 120 ml distilled water and make up to 180 ml

Add 2 % Agar = 4 g

Autoclave for 20 minutes

Cool to ~ 55°C

Add the following

10X D = 20 ml (final concentration = 2%)

Zeocin (100 mg/ml) = 200µl

Mix properly by swirling

Pour medium into plate to solidify

Store plates in the dark at 4 °C

Zeocin (100 mg/ml) Stock Solution (10 ml)

1g zeocin

Dissolve in 10 ml distilled water

Filter sterilize solution

Store at - 20°C in the dark.

VITA

ABDULKAREEM OLAKUNLE ODESINA

- Education: Master of Science in Biology, 2015. East Tennessee State University, Johnson City, TN.
- Bachelor of Science in Biochemistry, 2010. Olabisi Onabanjo University, Ogun, Nigeria.
- Professional Experience: Graduate Student Assistant, East Tennessee State University, Tennessee, Department of Biological Sciences, fall 2012 and fall 2014.
- Science Teacher, Otega Schools (annex), Ikorodu, Lagos, Nigeria, 2010 – 2011.
- Research Intern, Six month Student Industrial Work Experience Scheme, Olabisi Onabanjo University Teaching Hospital, Ogun, Nigeria, 2007.
- Presentations: Odesina A, and Kumar D. (2015). Characterization of SBIP68 a Putative Tobacco Glucosyltransferase and Its Role in Plant Defense. Phytochemical Society of North America. Urbana-Champaign, IL.
- Odesina A, and Kumar D. (2014). Characterization of SBIP-68 Putative Glucosyl Transferase Protein and its Role in Plant Defense. Appalachian Student Research Forum. Johnson City, TN.
- Odesina A, and Kumar D. (2013). SBIP-68 Glucosyl Transferase: Characterization and Role in Plant Defense. Appalachian Student Research Forum. Johnson City, TN.
- Odesina A. (2013). Characterization of SBIP-68 Tobacco Putative Glucosyl Transferase and Its Role in Plant Defense Mechanism. Seminar presentation at the Department of

Biological Sciences, East Tennessee State University,
Johnson City, TN.